

AD _____

Award Number: DAMD17-00-1-0236

TITLE: The Role of the Polypyrimidine Tract Binding Protein on
CD44 Splicing in Breast Cancer

PRINCIPAL INVESTIGATOR: Andrew Baraniak
Mariano A. Garcia-Blanco, Ph.D.

CONTRACTING ORGANIZATION: Duke University Medical Center
Durham, North Carolina 27710

REPORT DATE: June 2003

TYPE OF REPORT: Annual Summary

PREPARED FOR: U.S. Army Medical Research and Materiel Command
Fort Detrick, Maryland 21702-5012

DISTRIBUTION STATEMENT: Approved for Public Release;
Distribution Unlimited

The views, opinions and/or findings contained in this report are those of the author(s) and should not be construed as an official Department of the Army position, policy or decision unless so designated by other documentation.

Best Available Copy

20040720 063

REPORT DOCUMENTATION PAGE

Form Approved
OMB No. 074-0188

Public reporting burden for this collection of information is estimated to average 1 hour per response, including the time for reviewing instructions, searching existing data sources, gathering and maintaining the data needed, and completing and reviewing this collection of information. Send comments regarding this burden estimate or any other aspect of this collection of information, including suggestions for reducing this burden to Washington Headquarters Services, Directorate for Information Operations and Reports, 1215 Jefferson Davis Highway, Suite 1204, Arlington, VA 22202-4302, and to the Office of Management and Budget, Paperwork Reduction Project (0704-0188), Washington, DC 20503

1. AGENCY USE ONLY (Leave blank)		2. REPORT DATE June 2003	3. REPORT TYPE AND DATES COVERED Annual Summary (1 Jun 2000 - 31 May 2003)	
4. TITLE AND SUBTITLE The Role of the Polypyrimidine Tract Binding Protein on CD44 Splicing in Breast Cancer			5. FUNDING NUMBERS DAMD17-00-1-0236	
6. AUTHOR(S) Andrew Baraniak Mariano A. Garcia-Blanco, Ph.D.				
7. PERFORMING ORGANIZATION NAME(S) AND ADDRESS(ES) Duke University Medical Center Durham, North Carolina 27710 E-Mail: andrew.baraniak@duke.edu			8. PERFORMING ORGANIZATION REPORT NUMBER	
9. SPONSORING / MONITORING AGENCY NAME(S) AND ADDRESS(ES) U.S. Army Medical Research and Materiel Command Fort Detrick, Maryland 21702-5012			10. SPONSORING / MONITORING AGENCY REPORT NUMBER	
11. SUPPLEMENTARY NOTES				
12a. DISTRIBUTION / AVAILABILITY STATEMENT Approved for Public Release; Distribution Unlimited				12b. DISTRIBUTION CODE
13. ABSTRACT (Maximum 200 Words) <p>The cytogenetic and nuclear changes during breast tumor progression have been well documented, but the causes of these alterations are poorly understood. Changes in estrogen receptor status, gain in metastatic potential, accumulation of PNCs, and differential splicing of genes are changes seen in breast cancer cells during tumor progression. A strong connection between the splicing machinery and these subtle, significant, changes in gene expression have yet to be documented. Likely candidates are the alternative splicing factors, most notably the Polypyrimidine Tract Binding Protein (PTB). PTB is a known repressor of exon definition. During breast cancer progression, we believe, PTB's ability to repress exons is altered. To understand the changes in PTB function as cancer cells de-differentiate, an understanding of PTB mechanism must be attained. We are using the regulation of FGFR2 exon IIIb as a model system to study PTB mediated repression. We have mapped PTB binding sites and through the use of heterologous recruitment and RNAi mediated PTB depletion have clearly demonstrated PTB's function in the exon IIIb repression. Furthermore, we have defined the cell-type specific <i>cis</i>-regulatory elements responsible for overcoming PTB's repressive effects and have identified a potential <i>trans</i>-acting factor, Fox-1, that has been reported to antagonize PTB.</p>				
14. SUBJECT TERMS Polypyrimidine Tract Binding Protein (PTB), Fibroblast Growth Factor Receptor 2 (FGFR2), Alternative Splicing, Fox-1				15. NUMBER OF PAGES 144
				16. PRICE CODE
17. SECURITY CLASSIFICATION OF REPORT Unclassified	18. SECURITY CLASSIFICATION OF THIS PAGE Unclassified	19. SECURITY CLASSIFICATION OF ABSTRACT Unclassified	20. LIMITATION OF ABSTRACT Unlimited	

NSN 7540-01-280-5500

Standard Form 298 (Rev. 2-89)
Prescribed by ANSI Std. Z39-18
298-102

Table of Contents

Cover.....	1
SF 298.....	2
Table of Contents.....	3
Introduction.....	4
Body.....	5
Key Research Accomplishments.....	10
Reportable Outcomes.....	10
Conclusions.....	12
References.....	13
Appendices.....	14

Introduction

The broad, long-term goal of this project is to understand the mechanism of alternative exon repression mediated by the polypyrimidine tract binding protein (PTB). Little is known about this form of gene expression regulation in general, and even less is known about how this regulation is lost during the progression of cancers. The initial specific aims of this proposal were to investigate the mechanism of PTB action on the alternative splicing of CD44. These aims have since been amended to focus still on PTB mediated exon repression; however, now we are focusing on PTB's role in the alternative splicing of fibroblast growth factor receptor 2 (FGFR2). We believe that the molecular process through which PTB represses alternative exons is shared by many genes (Wagner and Garcia-Blanco, 2001); therefore, understanding PTB's role in the repression of FGFR2 exon IIIb can serve as a starting point for understanding its role in the repression of other exons that are alternatively spliced, especially those that change their splicing patterns during tumor progression. Recently, it was shown that the FGFR2 IIIb isoform played a critical role in the proper development of the mammary gland (Mailleux *et al* 2002). In addition, a subset of breast cancers has shown an increased expression of FGFR2, including one cell line, SUM-52PE, which solely expresses the IIIb isoform (Heiskanen *et al* 2001, Tannheimer *et al* 2000). A lot has been learned in the last three years on PTB's role in the repression of FGFR2 exon IIIb, and now we are currently beginning to understand the mechanisms through which PTB's effects can be counteracted. Hopefully these findings will allow for a mechanism that is generalizable for all alternative splicing events, including those that are directly pertinent to the field of breast cancer.

Body

In the annual report summarizing the first year of the funding period, fluorescent protein reporters capable of recapitulating *in vivo* PTB mediated exon-silencing of FGFR2 exon IIIb were described. To begin making the EGFP reporter constructs, we first cloned an intron into the open reading frame of the EGFP vector (clonetechn). Using the intron as a multiple cloning site, we created EGFP reporters containing FGFR2 exon IIIb and various deletions of either the Upstream Intronic Splicing Silencer (UISS), the Downstream Intronic Splicing Silencer (DISS), or both sequences. We have shown that both UISS and DISS bind PTB (Carstens *et al* 2000, Wagner and Garcia-Blanco 2002). When both silencing sequences are present in the reporter construct, exon IIIb is repressed thus allowing for the production of Green Fluorescent Protein; however, when either or both of the silencing sequences is deleted, exon IIIb is included and there is no detection of the Green Fluorescent Protein (Wagner *et al* 2003a). These results directly show that PTB mediated repression can be detected *in vivo*, and thus an *in vivo* assay for PTB activity has been established, which addresses the goals of task 1c in the statement of work.

In the midterm report summarizing the second year of the funding period, significant achievements in the understanding of PTB mediated exon IIIb repression were made. These achievements, most of which are described in the manuscript entitled "RNAi-mediated PTB depletion leads to enhanced exon definition" (Wagner and Garcia-Blanco 2002), include demonstrating that PTB is bound both upstream (Carstens *et al* 2000) and downstream of FGFR2 exon IIIb and that these binding sites are indeed important for silencing exon IIIb inclusion. In addition, we demonstrated that artificial recruitment of PTB to heterologous binding sites flanking exon IIIb can also elicit silencing, thus recruitment of PTB is sufficient to cause exon IIIb repression. Most importantly, we have used RNA interference (RNAi) to deplete PTB *in vivo* and show that this depletion leads to both an increase of exon IIIb inclusion in minigene constructs as well as the endogenous FGFR2 mRNA. These data prove the initial hypothesis of this proposal that states PTB is a repressor of exon inclusion. Furthermore, these data from the first and second year of funding address the goals outlined in task 1 and task 2 in the statement of work. In addition, we are currently in the midst of dissecting and identifying other elements that are crucial for the repression of exon IIIb (Wagner *et al* 2003b).

The development of the RNAi method to knock down endogenous levels of PTB has proven to be very important, as it has spawned three other manuscripts. The first of which involved a collaboration with Dr. Yan

Zeng in Dr. Bryan Cullen's laboratory, which was discussed in the midterm report and is cited at the end of this report (Zeng *et al* 2002). The second paper details PTB's involvement in IRES mediated translation, which is tangential in the study of PTB's function in relation to breast cancer, but it will be included in the appendix (Wagner *et al* 2003c). The third paper used RNAi on PTB to help understand how PTB can autoregulate its own protein levels via alternative splicing. This phenomenon is novel, and although it has not yet proven itself highly relevant to breast cancer progression, the process may later be proven to be important (Wollerton *et al* man in prep)

Having addressed PTB's role in the repression of exon IIIb inclusion, we wanted to understand how this repression is overcome in cell lines that include FGFR2 exon IIIb exclusively. Previously, two *cis*-acting cell-type specific regulatory elements have been identified that serve to activate exon IIIb inclusion and exon IIIc repression in epithelial cells (Del Gatto 1997, Carstens 1998, Jones 2001, Wagner *et al* manuscript submitted 2003d). These elements, termed the Intronic Activating Sequence 2 (IAS2) and Intronic Splicing Activator and Repressor (ISAR or IAS3), have been proposed to form a stem structure that allows for the cell-type specific inclusion of FGFR2 exon IIIb and repression of exon IIIc (Del Gatto 1997, Jones 2001, Muh 2002). We have shown that sequences within IAS2 and ISAR and their potential to form a stem have been highly conserved for over 600 million years (Mistry 2003), suggesting the importance of structure and perhaps sequence in the activation of exon IIIb inclusion and repression of exon IIIc inclusion. In order to delineate between the capability of stem formation and specific sequence composition of IAS2 and ISAR, we constructed minigene constructs that contained unrelated sequence substitutions for IAS2 and ISAR core (the stem forming sequence of ISAR). pI12DE-Rep, -Blue Blue(c), -Blue(c) Blue, -PyP, and -PyP Δ Bulge were capable of stem formation, whereas, pI12DE-Blue Blue, and Blue(c) Blue(c) were not able to form a stem structure, thus serving as a negative control (Appendix VII Fig 1B and 1C). The minigenes that were capable of stem formation rescued the function of IAS2 and ISAR core by allowing for the inclusion of exon IIIb and the repression of exon IIIc in the DT3 cell line, which normally includes exon IIIb (Appendix VII Fig 1D). These results agree with those published in the recent report by Muh, which demonstrate that unrelated stem forming sequences can substitute functionally for IAS2 and ISAR (Muh *et al* 2002). Having demonstrated that unrelated stem forming sequences can functionally substitute for IAS2 and ISAR core, we probed the stem-loop structure further to analyze the function of the predicted 2-nucleotide bulge of ISAR and the 735 nucleotide loop sequence separating IAS2 and ISAR core. By deleting and mutating the 2-nucleotide bulge sequence, we demonstrated that it served no function in the activation of exon IIIb or repression of exon IIIc (Appendix VII Fig

1E). After showing that the 2-nucleotide bulge had no effect on the proper splicing regulation of FGFR2, we demonstrated that a deletion of the loop sequence separating IAS2 and ISAR core also had no effect on the proper regulation of FGFR2 alternative splicing (Appendix VII Fig 2).

Having shown that neither the bulge nor the loop had an effect on the maintaining the cell-type specificity of FGFR2 alternative splicing, we sought to determine if the stem-loop structure was solely functioning through the approximation of elements upstream of IAS2 with elements downstream of ISAR core. This would provide one explanation for why random, unrelated stem-forming sequences could functionally substitute for IAS2 and ISAR core. To test whether the stem-loop structure was approximating sequences upstream of IAS2 to those downstream of ISAR core, we deleted the entire stem-loop structure, placing the nucleotide immediately upstream of the first base of IAS2 to the nucleotide immediately downstream of the last base of ISAR core, thus mimicking stem formation. Surprisingly, this construct retained the ability to include exon IIIb in DT3 cells 70% of the time for all single inclusion splicing events compared to the wild type, which included exon IIIb 90% of the time (Appendix VII Fig 3A and 3B). When a construct was unable to form a stem, such as the Blue Blue construct, exon IIIb was included only 20% of the time (Appendix VII Fig 3A and 3B). Having found that the approximation of these sequences was sufficient for exon IIIb inclusion in DT3 cells, we sought to mutate the region downstream of ISAR core to see if that had any effect on exon IIIb inclusion. Performing five base pair substitution mutations, we located an element in nucleotides 11-15 that had a significant effect on exon IIIb inclusion and exon IIIc repression. The C15 mutant caused a decrease in exon IIIb inclusion from 84% for wild type to 51% and an increase in exon IIIc inclusion from 16% to 49% (Appendix VII Fig 4).

Interestingly, the C15 mutant lies in the middle of GCAUG repeat downstream of ISAR core (Appendix VII Fig 4). Recently, it was reported that the pentanucleotide GCAUG repeat bound the splicing regulator Fox-1 (Jin *et al* 2003). In this paper, it was demonstrated that Fox-1 is involved in the alternative splicing regulation of the α -actinin gene, most likely due to Fox-1's ability to antagonize PTB function (Jin *et al* 2003). Due to these results, we obtained a cDNA clone of Fox-1 and overexpressed the protein in 293T cells, which normally repress exon IIIb, due in large part to the function of PTB. If Fox-1 were to antagonize PTB function, then it would be expected that overexpression of this protein would allow for the inclusion of exon IIIb in cells that normally repress exon IIIb. As can be seen in Figure 1, this was the case. When increasing amounts of Fox-1 were transfected into 293T cells, exon IIIb inclusion steadily increased.

The Fox-1 results have been obtained in the past couple of months, and there are still many experiments that need to be done to confirm its role in the activation of exon IIIb inclusion. A preliminary model suggests that the approximation of Fox-1 binding sites downstream of ISAR core to PTB binding sites upstream of IAS2, due to the formation of the IAS2-ISAR core stem structure, allows for Fox-1 to antagonize PTB function thus activating exon IIIb inclusion. We would still like to show that the sequence downstream of ISAR core is binding Fox-1, most likely using UV crosslinking or gel-mobility shift assays. To cement Fox-1's role in the activation of exon IIIb inclusion, we would like to knock out Fox-1 using RNAi in DT3 cells, which normally include exon IIIb, and demonstrate an increase in exon IIIc inclusion. In either case, the data gathered in the last year of funding has satisfied the goals presented in task 3 in the statement of work, and any new insight gathered from the Fox-1 data will aid in further studies implicating alternative splicing regulation with the progression of breast cancers.

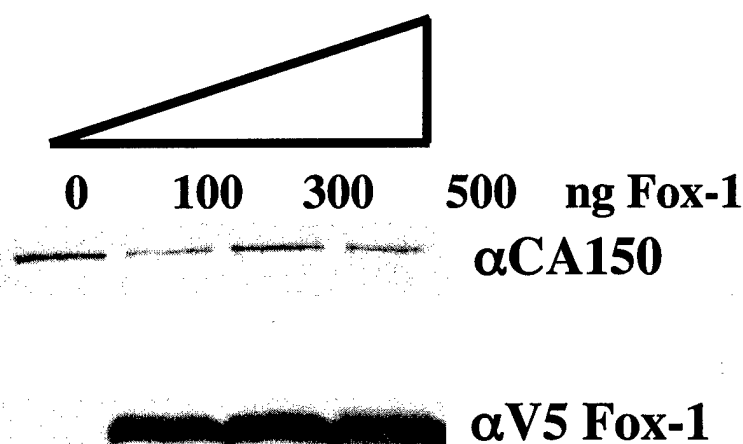
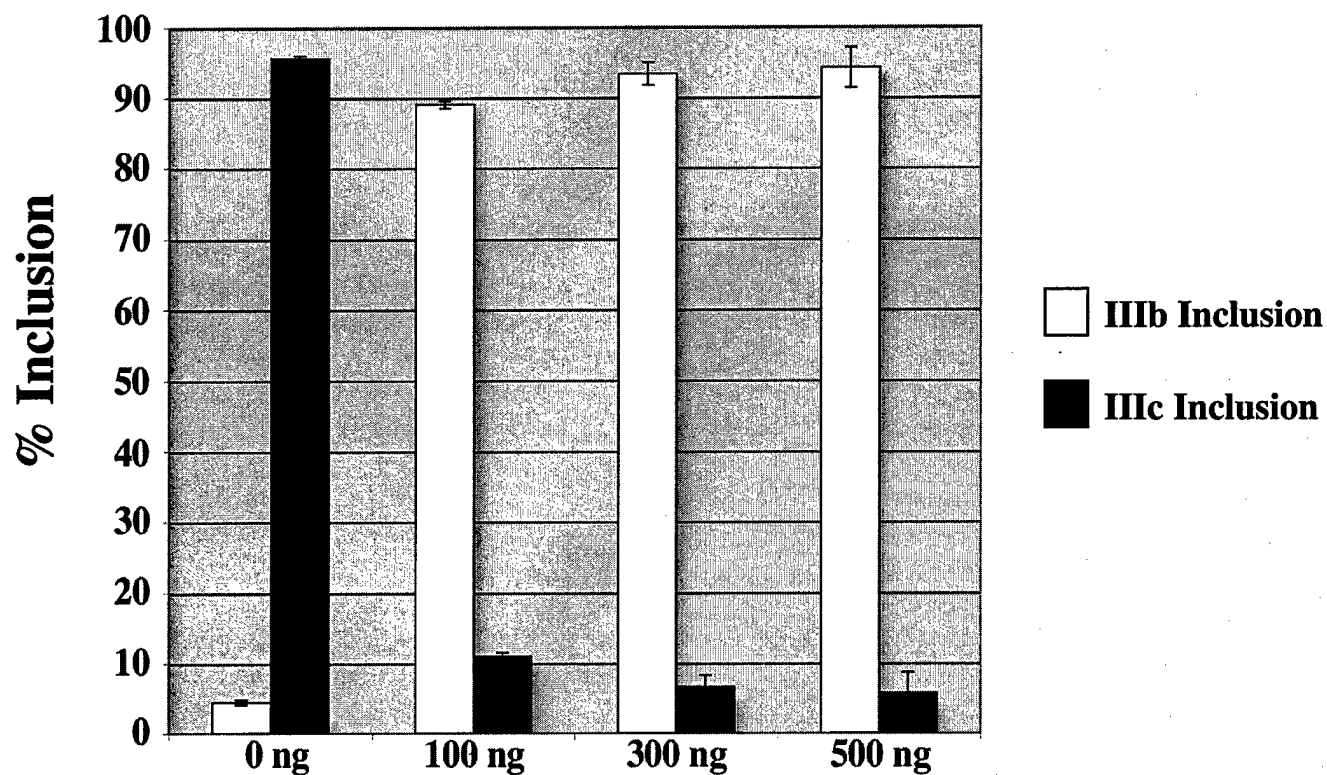


Figure 1: Transient transfections in 293T cells of increasing amounts of Fox-1 to determine its importance in regulation of FGFR2 minigene. As increasing levels of Fox-1 are transfected in the cells, exon 8 (IIIb) inclusion levels increase as exon 9 (IIIc) inclusion levels decrease. Western Blot to confirm overexpression of Fox-1. CA150 was used as a loading control to make sure that equivalent amounts of protein were being loaded for western analysis.

Key Research Accomplishments

- Designed EGFP minigenes that were capable of demonstrating PTB-mediated repression of exon IIIb
- Identified regions of PTB binding downstream of exon IIIb and defined them as splicing silencers
- Recruited PTB via heterologous MS2 fusion demonstrating PTB's sufficiency for exon IIIb repression
- Developed RNA interference protocol to transiently knock out PTB
- Demonstrated the function of endogenous PTB to repress endogenous FGFR2 IIIb inclusion using RNAi
- Defined and demonstrated cell-type specific elements, IAS2 and ISAR, capable of countering PTB's effects on exon IIIb repression
- Demonstrated that any stem forming structure could functionally substitute for IAS2 and ISAR to activate exon IIIb inclusion and repress exon IIIc inclusion
- Demonstrated that the sole purpose of the stem is to juxtapose sequences upstream of IAS2 to sequences downstream of ISAR
- Found sequence downstream of ISAR that functions to activate exon IIIb inclusion and repress exon IIIc inclusion, most likely through the recruitment of Fox-1
- Demonstrated that overexpression of Fox-1 in cells that normally include exon IIIc, serves to activate inclusion of exon IIIb, most likely due to Fox-1's capability to antagonize PTB's function

Reportable Outcomes

- Manuscript:** *Wagner EJ, Sessions O., Garcia-Blanco MA. 2003b. Characterization of the FGF-R2 Intronic Control Element. (man in prep).*
- Manuscript:** *Wollerton MC, Gooding CG, Wagner EJ, Garcia-Blanco MA, Smith CWJ. 2003. Polypyrimidine Tract Binding Protein Autoregulates via Alternative Splicing of Exon 11. (man in prep).*
- Manuscript:** **Wagner EJ, *Curtis ML, Eis PE, Garcia-Blanco MA. 2003d. The Application of the RNA Invader Assay™ to analyze FGF-R2 Alternative Splicing. (manuscript submitted). (*co-first authors)*
- Manuscript:** **Baraniak AP, *Lasda E, Wagner EJ, Garcia-Blanco MA. 2003. A Stem Structure Mediates Cell-Type Specific Splicing via Intronic Element Approximation. (manuscript submitted). (*co-first authors)*
- Manuscript:** *Wagner EJ, Florez P, Sessions O, Groemerier M, Garcia-Blanco MA. 2003c. RNAi-Mediated PTB Depletion Reveals a Requirement in IRES-Dependent Translation and Picornavirus Propagation. (manuscript submitted).*
- Manuscript:** *Wagner EJ, Baines A, Albrecht TA, Brazas RM, Garcia-Blanco MA. 2003a. Imaging Alternative Splicing in Living Cells. Methods in Molecular Biology, RNA-Protein Interaction Protocols (In press)*
- Manuscript:** *Mistry N, Harrington W, Lasda E, *Wagner EJ, *Garcia-Blanco MA. 2003. Of Urchin and Men: The Evolution of the FGF-R2 Alternative Splicing Unit. RNA. 9: 209-217. (*Co-corresponding Authors)*
- Manuscript:** *Zeng Y, Wagner EJ, Cullen BR. 2002. Both Natural and Designed Micro RNAs can inhibit the expression of Cognate mRNAs when expressed in Human Cells. Mol Cell. 9: 1327-1333*
- Manuscript:** *Wagner EJ and Garcia-Blanco MA. 2002. RNAi-mediated PTB depletion leads to enhanced exon definition. Mol Cell. 10: 943-9. Erratum in: Mol Cell. 2002 10: 1535*
- Manuscript:** *Wagner EJ and Garcia-Blanco MA. 2001. The Polypyrimidine Tract Binding Protein Antagonizes Exon Definition. Mol. Cell. Biol. 21: 3281-3288*
- Manuscript:** *Carstens RP*, Wagner EJ*, and Garcia-Blanco MA. 2000. An Intronic Splicing Silencer Causes Skipping of the IIIb exon of Fibroblast Growth Factor Receptor 2 through the Involvement of Polypyrimidine Tract Binding Protein. Mol. Cell. Bio. 20: 7388-7400 (*co-first authors). Please Note: This*

work was performed just prior to funding period but was published during funding period. The work presented in this paper is consistent with numerous aspects of the proposed research.

-Presentation: Poster Presentation at the Annual RNA Society Meeting held in Vienna, Austria 2003. Title of Abstract: Juxtaposition of conserved elements that likely function through the hormonally induced expression of Fox-1 activate cell-type specific inclusion of FGF-R2 exon IIIb (see appendix)

-Presentation: Poster Presentation at the Era of Hope Meeting held in Orlando, Florida 2002. Title of Abstract: Fluorescent Reporters to Recapitulate *in vivo* Alternative Splicing Regulation (see appendix)

-Presentation: Oral Presentation at the Annual RNA Society Meeting held in Madison, Wisconsin 2002. Title of Abstract: Quantitative Study of Alternative Splicing for the Fibroblast Growth Factor Receptor 2 Using the Invader RNA Assay (see appendix)

-Presentation: Poster Presentation at the Annual RNA Society Meeting held in Madison Wisconsin 2002. Title of Abstract: Characterizing Splicing Repressors of FGFR2 exon IIIb (see appendix)

-Presentation: Oral Presentation at the Annual RNA Society Meeting held in Banff, Alberta 2001. Title of Abstract: Cell-type specific Inclusion of FGFR2 IIIb is mediated by a central switch: the intronic control element (see appendix)

-Degrees: *Eric J. Wagner.* Received Doctor of Philosophy from the Program in Molecular Cancer Biology at Duke University. Title of Thesis: The Polypyrimidine Tract Binding Protein Antagonizes Exon Definition

-Awards: *Eric J. Wagner.* Student Researcher of the Year Award from the American Cancer Society; given to one Duke University student who is performing research in an ACS funded lab

Conclusions

Since the sequencing of the human genome, it has become clear that alternative splicing is more the rule than the exception. Estimates suggest that anywhere from 40% to 70% of genes undergo alternative splicing. As important as this process is, so little is known about the proteins involved and especially about their molecular mechanisms. The achievements in this report are significant in the fact that they provide strong evidence for the endogenous function of one of the regulators of alternative splicing; PTB, and we have identified another regulator of alternative splicing, Fox-1, which may serve to counteract the endogenous function of PTB. The alternative splicing of multiple genes have been found to change as breast cancer cells form and undergo tumor progression (as well as many other cancer cells), thus the function of the proteins governing this process is likely changing. Identifying and characterizing these proteins is integral to predict the changes in splicing patterns observed during tumor progression. The conclusion of this final report is straightforward: the function of endogenous PTB is to antagonize the exon definition of FGFR2 exon IIIb, fibronectin EIIb (Wagner 2002), and most likely exons from other genes. PTB mediated exon IIIb antagonism is counteracted by the cell-type specific stem structure formed between IAS2 and ISAR core. The sole function of this stem structure is to approximate sequences upstream of IAS2 with those downstream of ISAR core, one of which is the conserved GCAUG element found to bind the splicing regulator Fox-1 (Jin *et al* 2003). Exogenous expression of Fox-1 in cells that normally include FGFR2 exon IIIc has been demonstrated to activate the inclusion of FGFR2 exon IIIb, possibly due to Fox-1's ability to antagonize PTB's endogenous function.

References

1. Wagner E.J. and Garcia-Blanco MA. 2001. The Polypyrimidine Tract Binding Protein Antagonizes Exon Definition. *Mol. Cell. Biol.* 21: 3281-3288
2. Mailleux, A. A., Spencer-Dene, B., Dillon, C., Ndiaye, D., Savona-Brown, C., Itoh, N., Kato, S., Dickson, C., Thiery, J. P., and Bellusci, S. 2002. Role of FGF10/FGFR2b signaling during mammary gland development in the mouse embryo. *Development* 129: 53-60.
3. Heiskanen, M., Kononen, J., Barlund, M., torhorst, J., Sauter, G., Kallioniemi, A., and Kallioneimi, O. 2001. CGH, cDNA and tissue microarray analyses implicate FGFR2 amplification in a small subset of breast tumors. *Anal Cell Pathology* 22:229-34.
4. Tannheimer, S. L., rehemtulla, A., and Ethier, S. P. 2000. Characterization of fibroblast growth factor receptor 2 overexpression in the human breast cancer cell line SUM-52PE. *Breast Cancer Research* 2:311-20.
5. Carstens R.P., Wagner E.J., and Garcia-Blanco M.A. 2000. An Intronic Splicing Silencer Causes Skipping of the IIIb exon of Fibroblast Growth Factor Receptor 2 through the Involvement of Polypyrimidine Tract Binding Protein. *Mol. Cell. Bio.* 20: 7388-7400.
6. Wagner E.J. and Garcia-Blanco M.A. 2002. RNAi-mediated PTB depletion leads to enhanced exon definition. *Mol Cell.* 10: 943-9. Erratum in: *Mol Cell.* 2002 10: 1535.
7. Wagner E.J., Baines A., Albrecht T.A., Brazas R.M., Garcia-Blanco M.A. 2003. Imaging Alternative Splicing in Living Cells. *Methods in Molecular Biology, RNA-Protein Interaction Protocols (In press)*.
8. Del Gatto F., Plet A., Gesnel M.C., Fort C., and Breathnach R. 1997. Multiple interdependent sequence elements control splicing of a fibroblast growth factor receptor 2 alternative exon. *Mol Cell Biol* 17:5106-16.
9. Carstens R.P., McKeehan W.L., and Garcia-Blanco M.A.. 1998. An intronic sequence element mediates both activation and repression of rat fibroblast growth factor receptor 2 pre-mRNA splicing. *Mol Cell Biol* 18:2205-17.
10. Jones R.B., Carstens R.P., Luo Y., and McKeehan W.L. 2001. 5'- and 3'-terminal nucleotides in the FGFR2 ISAR splicing element core have overlapping roles in exon IIIb activation and exon IIIc repression. *Nucleic Acids Res* 29:3557-65.
11. *Wagner EJ, *Curtis ML, Eis PE, Garcia-Blanco MA. 2003. The Application of the RNA Invader Assay™ to analyze FGF-R2 Alternative Splicing. (*manuscript submitted*). (*co-first authors).
12. Muh S.J., Hovhannisyan R.H., and Carstens R.P. 2002. A Non-sequence-specific double-stranded RNA structural element regulates splicing of two mutually exclusive exons of fibroblast growth factor receptor 2 (FGFR2). *J Biol Chem* 277:50143-54.
13. Mistry N., Harrington W., Lasda E.L., Wagner E.J., and Garcia-Blanco M.A. 2003. Of urchins and men: evolution of an alternative splicing unit in fibroblast growth factor receptor genes. *RNA* 9:209-17.
14. Jin Y., Suzuki H., Maegawa S., Endo H., Sugano S., Hashimoto K., Yasuda K., and Inoue K. 2003. A vertebrate RNA-binding protein Fox-1 regulates tissue-specific splicing via the pentanucleotide GCAUG. *Embo J* 22:905-12.

Juxtaposition of conserved elements that likely function through the hormonally induced expression of Fox-1 activate cell-type specific inclusion of FGF-R2 exon IIIb

Andrew P. Baraniak and Mariano A. Garcia-Blanco

Department of Molecular Genetics and Microbiology, Duke University Medical Center
Duke University, Durham, NC 27710

Alternative splicing of the fibroblast growth factor receptor 2 (FGF-R2) occurs in a cell-type specific manner with the mutually exclusive use of either exon IIIb or exon IIIc. Specific inclusion of exon IIIb is observed in the epithelial-like DT3 cell line, whereas exon IIIc inclusion is observed in the related but fibroblast-like AT3 cell line. In DT3 cells, the Intronic Activating Sequence 2 (IAS2) and the Intronic Splicing Activator and Repressor (ISAR) *cis*-elements in the FGF-R2 pre-mRNA activate exon IIIb inclusion and repress inclusion of exon IIIc. The function of these elements counters exon IIIb silencing, which is mediated by PTB and other factors yet to be identified. We and others have strong data that support the existence and the functional importance of a stem formed between IAS2 and ISAR. Surprisingly, however, juxtaposing sequences immediately upstream of IAS2 with sequences immediately downstream of ISAR core by deleting the entire stem-loop region had no effect on the proper cell-type specific alternative splicing of FGF-R2. These data demonstrate that the sole purpose of the IAS2-ISAR core stem is to approximate sequences upstream of IAS2 with those downstream of ISAR.

A strong candidate for an approximated sequence downstream of ISAR core is the conserved GCAUG repeat, which has been shown to bind the Fox-1 splicing regulator. GCAUG repeats have been previously implicated in alternative splicing regulation. We will demonstrate that a GCAUG sequence downstream of ISAR core is important for activation of exon IIIb and repression of exon IIIc inclusion. In 293T cells, which normally skip exon IIIb, Fox-1 expression dramatically increases IIIb inclusion from 5% to over 90%, strongly suggesting that Fox-1 is important for the activation of exon IIIb. We are currently performing RNAi on Fox-1 in cells that include exon IIIb to confirm that this splicing regulator is essential for the cell-type specific splicing of FGF-R2 transcripts.

Taken together our data suggest that the approximation of the Fox-1 binding site close to the silencer sequences downstream of exon IIIb is responsible for the de-repression of this exon. This de-repression is precisely the type of function predicted for Fox-1 as it has been shown to antagonize the repression of PTB on the alpha-actinin NM exon (Jin *et al* 2003). Furthermore, it is intriguing that Fox-1 expression has been shown to be upregulated by androgens and DT3 cells, but not AT3 cells, are androgen dependent. We favor a model, which we believe is unprecedented, where inclusion of exon IIIb is determined in response to a hormonal signal.

II. Abstract for Poster Presentation at the Era of Good Hope Meeting in Orlando, Florida

Fluorescent Reporters to Recapitulate *in vivo* Alternative Splicing Regulation

Eric J. Wagner, Andrew Baraniak, & Mariano Garcia-Blanco

Department of Molecular Genetics & Microbiology, Duke University Medical Center

Fibroblast growth factor receptor 2 (FGF-R2) alternative splicing occurs in a highly tissue restrictive fashion. The mutually exclusive inclusion of exon IIIb or IIIc results in receptors with different ligand binding specificities. The general profile of FGF-R2 splicing demonstrates that the IIIb exon is predominantly included in epithelial cells while the IIIc exon is included in mesenchymal tissues. In recent elegant experiments, either the IIIb or IIIc exon has been knocked out in mice. FGF-R2-IIIb^{-/-} mice survive to term but show severe dysgenesis and agenesis of many internal organs. Specific knockout of FGF-R2-IIIc results in an embryonic lethality, however, hemizygous knockouts demonstrate many of the physical abnormalities associated with Apert's and Pfeiffer's syndromes.

Our lab has been studying the mechanisms of FGF-R2 alternative splicing using two rat cell lines that splice the endogenous FGF-R2 either to the IIIb exon or the IIIc exon, exclusively. Using this system we have identified several *cis* regulatory elements. In AT3 cells, which include IIIc, we have found that two Intronic Splicing Silencers (ISS) flank the IIIb exon and are each required for its repression. In DT3 cells, two cell-type specific *cis* elements, termed the Intronic Activating Sequence 2 (IAS2) and the Intronic Splicing Activator and Repressor (ISAR) have been identified to overwhelm the repressive effect of the flanking ISS. These two elements can form a putative secondary structure that we believe physically interferes with the activity of downstream ISS due to its proximity with IAS2. Our research on the mechanism of FGF-R2 alternative splicing has focused primarily on *in vitro* systems and tissue culture cell lines. We are interested in studying the physiological relevance of these mechanisms within the living animal to gain insight both on the developmental regulation of FGF-R2 alternative splicing as well as the regulation within the adult mouse.

We are developing a versatile set of fluorescent reporters using both GFP and RFP. Within the GFP reading frame we have introduced FGF-R2 exon IIIb as well as its regulatory *cis* elements. Inclusion of the IIIb exon within GFP cDNA results in an insertion, which disrupts fluorescence; only cells that skip the exon will fluoresce.

Using this reporter, we have been able to demonstrate striking cell-type specific GFP fluorescence. We are also introducing the IIIc exon as well as its *cis* element regulatory sequences into the RFP reading frame. We are performing experiments aimed at illustrating cell-type specific fluorescence of RFP. These reporters, when used in concert, act as complementary measurements of activity of the splicing factors responsible for tissue-specific FGF-R2 alternative splicing.

The long-term goal of these reporters is to elucidate the alternative splicing changes that occur in tumors *in situ*. Many genes undergo significant alternative splicing changes as breast cancer tumors progress; CD44 is a notable example. The GFP reporter has been designed in such a way as to accommodate the study of virtually any alternatively spliced exon. The potential uses of this reporter in breast cancer research will be discussed.

III. Abstract for Oral Presentation at Annual RNA Society Meeting in Madison, Wisconsin 2002

Quantitative Study of Alternative Splicing for the Fibroblast Growth Factor Receptor 2 Using the Invader RNA Assay

Eric J. Wagner¹, Michelle L. Curtis², Peggy S. Eis², & Mariano Garcia-Blanco¹

¹ Department of Molecular Genetics and Microbiology
Duke University Medical Center, Durham NC 27710

² Third Wave Technologies, Madison WI 53719

The ability to precisely differentiate between mRNA isoforms is critical to the study of alternative splicing. Many currently used detection methods suffer from difficulty, high cost, lack of reproducibility, insufficient quantification, and most important, lack of specificity. The Invader RNA assay, which specifically and quantitatively measures zeptomole levels of RNA, appeared to be ideal for the quantification of alternative mRNAs.

We applied this technology to investigate the alternative inclusion of exon IIIb or exon IIIc in mRNAs encoding Fibroblast Growth Factor Receptor 2 (FGF-R2) in two related cell lines derived from the rat Dunning prostate tumor, DT3 and AT3. DT3 cells used exon IIIb and AT3 included exon IIIc. IIIc inclusion in AT3 cells requires the silencing of IIIb and is driven by strong splice sites bordering the IIIc exon. IIIb inclusion in DT3 cells requires two regulatory elements, ISAR and IAS2, which jointly activate exon IIIb and repress exon IIIc. In this study, we transfected several FGF-R2 minigenes containing various deletions of IAS2 and ISAR into DT3 and AT3 cells and used the Invader assay to distinguish and quantify the splicing products. The IIIb and IIIc Invader probe sets were highly specific for their respective targets (i.e., no cross-reactivity). Further, we compared Invader assay results with RT-PCR results. Whereas both methods yielded similar splicing profiles, only the Invader assay precisely quantified small variations in the absolute number of spliced products. This study indicates the Invader RNA assay is a highly specific and quantitative alternative to current detection methods.

IV. Abstract for Poster Presentation at Annual RNA Society Meeting in Madison, Wisconsin 2002

Characterizing Splicing Repressors or FGF-R2 Exon IIIb

Eric J. Wagner & Mariano Garcia-Blanco

Department of Molecular Genetics and Microbiology
Duke University Medical Center, Durham NC 27710

The tissue specific regulation of fibroblast growth factor receptor 2 (FGF-R2) pre-mRNA splicing results in the mutually exclusive use of either the IIIb exon or the IIIc exon. Choice of either of these exons results in receptors with differing ligand binding properties. To study this regulation, we use the well-differentiated DT3 rat prostate carcinoma cell line, which includes only the IIIb exon, while the poorly differentiated AT3 rat prostate carcinoma cell line includes exon IIIc.

Downstream of exon IIIb lies an Intronic Control Element (ICE) which elicits multifunctional regulation on both exon IIIb and IIIc. One of these functions is to silence exon IIIb. Within the ICE are 7 UCUU motifs, which are required for efficient silencing of exon IIIb, and that bind PTB. A critical role for PTB is supported by the following: We have previously shown that overexpression of PTB enhances the silencing of IIIb and now we show that recruitment of a PTB-MS2 fusion protein to a heterologous binding site within the ICE leads to silencing of IIIb. We also show that specific depletion of PTB in vivo using RNA interference leads to an increase in exon IIIb inclusion. We have found that minigenes with several UCUU elements deleted are predictably more sensitive to the levels of PTB in the cell. The increase in exon IIIb inclusion can be partially rescued by overexpression of human PTB, which is encoded by a mRNA expected to be partially resistant to RNAi.

A second silencing element has been found at the 5' end of the ICE, which we believe does not bind PTB. This sequence is highly conserved among FGF-R2 genes from rat to sea urchin. We are using single point mutations that destroy silencing to design a purification scheme to identify this factor(s). We will discuss the progress of this purification.

V. Abstract for Oral Presentation at Annual RNA Society Meeting in Banff, Alberta 2001

Cell-type specific inclusion of FGF-R2 exon IIIb is mediated by a central switch: the intronic control element.

**Eric Wagner, Andrea Baines, Russ Carstens, and Mariano Garcia-Blanco
Department of Genetics, Duke University**

Tissue specific alternative splicing of fibroblast growth factor receptor 2 (FGF-R2) pre-mRNA results in the mutually exclusive use of exons IIIb or IIIc; choice of exon inclusion determines the ligand specificity and has profound physiological consequences. The well-differentiated DT3 rat prostate cell line includes IIIb, while the poorly differentiated AT3 rat prostate line includes IIIc. We will present experiments directed at unraveling the cell-type specific use of IIIb or IIIc as well as a system designed for the study of FGF-R2 splicing in living cells or transgenic animals.

In both DT3 and AT3 cells, two intronic splicing silencers (ISS) located upstream of exon IIIb (UISS) and downstream (DISS) promote its exclusion. Both ISS have multiple binding sites for the Polypyrimidine Tract Binding Protein (PTB) and PTB is a major player in mediating silencing of IIIb via the UISS. Although silencing via the DISS also involves PTB; analysis revealed a critical requirement for other factors that bind a conserved UGCUU motif, this will be discussed. We believe the ISS elements, in large measure via PTB, form the borders of a zone of silencing; IIIb sits in the middle of this zone. In DT3 cells, however, the ISS are countered by two cis-acting elements located between IIIb and IIIc; these elements working in concert activate IIIb, and independently repress IIIc. These intronic splicing activators and repressors (ISAR and ISAR2), which have no apparent function in AT3 cells, contain complementary sequences and can form a stem (as proposed by R. Breathnach). ISAR2 is embedded within the DISS; given this arrangement it's likely that an ISAR-ISAR2 stem will disrupt ISS function. The DISS elements and the overlapping ISAR2 form a master switch for cell-type specific regulation of IIIb inclusion; we have named this switch: intronic control element (ICE).

In order to study the interplay between the ISS and ISAR elements during development or tumor progression we have developed a system that relies on the expression of Green Fluorescent Protein. We will show the system to be a versatile and accurate reporter of ISS and ISAR function. We will also discuss applications of the system to study alternative splicing in transgenic animals and in tumors in situ.

Imaging Alternative Splicing in Living Cells

Eric J. Wagner^{1,3,‡}, Andrea Baines^{1,†}, Todd Albrecht¹, Robert M. Brazas¹, and

Mariano A. Garcia-Blanco^{1,2,*}

Departments of ¹Molecular Genetics and Microbiology and ²Medicine, ³Program in

Molecular Cancer Biology, Duke University Medical Center

Durham, North Carolina 27710

‡ Eric J. Wagner is at the Department of Biochemistry and Biophysics, Program in Molecular Biology and Biotechnology, CB#7100, University of North Carolina, Chapel Hill, NC 27599.

† Andrea Baines is at the Medical Scientist Training Program, University of Michigan, 2965 Taubman Medical Library, 1150 W. Medical Center Drive, Ann Arbor, MI 48109-0619.

*Correspondence to: M. A. Garcia-Blanco (garci001@mc.duke.edu).

Abstract

We have developed an *in vivo* reporter of alternative splicing decisions, which allows for the determination of FGF-R2 splicing patterns without destruction of cells. This method has broad applications that include the study of other alternatively spliced genes, in tissue culture and in whole animals, and may be useful in creating imaging markers for the study of tumor progression and metastasis. In this chapter we present one embodiment of this methodology using fluorescence reporters. As with any new assay, a series of experiments were performed to validate the method. In this chapter, we document some of these experiments.

1.0 Introduction

1.1. Alternative splicing

Versatility, or “multitasking”, by a relatively small number of genes may be absolutely required to establish the development and function of metazoans (1,2).

Complex genes in metazoans can each encode multiple protein products by differentially selecting which exons will be included in a mature transcript; this process is known as alternative splicing (3), likely to be the most important engine driving the diverse array of proteins observed in any one cell, the proteome. Alternative RNA synthesis and

processing yields different mRNAs from one gene by altering one or all of the following:

1) the transcription initiation site, thus modifying the 5' end of the RNA, 2) the site of cleavage and polyadenylation, thus altering the 3' end of the transcript, and finally 3) the definition of exons, providing for the different assortment of these packets of coding information. Alternative splicing is observed among pre-mRNAs from over two thirds of protein-coding genes in humans (4, 20). Alternative splicing can be divided into four general categories: the choice to remove or not to remove an intron, the alternative use of 5' splice sites or 3' splice sites that will change the length an exon, and the choice between exon inclusion and exon skipping. This last form of alternative splicing involves one or more alternatively used exon(s) between two exons that are constitutively included.

1.2 Alternative splicing of FGF-R2 transcripts

Even though the methodology described is generally applicable to many examples of alternative splicing (*see Note 1*), here we will focus on the mutually exclusive choice made between two exons FGF-R2IIIb (IIIb) or FGF-R2IIIc (IIIc) (5-7, 11-16). Although

exons IIIb and IIIc encode homologous sub-domains, the differences between them are sufficient to dramatically alter the ligand-binding specificity of the FGF-R2 isoforms. The choice between IIIb and IIIc is tissue specific. Epithelial cells and well-differentiated prostate tumors of epithelial origin (e.g. DT3 rat prostate tumors) include only IIIb, whereas mesenchymal cells or de-differentiated prostate carcinomas (e.g. AT3 rat prostate tumors) include only IIIc (14). The IIIb/IIIc choice must be dictated by differences in the splicing machinery in different cells (i.e., DT3 vs. AT3) and by unique cis-acting elements in FGF-R2 transcripts. The identities of these trans-acting factors and cis-elements have led to a model for the tissue-specific regulation of IIIb/IIIc choice (5, 12,13, 15-17) (**Figure 1**). The choice of FGF-R2 isoforms critically depends on the following cis-acting elements: Weak splice sites border the IIIb exon and contribute to poor exon definition (10). An hnRNP A1 binding site in exon IIIb mediates poor recognition of this exon (11). Intronic splicing silencers (ISS) flank exon IIIb, and mediate profound repression of IIIb inclusion (12,15). This silencing is mediated by the polypyrimidine tract binding protein (PTB) (15). In fibroblasts, these repressors of exon IIIb dictate exon choice, whereas in epithelial cells these negative cis-elements are counteracted to activate exon IIIb and repress exon IIIc. An intronic splicing activator and repressor (ISAR) and an intronic activating sequence (IAS2) are located in the intron between IIIb and IIIc and are absolutely required for cell-type specific activation of IIIb (5,13). These elements are also required for IIIc repression (Wagner et al, manuscript in preparation).

1.3. Methods to study alternative splicing of FGF-R2 transcripts

Most current methods used to study alternative splicing in mammals employ two general approaches. Biochemical analysis involves the use of cellular or subcellular extracts capable of recapitulating splicing reactions *in vitro*. The advantage to this approach is it facilitates the study of individual proteins using classical biochemistry; the disadvantages are that, to date, many cells types have not produced splicing-competent nuclear extracts and most available extracts can only partially recapitulate splicing decisions made *in vivo*. A molecular genetics approach involves the use of minigenes where genomic sequence from alternatively spliced genes are inserted into mammalian expression vectors and then transfected into cells in culture that regulate the alternative splicing event of interest. The advantage to this approach is that it facilitates the discovery of *cis* elements and is experimentally facile. This approach combined with the use of RNA interference (see **Chapter** __ in this volume) can lead to the identification of *trans*-acting factors (15). Additionally the use of knockout mice has led to an understanding of the roles of a few alternative splicing factors (e.g., Nova-1)(18). The details of the RNA transactions in these cases were obtained by lysing the cells and analyzing the isolated RNA. In some cases alternative decisions have been visualized in fixed tissues using *in situ* hybridization. All of these approaches, although quite useful, do not report on splicing in real time.

We have developed an *in vivo* reporter of alternative splicing decisions (see **Note 2**), which allows for the determination of FGF-R2 splicing patterns without destruction of cells. This method has broad applications that include the study of other alternatively spliced genes, in tissue culture and in whole animals, and may be useful in creating imaging markers for the study of tumor progression and metastasis. In this chapter we

present one embodiment of this methodology using fluorescence reporters (see **Note 3**). As with any new assay, a series of experiments were performed to validate the method. In this chapter, we document some of these experiments. We describe the creation of these fluorescent splicing reporters and demonstrate the correlation between the alternative splicing of the reporter and the fluorescence seen in the cells.

2. Materials

2.1 Plasmids

1. Plasmid pEGFPN1: pEGFPN1 (Clontech, Inc.) has a multi-cloning site (MCS) between the immediate early promoter of CMV (PCMV IE) and EGFP coding sequences and an SV40 polyadenylation signal downstream of the EGFP open reading frame (orf) to direct proper processing of the 3' end of the mRNA. A neomycin-resistance cassette (neo^r) allows stably transfected eukaryotic cells to be selected using geneticin (also G418) and a kanamycin resistance marker is used for selection of kan^r in *E. coli*. A complete description and sequence of this vector can be found at the clontech website address:
<http://www.clontech.com/techinfo/vectors/vectorsE/pEGFP-N1.shtml>.
(see **Note 4**).
2. Plasmid pGInt: Plasmid pGInt was constructed by introducing an intron from pI-12 (15) into sequences encoding the EFGR orf in pEGFPN1. (see **Note 5**).
3. Plasmid pGIIb: The rat FGF-R2 exon IIIb, and upstream and downstream intronic sequences flanking the exon including UISS and ICE, was subcloned into pGInt (**Figure 2**).

4. Plasmids pGΔUISS, pGΔICE and pGΔΔ: Plasmid pGΔUISS, pGΔICE and pGΔΔ are identical to pGIIIb except that the UISS, ICE or both were respectively deleted (**Figure 2**).
5. Plasmid pcDNA5/FRT/TO (Invitrogen, Inc.). This plasmid is similar to standard cytomegalovirus (CMV) immediate early promoter driven mammalian expression vectors except for the presence of three important features: First, there is the FRT site, which is a recognition/target sequence for the yeast 2μ plasmid site-specific recombinase, Flp. The presence of this site allows for this plasmid to be integrated into a second specific FRT site located within a host cell chromosome by Flp dependent-, site-specific recombination (see **Figure 3**). Second, the CMV promoter has two tetracycline (tet) repressor operators within it, making this promoter sensitive to the presence of tet repressor. In the absence of tetracycline, the tet repressor will bind the operator and repress the CMV promoter and there will be no expression of the gene of interest. Upon addition of tetracycline, expression of the gene of interest will be induced strongly (Tet-ON), similar to the levels seen using the standard CMV promoter. (see **Note 6**). Third, this plasmid backbone contains a hygromycin resistance gene that is just downstream of the FRT site and lacks a mammalian promoter. The promoter for the hygromycin resistance gene is acquired upon integration into the chromosomal FRT site, which prevents spurious integration events from being selected (see **Figure 3**)(see **Note 7**).
6. Plasmids pcDNA5/FRT/TO-Gint, pcDNA5/FRT/TO-GIIIb, pcDNA5/FRT/TO-G ΔUISS, pcDNA5/FRT/TO-GΔ,Δ. Each of these plasmids has the EGFP

region including the intron and IIIb sequences from pGInt, pGIIIb, pGAUISS and pGΔ,Δ cloned into the polylinker region of pcDNA5/FRT/TO downstream of the CMV immediate early promoter. These plasmids can be integrated into a chromosomal FRT site using Flp recombinase (see below for details).

7. Plasmid pOG44. This vector expresses a temperature sensitive mutant of the yeast 2μ plasmid-derived Flp recombinase under the control of the CMV immediate early promoter. It is used as a source of Flp recombinase during Flp-mediated recombination into the chromosomal FRT site. See Invitrogen's website for additional details (www.invitrogen.com).

2.2 Cell culture and transfections

1. DT3 and AT3 cell lines are derivatives of the rat Dunning prostate tumor and were kindly given to the laboratory by Dr. Wallace McKeehan (Texas A & M University Health Sciences Center, Houston, TX). These cells were maintained in DMEM-L (media described below).
2. Flp-In T-Rex 293 Cell Line (Invitrogen, Inc.). These cells, which are derived from standard human embryonic kidney 293 cells (ATCC, CRL-1573), were purchased from Invitrogen, Inc. Flp-In T-Rex 293 cells have a single copy of a FRT site integrated due to the stable transfection of the pFRT/lacZeo plasmid (Invitrogen, Inc.). Invitrogen has demonstrated high level expression from pcDNA5/FRT/TO derived vectors integrated at this chromosomal FRT location. The pcDNA6/TR tet repressor expression vector (Invitrogen, Inc.) has also been stably integrated yielding high level constitutive expression of tet repressor.

Therefore, in the absence of tetracycline, there will be no expression from pcDNA5/FRT/TO integrated plasmids, while there will be strong expression in the presence of tetracycline. These cells were maintained in DMEM-High Glucose (Invitrogen) with tetracycline-free 10% fetal bovine serum (see **Note 8**), L-glutamine, penicillin/streptomycin, 100 µg/ml Zeocin, and 15 µg/ml blasticidin.

3. Dulbecco's modified eagle medium with low glucose, L-glutamine, 110 mg/L sodium pyruvate and pyridoxine hydrochloride (DMEM-L). (AT3 and DT3 cell lines). Dulbecco's modified eagle medium with high glucose, L-glutamine, 110 mg/L sodium pyruvate and pyridoxine hydrochloride (DMEM-H). (Flp-In T-Rex 293 cell line). Unless otherwise indicated tissue culture supplies were obtained from Invitrogen, Inc.
 4. Fetal bovine serum (FBS) was heat inactivated at 56° C for 30 min (Hyclone, Inc.).
 5. Penicillin - streptomycin (100X -10,000 units/ml).
 6. Trypsin-EDTA (0.05% Trypsin, 0.53 mM EDTA-4Na).
 7. Dulbecco's Phosphate Buffered Saline (PBS).
 8. OPTI-MEM reduced serum medium with 1X HEPES buffer, L-glutamine and without phenol red was used for transfection media (Invitrogen, Inc.).
- Fluorescence detection was done in DMEM maintenance media.
9. Lipofectamine (Invitrogen, Inc).
 10. FuGENE 6 (Roche Molecular Biochemicals).

11. Geneticin (G418): stock solution is 50 mg/ml (Invitrogen, Inc.).
12. Zeocin: stock solution is 100 mg/ml. (Invitrogen, Inc.).
13. Blasticidin: stock solution is 10 mg/ml (Invitrogen, Inc.).
14. Qiaquick PCR purification kit (Qiagen) for purification of DNA fragments for transfection.
15. Hygromycin: stock solution is 50 mg/ml (Invitrogen, Inc)

2.3 Fluorescent microscopy

1. Leica DMRA Fluorescent Microscope.
2. Chroma FITC Filter Set #41001.
3. SPOT Digital Camera (Diagnostic Instruments).
4. SPOT RT Software for image acquisition (Diagnostic Instruments).
5. Dell Dimension 4100 computer.
6. Glass slides, glass coverslips and all other conventional microscopic supplies are used.
7. Crystal/Mount Aqueous/Dry Mounting Medium (Biomeda).

2.4 Fluorescence activated cell sorter

1. FACSCaliber flow cytometer with 488 nm argon laser (Becton Dickinson). The instrument is part of the Duke University Comprehensive Cancer Center fluorescence activated cell sorter shared resource facility (Dr. J. Michael Cook, Director).
2. Standard 530 nm FITC Bandpass Filter.
3. CELLQuest Software was used for fluorescence analysis.

3 Methods

3.1. Cell culture conditions

1. All cell lines are maintained in T75 vented tissue culture flasks (Corning) at 37°C with 5% carbon dioxide in vented cap. Transfections are performed in 6 well plates (Falcon)(see **Note 9**).
2. Cell lines are replaced every 3 months with frozen stocks from liquid nitrogen. Cells are thawed by placing a 1 ml frozen stock in 37°C water bath. The entire 1 ml aliquot is then placed in a T25 tissue culture flask with 5 ml of maintenance media and placed at 37C with 5% carbon dioxide.
3. Cell lines are prepared for liquid nitrogen storage by treating a T75 tissue culture flask with 1.5 ml of trypsin at 37°C until all cells have detached. Trypsinized cells are resuspended with 8.5 ml of DMEM growth media and placed in a sterile 15 ml conical tube and centrifuged at 3,000 rpm for 1 min in a table top clinical centrifuge (International Equipment Company) with a fixed-angle rotor. The supernatant fraction is removed and the cell pellet is resuspended in 3 ml of maintenance media with 10% (v/v) DMSO. 1 ml aliquots are distributed into 1.5 ml cryogenic tubes (Nalgene, Inc). Cells are placed in a freezing chamber (Nalgene, Inc) containing isopropanol at -80°C for 24 hr and then moved to liquid nitrogen.
4. Passage cells once the cell monolayer is confluent. Cells in a T75 flask are treated with trypsin as described above and resuspend by adding 8.5 ml of maintenance media in addition to the 1.5 ml of trypsin. Add 1 ml of the

resuspended cells to a T75 flask already containing 9 ml of maintenance media.

3.2. Transfections with conventional vectors

1. Plate cells in 6 well plates the day before transfection (~ 20 hr before transfection) at a dilution of 3×10^5 cells/well.
2. Linearize plasmids pGInt and derivatives (but not the plasmids containing FRT sites) by digestion with Apa LI at 37° C (see **Note 10**).
3. For transfection, add 5 μ L of lipofectamine reagent to 95 μ L with OPTI-MEM in a 1.5 ml microcentrifuge tube and incubate at room temperature for 2 min.
4. In a separate 1.5 ml microcentrifuge tube bring 1 μ g of linearized plasmid DNA to a total volume of 100 μ L with OPTI-MEM.
5. Mix the 100 μ L of plasmid DNA with the 100 μ L of diluted lipofectamine reagent (both in OPTI-MEM) and incubate at room temperature for 20 min.
6. Add 800 μ L of OPTI-MEM to the 200 μ L plasmid DNA and lipofectamine solution.
7. Wash one well of 6-well plate twice with 2 ml of OPTI-MEM then replace media with 1 ml of lipofectamine reagent and plasmid DNA solution.
8. Incubate for 4 hr at 37° C with 5% carbon dioxide.
9. Replace media with 2 ml of maintenance media and allow cells to recover for 24 hrs at 37° C with 5% carbon dioxide.
10. Replace 2 ml of maintenance media with 2 ml of this media containing a 1:100

dilution of the stock Geneticin antibiotic (500 ug/ml final concentration)

3.2.1. Frt/Flp vectors . **Figure 3** illustrates the overall approach used to integrate the pcDNA5/FRT/TO expression vectors into a single chromosomal FRT site per cell using Flp recombinase. The following steps were used to integrate the pcDNA5/FRT/TO - EGFP series of vectors:

1. The Flp-In T-Rex cells are seeded in T75 tissue culture flasks 1 day prior to transfection so that 24 hrs later (the day of transfection) they will be approximately 75% confluent (see **Note 11**). The total amount of media in the flask was 10 ml (see **Note 12**)
2. For each T75 flask to be transfected, the following transfection mix is made in this order:
 - a. Place 800 μ L of OPTI-MEM into a sterile polystyrene tube.
 - b. Add 48 μ L of FuGENE 6 to the OPTI-MEM below the surface.
 - c. The FuGENE 6 and OPTI-MEM are mixed by flicking the tube five times.
 - d. Add a mixture of 14.4 μ g of pOG44 and 1.6 μ g of pcDNA5/FRT/TO (each expression vector should be done separately) to the tube and flick five more times.
 - e. Allow this mixture to sit for 25 min at room temperature.
 - f. Add the transfection mixture to the flask of Flp-In T-Rex 293 cells, mix thoroughly (see **Note 13**), and place back in the incubator at 37°C, 5% CO₂ for 48 hrs.

3. After allowing the cells to grow for two days, trypsinize each flask and replate into media supplemented with 15 $\mu\text{g/ml}$ blasticidin and 150 $\mu\text{g/ml}$ hygromycin.
4. Allow the cells to grow in this selective media until large colonies of stable transfectants form in the flask. Change the media every three days during this incubation.
5. Trypsinize the flask and then replate into a T75 flask in the same selective media. (see **Note 14**)
6. After sufficient numbers of blasticidin/hygromycin resistant cells were produced, the cells are ready for flow cytometry analysis.

3.3 Fluorescent microscopy

1. Cells are plated at $3 \times 10^5/\text{well}$ in a six well plate, where each well contained a sterile glass coverslip.
2. The following day, remove the media and wash the cells once with 2 ml PBS.
3. In the chemical fume hood, remove the PBS and then add 2 ml of PBS-fix (PBS with 3.7% formaldehyde made fresh) to the wells and then incubate at room temperature for 15 min.
4. Remove the PBS-fix and add 2 ml of 20mM NH_4Cl to quench the formaldehyde.
5. Cells are then washed once more with PBS and then the coverslip is placed onto a conventional glass microscope slides containing one drop of

antifade/sealant (Biomeda).

6. Visualize the cells on a Leica DMRA Fluorescent Microscope using a Chroma FITC Filter Set #41001. Images are acquired using SPOT RT Software (Diagnostics Instruments) and further processed using Photoshop 5.5 (Adobe).

3.4 Fluorescence activated cell sorter

1. Wash stable cell lines within T-25 tissue culture flask with 4 ml of PBS.
2. Add 0.5 ml Trypsin-EDTA and incubate at 37°C with 5% carbon dioxide until cell monolayer is resuspended.
3. Once cells have detached, add 4.5 ml DMEM 10%FBS to inactivate trypsin.
4. Count cells on hemocytometer and dilute to a density of 5×10^5 cells in 500 μL DMEM 10%FBS.
5. Add 500 μL of cells to 5 ml polystyrene round-bottom tube from Falcon for FACS analysis.
6. FACS analysis was performed at the Comprehensive Cancer Center Flow Cytometry shared resource at the Duke University Medical Center.
7. FACS analysis is performed on a Beckon Dickinson FACS Caliber machine with a 488 nm laser.
8. Mean EGFP is the average emission in Relative Fluorescence Units (RFU) of ~10,000 cells that reside within a gated value set at a threshold above background fluorescence.

3.5. Measuring exon IIIb inclusion using pGIIIb plasmids.

The plasmid pEGFPN1 (Clontech), which can drive EGFP expression in both DT3 and AT3 cells, was used to construct the pG family of alternative splicing reporter vectors. Cells transfected with either pEGFP-N1 or pGInt expressed high levels of EGFP as detected by fluorescence microscopy and FACS (**Figure 4A** and data not shown). The high expression of EGFP corresponded to efficient splicing of the intron in pGInt transcripts and we concluded that pGInt could report on the constitutive removal of the pI-12 intron.

We sought to construct plasmids, which could report on regulated splicing events. To this end, we interrupted the intron in pGInt with the rat FGF-R2 exon IIIb and its flanking intronic splicing silencers, the upstream intronic splicing silencer (UISS) and the downstream intronic control element (ICE) ((15) see **Materials** and **Figures 2 & 5A**). If UISS and ICE function properly exon IIIb will be silenced (skipped) and the predominant mature transcript will encode EGFP. If, on the other hand, UISS and/or ICE are compromised, exon IIIb will be included, the EGFP orf will be disrupted and EGFP expression will be diminished. When pGIIIb was stably transfected into DT3 cells, high levels of fluorescence were observed (**Figure 5B**)(see **Note 15**). Deletion of either UISS or ICE, which has been shown to dramatically increase the amount of exon IIIb inclusion (12,15), led to decreased EGFP expression (**Figure 5B**). To confirm the results of fluorescence microscopy, we quantified the levels of EGFP fluorescence by FACS (**Figure 5C**). We directly examined the alternative splicing of the pGIIIb reporters using RT-PCR analysis and demonstrated an excellent correlation between the alternative

splicing pattern and the levels of EGFP fluorescence (**Figure 6**) (see **Note 16**). These data demonstrate the pGIIIb vectors can accurately report on the silencing of exon IIIb.

3.5.1. Advantages of Frt/Flp vectors

Although the pGIIIb vectors were a good first step they suffered from several limitations. First, the level of EGFP expression varied significantly from cell to cell in the selected population. Indeed there was a considerable pool of cells that expressed very low levels of EGFP. Second, the expression of EGFP from pGInt (or pEGFPN1) was much higher for DT3 cells than for AT3 cells (data not shown). In order to correct these problems we decided to transport our reporters into the pcDNA5/FRT/TO plasmid system (see **Section 2.2.2.**). The site specific integration of the splicing reporters into the FRT site in Flp-In T-Rex 293 cells (**Section 2.2.2**) leads to high levels of EGFP expression in the presence of tetracycline and this expression was more homogenous than that obtained with conventional transfection methods (**Figure 7**). Analysis of cells harboring pcDNA5/FRT/TO-GIIIb vectors revealed a twenty-fold decrease in EGFP expression when the UISS and ICE silencer elements were deleted (**Figure 7**). These and other data (not shown) have convinced us that these FRT vectors are superior splicing reporters in living cells. Presently we are constructing DT3 and AT3 cells bearing single FRT sites to carry out a similar analysis in these cell lines.

4.0 Notes

1. The case of FGFR2 alternative splicing may represent a unique case since the most important *cis*-acting elements are localized within the introns. In other cases where exonic splicing enhancers (ESE) or exonic splicing silencers (ESS) are critically important it will be necessary to further engineer the reporter systems.
2. It is important to note that these reporters do not directly assay the splicing of FGF-R2 transcripts but rather report on the activity of *cis*-acting elements of alternative splicing.
3. Currently we are constructing a parallel series of reporters based on firefly and renilla luciferase genes.
4. When working with pEGFPN1 there seems to always be a band at 500 nt that copurifies full length plasmid from maxi/minipreps so uncut vector must be run next to anything that is to be screened for cloning purposes.
5. The specific location at which to divide the coding region of EGFP was chosen based on a division that would result in consensus splice junction sequences. The pI-12 intron was specifically engineered to contain a multiple cloning sites in the center to facilitate the insertion of other exonic and intronic sequences. This intron contains a highly optimized branchpoint and polypyrimidine tract and perfect consensus

matches at both the 5' and 3' splice sites. Sequences encoding amino acids 1-35 of EGFP were PCR amplified using pEGFPN1 as a template and primers 5'GFP-F (5'-CCGGCTCGAGGCCACCATGG TGAGCAAGGG-3') and 5'GFP-R (5'-CCGGGAATTTCGGATCCATACTCACCT CGCCCTCGCCGGAC ACGC-3').

These primers were designed with overhangs such that they generated a product containing an XhoI restriction site at the 5' end and EcoRI and BamHI sites at the 3' end, as well as a consensus-matching 5' splice site. Sequences encoding amino acids 36-239 of EGFP were PCR amplified using pEGFPN1 as a template and primers 3'GFP (5'-CCGGGGGGCCC TTTCCTTTTT TTTCCTCAGG GCGATGCCAC CTACGGCAA-3') and 3'GFP-R (5'-CCGGGCGGCC GCTTTACTTG TACAGCTCGT CC-3'). These primers included overhangs that generated a product containing an ApaI site, polypyrimidine tract, branch point, and 3' splice site ahead of the second half of the EGFP coding region. The multicloning site of the intron of pI-12 (*14*) was inserted between the BamHI site and the ApaI site of the intron generating an intron with a final length of 131 nt.

6. In the absence of tet repressor, the pcDNA5/FRT/TO will behave as CMVp driven mammalian expression vector. In addition, there are other pcDNA5/FRT vectors available that have different features than pcDNA5/FRT/TO (See www.invitrogen.com for additional details).
7. See www.invitrogen.com for more details on the pcDNA5/FRT/TO backbone and its use.

8. The tet inducible system used here is extremely sensitive to the presence of low levels of tetracycline. Therefore, if tight control of the CMVp/2X Tet Op promoter is desired, it is important the FBS used during cell culture lack any tetracycline. We have used two sources of tet-free FBS with good success (Cat. # 8630-1 BD Clontech and Cat.# SH30070.03T, Hyclone, Inc.)
9. Falcon 6 well plates were used for transfection because non-Falcon plates resulted in detachment of AT3 cells following the transfection protocol.
10. Linearization of plasmids at the ApaL1 site probably led to loss of CMV promoter activity in a significant percentage of transfected cells. This may be due to trimming or recombination of the linearized plasmids after transfection into cells.
11. We have found that the degree of confluence of the cells is not critical for these transfections. The transfection efficiency may vary, but hygromycin/blasticidin resistant colonies will be produced at various cell densities. If optimization of stable cell production is critical, then the transfection reagent used and complete transfection protocol should be optimized. This may involve altering the pOG44:pcDNA5FRT/TO ratio during transfection in order to increase the number of stable integrants produced.

12. During transfection, we leave out all antibiotics including blasticidin, zeocin, penicillin, and streptomycin. The presence of antibiotics during transfection can lead to cell death.
13. When dispersing the transfection mixture, use a back and forth motion instead of a rotary motion to avoid piling the FuGENE6/DNA complexes in the middle of the flask.
14. The colonies are dispersed and replated in a smaller flask in order to increase the growth rate of the stably transfected cells.
15. The same results were obtained in AT3 cells. In DT3 cells exon IIIb is silenced in pGIIIb because the cell-type specific activators IAS2 and ISAR are not included in the vector.
16. The fold change in the levels of exon IIIb inclusion for reporters with deletions relative to the pGIIIb is plotted against the fold change in fluorescence as measured by FACS of the reporters with deletions relative to pGIIIb, a correlation could be seen. In fact, the fold changes were identical for the pG Δ UISS and the pG Δ ICE. The pG Δ , Δ fold changes was not in complete agreement although the same trend was observed. The reason for this minor discrepancy is not known but may be due to a competitive advantage for the exon IIIb skipped product in RT-PCR (Wagner et al, manuscript in preparation) or to a lower than expected level of the transcripts that

include the IIIb exon since it is likely subject to nonsense mediated decay (NMD) (18).

Acknowledgements

This work was supported by grants (RO1GM63090 and R21CA97502) to M.A.G-B. E.J.W. was supported by a fellowship from the DOD.

References

1. Claverie, J. M. (2001). Gene number. What if there are only 30,000 human genes? *Science* **291**, 1255-7.
2. Venter, J. C., et al. (2001). The sequence of the human genome. *Science* **291**, 1304-51.
3. Black, D. L. (2000). Protein diversity from alternative splicing: a challenge for bioinformatics and post-genome biology. *Cell* **103**, 367-70.
4. Modrek, B. and Lee, C. (2002). A genomic view of alternative splicing. *Nat. Genet.* **30**, 13-9.
5. Roberts, G. C. and Smith, C. W. (2002). Alternative splicing: combinatorial output from the genome. *Curr. Opin. Chem. Biol.* **6**, 375-83.
6. Del Gatto, F., Plet, A., Gesnel, M. C., Fort, C. and Breathnach, R. (1997). Multiple interdependent sequence elements control splicing of a fibroblast growth factor receptor 2 alternative exon. *Mol. Cell. Biol.* **17**, 5106-16.

7. Del Gatto, F., Gesnel, M. C. and Breathnach, R. (1996). The exon sequence TAGG can inhibit splicing. *Nucl. Acids Res.* **24**, 2017-21.
8. Del Gatto, F. and Breathnach, R. (1995). Exon and intron sequences, respectively, repress and activate splicing of a fibroblast growth factor receptor 2 alternative exon. *Mol. Cell. Biol.* **15**, 4825-34.
9. Del Gatto-Konczak, F., Olive, M., Gesnel, M. C. and Breathnach, R. (1999). hnRNP A1 recruited to an exon in vivo can function as an exon splicing silencer. *Mol. Cell. Biol* **19**, 251-60.
10. Carstens, R. P., Wagner, E. J. and Garcia-Blanco, M. A. (2000). An intronic splicing silencer causes skipping of the IIIb exon of fibroblast growth factor receptor 2 through involvement of polypyrimidine tract binding protein. *Mol. Cell. Biol.* **20**, 7388-400.
11. Carstens, R. P., McKeehan, W. L. and Garcia-Blanco, M. A. (1998). An intronic sequence element mediates both activation and repression of rat fibroblast growth factor receptor 2 pre-mRNA splicing. *Mol. Cell. Biol.* **18**, 2205-17.
12. Carstens, R. P., Eaton, J. V., Krigman, H. R., Walther, P. J. and Garcia-Blanco, M. A. (1997). Alternative splicing of fibroblast growth factor receptor 2 (FGF-R2) in human prostate cancer. *Oncogene* **15**, 3059-65.
13. Wagner, E. J. and Garcia-Blanco, M. A. (2002). RNAi-mediated PTB depletion leads to enhanced exon definition. *Mol. Cell* **10**, 943-9.
14. Wagner, E. J. and Garcia-Blanco, M. A. (2001). Polypyrimidine tract binding protein antagonizes exon definition. *Mol. Cell. Biol.* **21**, 3281-8.

15. Del Gatto-Konczak, F., Bourgeois, C. F., Le Guiner, C., Kister, L., Gesnel, M. C., Stevenin, J. and Breathnach, R. (2000). The RNA-binding protein TIA-1 is a novel mammalian splicing regulator acting through intron sequences adjacent to a 5' splice site. *Mol. Cell. Biol.* **20**, 6287-99.
16. Gilbert, E., Del Gatto, F., Champion-Arnaud, P., Gesnel, M. C. and Breathnach, R. (1993). Control of BEK and K-SAM splice sites in alternative splicing of the fibroblast growth factor receptor 2 pre-mRNA. *Mol. Cell. Biol.* **13**, 5461-8.
17. Jensen, K. B., Dredge, B. K., Stefani, G., Zhong, R., Buckanovich, R. J., Okano, H. J., Yang, Y. Y. and Darnell, R. B. (2000). Nova-1 regulates neuron-specific alternative splicing and is essential for neuronal viability. *Neuron* **25**, 359-71.
18. Jones, R. B., Wang, F., Luo, Y., Yu, C., Jin, C., Suzuki, T., Kan, M. and McKeehan, W. L. (2001). The nonsense-mediated decay pathway and mutually exclusive expression of alternatively spliced FGFR2IIIb and -IIIc mRNAs. *J. Biol. Chem.* **276**, 4158-67.

Figure legends.

Figure 1. A model for the regulation of FGF-R2 alternative splicing. Several factors have been implicated in mediating IIIb silencing; the polypyrimidine tract binding protein (PTB) binds the ISS elements that flank IIIb and silences this exon (15). HnRNP A1 has also been implicated in IIIb silencing. Artificial recruitment of hnRNP A1 protein to IIIb leads to decreased IIIb inclusion (11). IIIb inclusion is likely mediated by an epithelial specific factor, which we posit interacts with and stabilizes a secondary structure predicted to be formed by ISAR-IAS2 base pairing (5,16). Given the overlap between IAS2 and the downstream silencers within ICE, it is likely that the putative ISAR-IAS2 secondary structure perturbs silencer function.

Figure 2. Schematics of EGFP reporters used to image alternative splicing. All constructs represented have the backbone sequence of pEGFPN1 (Clontech, Inc). The pGInt reporter contains an intron derived from pI-12 inserted within the EGFP open reading frame (see materials and methods). The pGIIIb reporter is identical to pGInt with the exception of having FGF-R2 exon IIIb as well as the flanking intronic elements, UISS and ICE, inserted between the BamHI and ApaI sites of the intron (see materials and methods). The pGAUISS, pGAICE, and pGA Δ reporters are identical to pGIIIb with the exception of having either the UISS or the ICE (or both) intronic elements deleted.

Figure 3. The Flp-In T-Rex system (Invitrogen, Inc.) for creating tetracycline-inducible stable cell lines. A cell line is created that contains the pFRT/lacZeo vector integrated at a single chromosomal location and multiple copies of the pcDNA6/TR tet repressor

expression vector. This cell line is then transfected with the pcDNA5/FRT/TO expression vector containing the gene of interest (G.O.I.) and the pOG44 Flp recombinase expression vector. The Flp recombinase catalyzes the recombination of the pcDNA5/FRT/TO vector (through its FRT site) and the chromosomal FRT site, which is part of the integrated pFRT/lacZeo. The integration of the expression vector disrupts the lacZeo fusion gene expression and induces the expression of the hygromycin resistance gene making the stably transfected cells hygromycin resistant. After the stable cells have been allowed to grow as a polyclonal population in the absence of tetracycline, the expression of the G.O.I. can be induced by the addition of tetracycline.

Figure 4. The placement of an intron in EGFP results in complete splicing in vivo and high level of GFP fluorescence. A. DT3 and AT3 cells were transfected with both EGFP vector as well as the newly created pGInt vector and subject to stable selection using geneticin. High levels of fluorescence were seen in both cell lines using either vector. The exposure time for the images presented here has been normalized to the pEGFP fluorescence in DT3 cells and thus may be compared. The increase in GFP fluorescence observed from the intron containing EGFP vector was apparent in this experiment and repeated in subsequent experiments. B. The results of RT-PCR analysis using exonic primers that flank the intron insertion of pGInt. Total splicing of the pI-12 intron was observed in DT3 cells, as well as AT3 cells (not shown).

Figure 5. The pGIIIb reporter plasmids successfully report the splicing regulation of the UISS and the ICE intronic splicing silencers. A. Four splicing reporters were constructed

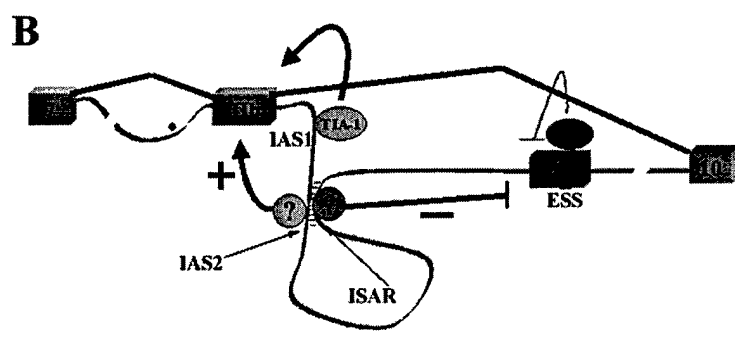
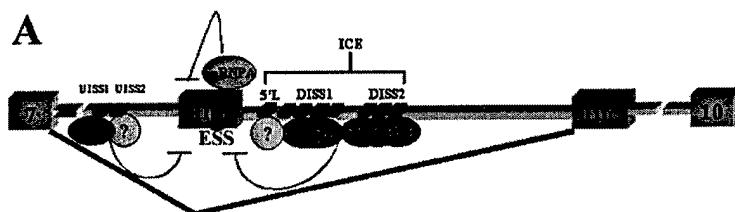
containing various deletions of the intronic splicing silencers located in the UISS or ICE.

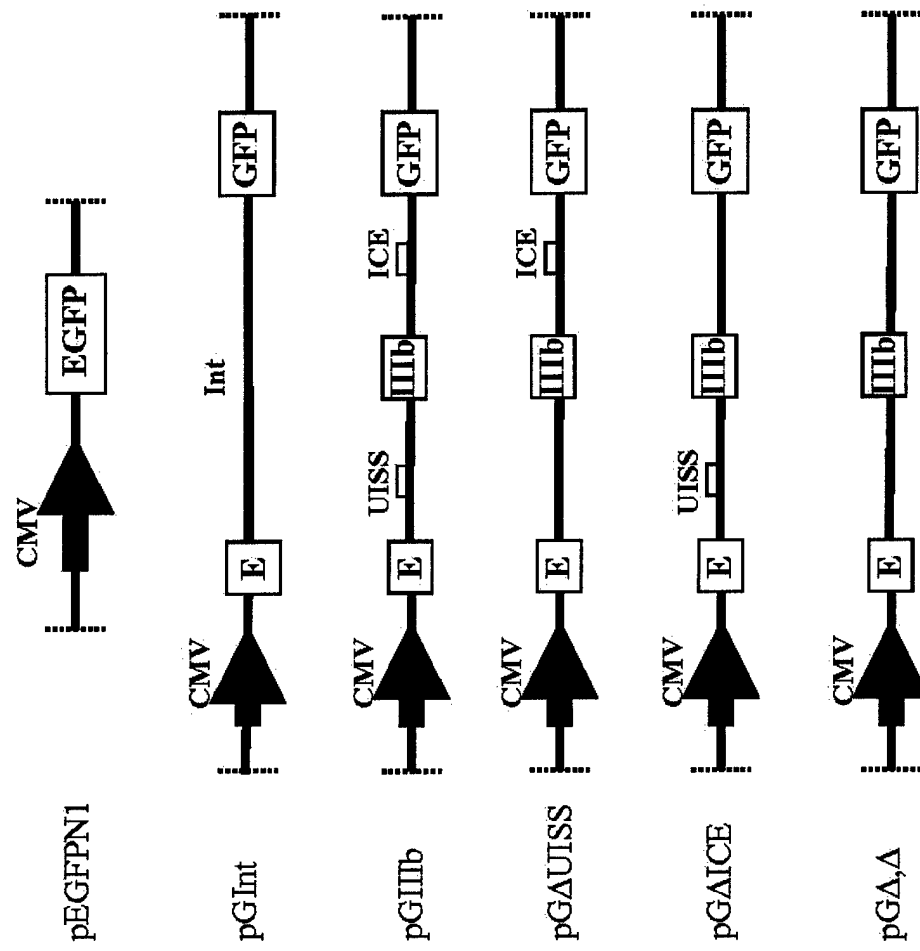
B. These four reporters were transfected into DT3 cells and then were subject to stable selection. The cells were then analyzed for GFP fluorescence. Near identical results were seen with the transfection of AT3 cells (not shown). C. The FACS analysis of the fluorescing cells of panel B quantified GFP levels.

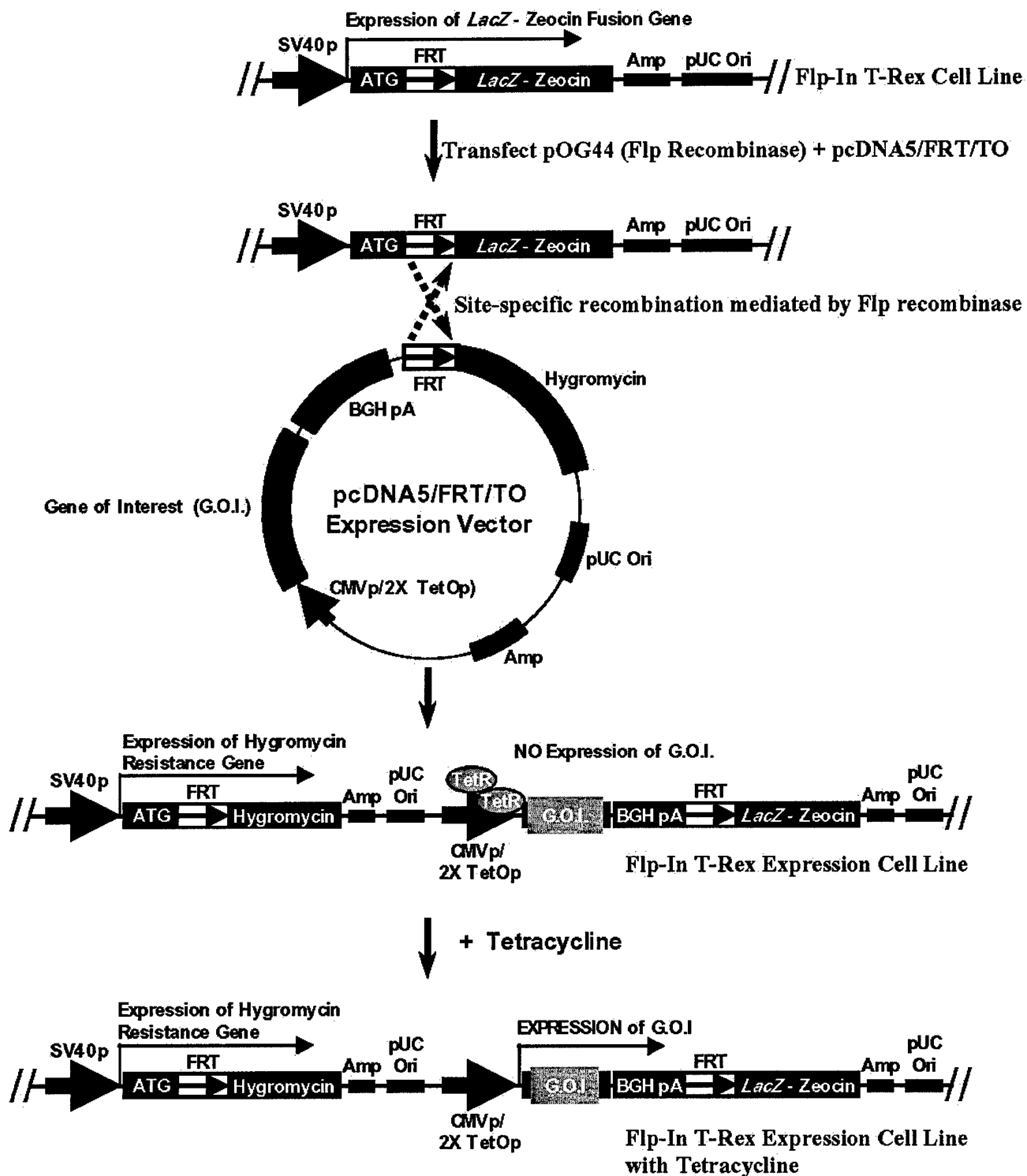
Figure 6. The levels of fluorescence of DT3 cells stably transfected with pGIIIb reporters correlates with the results of RT-PCR analysis of the *in vivo* splicing patterns.

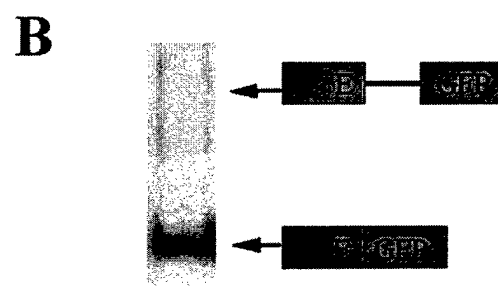
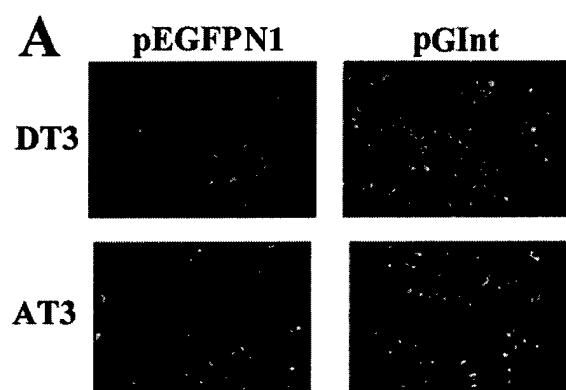
A. The results of RT-PCR analysis using EGFP specific primers demonstrate increased exon IIIb inclusion as the silencer sequences are deleted. B. The fold change in exon IIIb inclusion compared to the pGIIIb is plotted against the fold change in FACS analysis for the same constructs. The fold changes are consistent with each other with the exception of pG $\Delta\Delta$ (see Note 16).

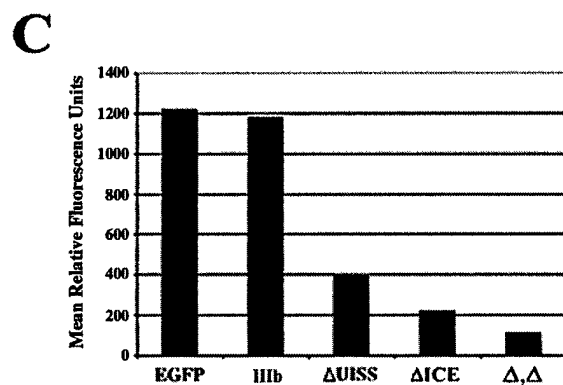
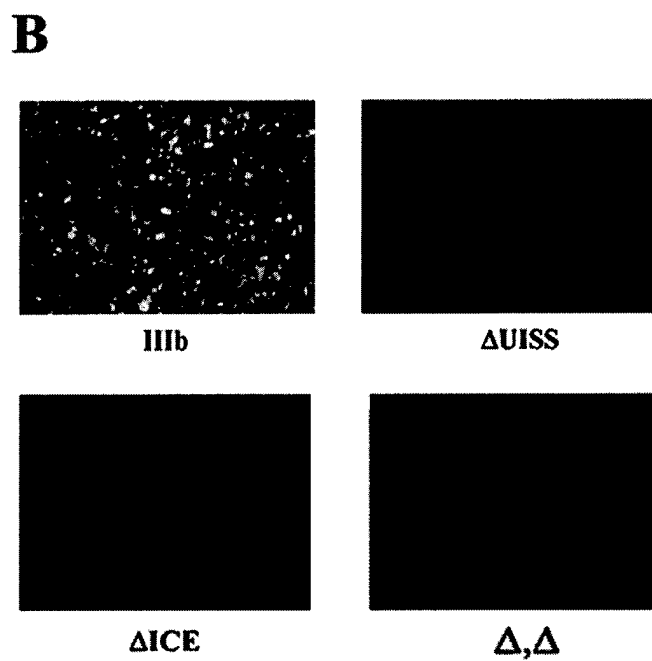
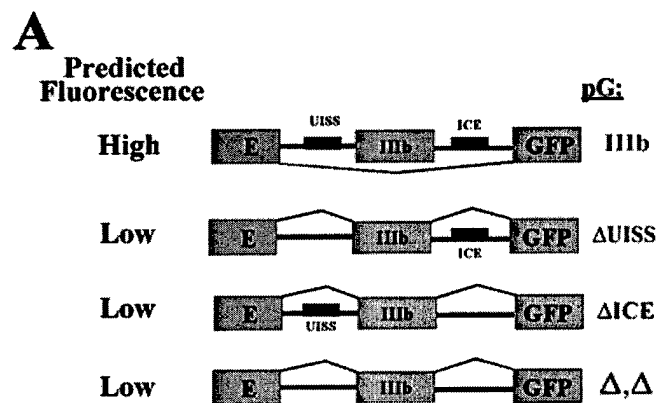
Figure 7. The pcDNA5/FRT/TO-G plasmids provide an efficient and facile system to study silencing of exon IIIb in HEK293 cells. The mean EGFP fluorescence is plotted vs. the HEK293 cells grown in the absence (-) or presence (+) of 12.5 $\mu\text{g/ml}$ tetracycline and harboring the indicated pcDNA5/FRT/TO-G plasmid in the unique genomic FRT site.



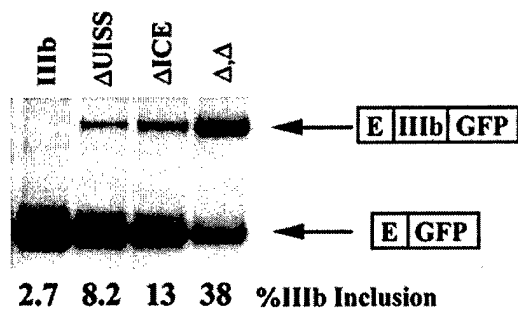




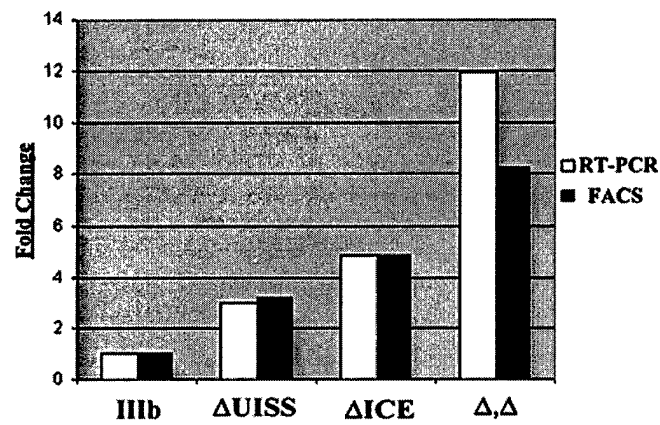




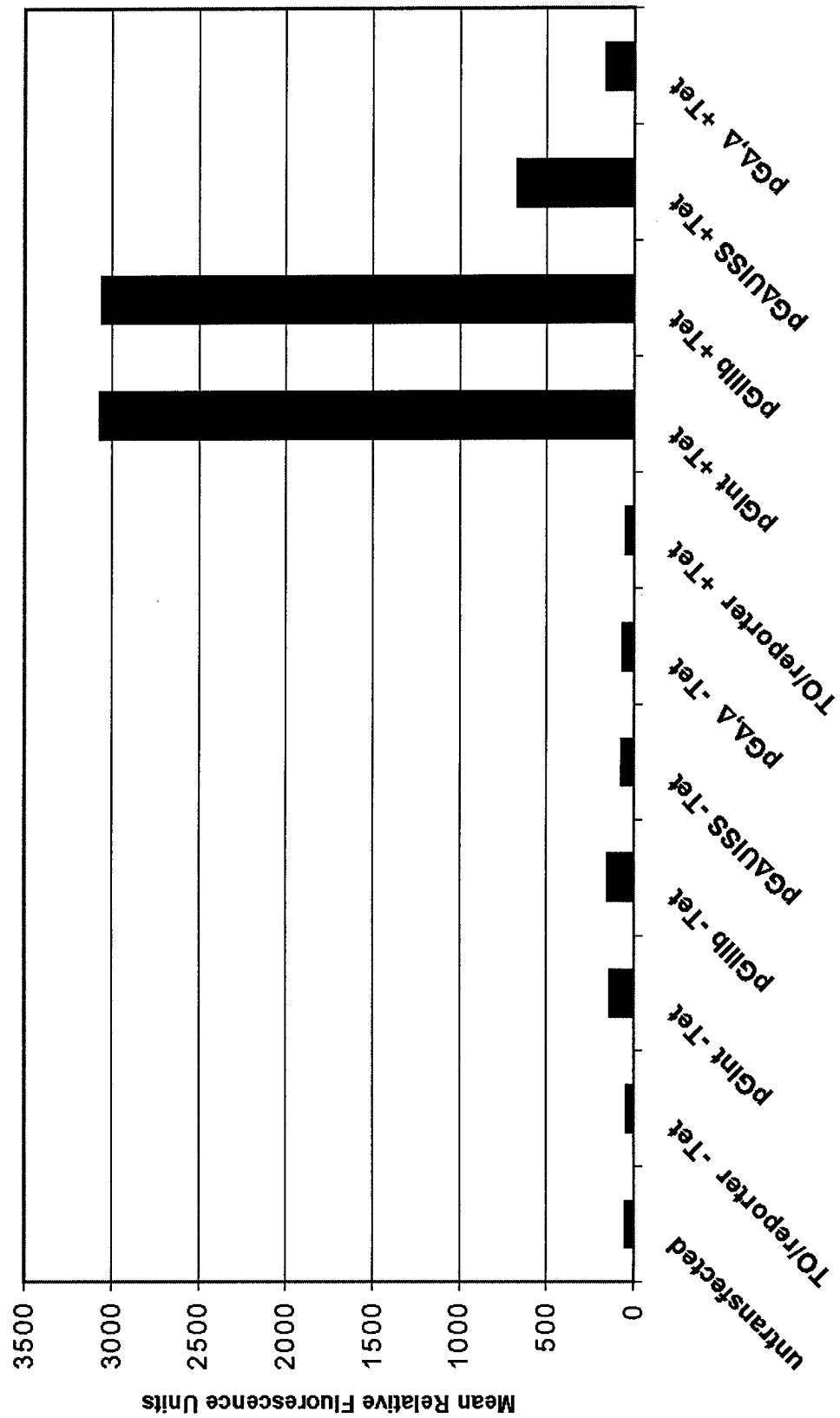
A



B



Stable EGFP transfections in 293 TREX cells



A Stem Structure in FGFR2 Transcripts Mediates Cell-Type Specific Splicing by Approximating Intronic Control Elements

Andrew P. Baraniak^{1,†}, Erika L. Lasda^{1,†}, Eric J. Wagner^{1,3,‡},
Mariano A. Garcia-Blanco^{1,2,*}

¹Department of Molecular Genetics and Microbiology, ²Department of Medicine,
³Program in Molecular Cancer Biology, Duke University Medical Center, Durham, NC,
27710

Running Title: Approximation of intronic control elements activates FGFR2 exon IIIb

Keywords: fibroblast growth factor receptor 2 (FGFR2), alternative splicing, RNA duplex, approximation, intronic control elements

[†] A. P. Baraniak and E. L. Lasda contributed equally to this manuscript

*To whom correspondence should be addressed: Box 3053, Duke University Medical Center, Durham N.C. 27710. Phone (919) 613-8632. Fax (919) 613-8646. Email: garci001@mc.duke.edu

[‡]Current address for E. J. Wagner: Department of Biochemistry and Biophysics, Program in Molecular Biology and Biotechnology, CB# 7100, University of North Carolina, Chapel Hill, North Carolina 27599

ABSTRACT

Alternative splicing of the fibroblast growth factor receptor 2 (FGFR2) occurs in a cell-type specific manner with the mutually exclusive use of exon IIIb or exon IIIc. Specific inclusion of exon IIIb is observed in epithelial cells, whereas exon IIIc inclusion is seen in mesenchymal cells. Epithelial specific activation of exon IIIb and repression of exon IIIc are coordinately regulated by the Intronic Activating Sequence 2 (IAS2) and the Intronic Splicing Activator and Repressor (ISAR) elements in the FGFR2 pre-mRNA. Previously it has been suggested that IAS2 and a 20-nucleotide "core" sequence of ISAR form a stem structure that allows for the proper regulation of FGFR2 alternative splicing. Replacement of IAS2 and ISAR core with random sequences capable of stem formation resulted in the proper activation of exon IIIb and repression of exon IIIc in epithelial cells. Given the high degree of phylogenetic conservation of the IAS2-ISAR core structure and the fact that unrelated stem forming sequences could functionally substitute for IAS2 and ISAR, we postulated that the stem structure facilitated the approximation of intronic control elements. Indeed, deletion of the entire stem-loop region and juxtaposition of sequences immediately upstream of IAS2 with sequences immediately downstream of ISAR core maintained proper cell-type specific inclusion of exon IIIb. These data demonstrate that IAS2 and ISAR core sequences are dispensable for the cell-type specific activation of exon IIIb and thus the major, if not sole, role of the IAS2-ISAR stem is to approximate sequences upstream of IAS2 with sequences downstream of ISAR core. The downstream sequence is very likely a highly conserved GCAUG element, which we show was required for efficient exon IIIb activation.

INTRODUCTION

Fibroblast growth factor receptor 2 (FGFR2) contains a single transmembrane domain, an intracellular tyrosine kinase domain, and an extracellular fibroblast growth factor (FGF) binding domain, which is composed of immunoglobulin-like domains (Ig) II and III. Alternative splicing of FGFR2 transcripts produces two variants of the Ig-III domain with different carboxy-terminal halves, which lead to distinct ligand binding specificity. The two forms of the Ig-III domain are derived from the tissue-specific inclusion of either exon IIIb or exon IIIc (36, 44). FGFR2(IIIb) primarily binds FGF10 and FGF7 and is the isoform of choice in epithelial cells, whereas FGFR2(IIIc) binds FGF2 with high affinity and is predominantly expressed in mesenchyme (36, 51). Proper cell-type specific expression of each isoform is essential for maintaining FGF/FGFR2 signaling that governs epithelial-mesenchymal interactions required for organogenesis in mouse embryos (12, 22). Mutations that alter the ligand specificity of FGFR2(IIIc) or those that lead to inappropriate expression of exon IIIb in mesenchyme have been linked to several developmental syndromes in humans (22, 43, 52). The physiological importance of regulating FGFR2 isoform choice is highlighted further by studies that show a switch from FGFR2(IIIb) to FGFR2(IIIc) during the progression of prostate carcinomas (6, 51).

The mutually exclusive incorporation of exon IIIb or exon IIIc is regulated by the complex interplay of *cis*-acting elements in the FGFR2 pre-mRNA and *trans*-acting factors, some of which appear to be cell-type specific. To study the mechanism of regulation, we have employed two cell lines derived from Dunning rat prostate tumors. The DT3 cell line is a well-differentiated carcinoma and expresses FGFR2(IIIb)

exclusively, whereas the AT3 cell line is poorly differentiated and solely expresses FGFR2(IIIc) (51). Skipping of exon IIIb in AT3 cells is facilitated by the presence of weak splice sites flanking this exon, an exonic silencing sequence (ESS) in exon IIIb, and two intronic silencing elements. The Upstream Intronic Splicing Silencer (UISS) and the Downstream Intronic Splicing Silencer (DISS), which resides within the Intronic Control Element (ICE), flank exon IIIb (8, 14, 20, 50). The ESS functions to recruit hnRNP A1 to exon IIIb thereby repressing its inclusion (17), while UISS and ICE antagonize exon IIIb definition by binding the polypyrimidine tract binding protein (PTB) and other factors yet to be characterized (8, 49, 50). The silencing of exon IIIb is countered in epithelial cells by the action of several *cis*-acting elements. The Intronic Activating Sequence 1 (IAS1), which is located downstream of exon IIIb, serves as a binding site for the splicing factor TIA-1. The binding of TIA-1 to IAS1 has been demonstrated to activate the weak 5' splice site of exon IIIb as well as weak splice sites of other exons (16). The Intronic Activating Sequence 2 (IAS2) is located in the middle of the DISS within the ICE while the Intronic Splicing Activator and Repressor (ISAR, also known as IAS3) is located over 700 nucleotides downstream of IAS2. Both of these cell-type specific elements serve to activate the inclusion of exon IIIb (7, 14, 15). IAS2 and ISAR also function to repress exon IIIc inclusion in a cell-type specific manner (7, 28, Wagner *et al* manuscript submitted). It is believed that IAS2 and a portion of ISAR, hereafter referred to as ISAR core, activate exon IIIb inclusion by creating a stem structure that disrupts the silencing activity of UISS and ICE (15, 28, 40, 49).

We have shown that sequences within IAS2 and ISAR and their potential to form a stem have been highly conserved for over 600 million years (38), suggesting the

importance of structure and perhaps sequence in the activation of exon IIIb inclusion and repression of exon IIIc inclusion. Recently it has been shown that similar stem structures are predicted to form in FGFR1 in several species (40). In addition, it was shown that other sequences capable of stem formation can functionally substitute for IAS2 and ISAR (40).

In this study, we demonstrate that some unrelated stem forming sequences, but not all, can functionally substitute for IAS2 and ISAR core. We also find that the 735 nucleotides separating IAS2 and ISAR core serve no function in the regulation of FGFR2 exon choice. Most importantly, we determine that the major function, if not the only function, of the IAS2-ISAR core stem is to approximate intronic sequences upstream of IAS2 to sequences downstream of ISAR core. Splicing precursors where these sequences have been juxtaposed are capable of recapitulating cell-type specific splicing independent of IAS2 and ISAR core. We also identified sequences downstream of ISAR core that are important for cell-type specific exon IIIb inclusion and exon IIIc repression. Finally, having shown the importance of sequences downstream of ISAR core, we determined that a minimal distance between ISAR and the 3' splice site must be maintained for the proper regulation of exon IIIb inclusion.

MATERIALS AND METHODS

Plasmid Construction. The plasmid DNA constructs used in this study were made using standard cloning techniques described previously (7). The previously described minigenes pI-11 and pI-11 FS (7) are hereafter referred to as pI12 and pI12DE-WT (double exon-*wild type*). To create minigenes containing only exon IIIb, PCR amplification of parental DE constructs with primers INT3BF2 and INT2R2 (7) was followed by digestion with *SpeI* and *XhoI*. The PCR products were cloned back into the *XbaI* and *XhoI* sites of pI-12. To create minigenes containing only exon IIIc, parental DE constructs were digested with *XbaI* and *XhoI* and cloned into pI12. The pI12DE-Rep, -Blue, -Blue(c), and -PyPu splicing constructs were created by digesting pI12DE-ΔIAS2 (Wagner *et al* manuscript submitted) with *ClaI* and performing nondirectional annealed oligo cloning with the following oligos: IAS2 Rep F, IAS2 Rep R, IAS2 Blue F, IAS2 Blue R, IAS2 PyPu F, IAS2 PyPu R. To create pI12DE-Blue Blue, -Blue Blue(c), -Blue(c) Blue, -Blue(c) Blue(c), -PyPu, and -PyPuΔBulge, a portion of the plasmids containing substitutions in IAS2 were subcloned into pBluescript (Stratagene) using *XbaI* and *XhoI*. These plasmids were then digested with *NdeI* and *NsiI* to remove ISAR, and annealed oligo cloning was performed to replace ISAR core, within the *wt* ISAR sequence, with the following oligos: ISAR Blue F, ISAR Blue R, ISAR Blue(c) F, ISAR Blue(c) R, ISAR PyPu F, ISAR PyPu R, ISAR PyPu ΔBulge F, ISAR PyPu ΔBulge R. The FGFR2 sequence cloned into pBluescript was then subcloned back into pI12DE-WT digested with *XbaI* and *XhoI*. To create the following minigenes, the *XbaI/XhoI* fragment of pI12DE-WT was subcloned into pBluescript (Stratagene) and then subjected to QuikChange mutagenesis (Stratagene): pI12DE-ΔU, -ΔG, -+G, -ΔBulge, -C5, -C10, -

C15, -C20, -C25, -C30, -C11, -C13, -C14, and -C16. To create pI12DE-ΔLP, PCR amplification of pI12DE-WT with the following primer sets, INT3BF2 with IAS2-cla-R and INT3CR (7) with HinP1I-ISAR-F, was followed by digestion with *SpeI/ClaI* and *XhoI/HinP1I*, respectively. The PCR products were sequentially cloned into pI12 digested with *XbaI* and *ClaI*, then *ClaI* and *XhoI*. The minigenes pI12IIIb-ΔISARΔ193, -+ISARΔ193, and -ISAR+58 were obtained through PCR amplification using the primer INT3BF2 with the following primers: ΔISARΔ193 R, +ISARΔ193 R, and ISAR+58 R, respectively. The PCR products were digested with *SpeI* and *XhoI* and cloned into pI12 digested with *XbaI* and *XhoI*. To create pI12IIIb-ISAR BS1 and pI12IIIb-ISAR BS2, PCR amplification of pBluescript (Stratagene) using the primer sets BS 100 F and BS 293 R and BS 1500 F and BS 1693 R was followed by digestion of the PCR products with *XhoI*. The digested PCR products were cloned into pI-12 +ISAR Δ193 IIIb digested with *XhoI*. pI12DE-ΔSTLP was cloned by PCR amplification of pI12DE-WT with the following primer sets, INT3BF2 with del-stem-loop-R and del-stem-loop-F with INT3CR (7), followed by digestion with *SpeI/ClaI* and *BsmBI/XhoI* respectively. The PCR products were sequentially cloned into pI12 digested with *XbaI/ClaI* and then *BsmBI/XhoI*. All constructs utilizing PCR amplification were sequenced for verification. All oligo sequences will be provided upon request.

Cell Culture and Transfection. AT3 and DT3 cells were maintained in Dulbecco's modified essential media (low glucose) supplemented with 10% fetal bovine serum (Hyclone). Stable transfections were performed as previously described (7) with one exception, after trypsinization, the cells were reseeded in 25-cm² flasks containing 500 μg/mL of Geneticin (Gibco) for selection of stable cell populations.

RNA Isolation and RT-PCR assay of transfected minigenes. Cellular RNA for RT-PCR and the Invader® RNA assay was isolated using the method of Chomczynski and Sacchi (10) or Trizol (Invitrogen). RT-PCR reactions using T7 and SP6 primers were performed as previously described (7). PCR products were either loaded directly onto 5% nondenaturing acrylamide gels or added to restriction digests with either *Ava*I or *Hinc*II (New England Biolabs). Analysis and quantification of PCR products from double exon digests was performed as previously described (8). Analysis and quantification of PCR products from single exon constructs (IIIb or IIIc) was performed in the following manner. Phosphoimager quantification of single inclusion (U-IIIb-D or U-IIIc-D) and skipped bands (U-D) was performed with ImageQuant. A ratio of included to skipped products was calculated by dividing single inclusion by the sum of single inclusion plus molar equivalents of the skipped product. The formula for IIIb inclusion is: $\text{IIIb inc.}/(\text{IIIb inc.} + (1.6 * \text{skipped product}))$.

Invader® RNA assay. The Invader® RNA assay (Third Wave Technologies, Madison, WI) was carried out essentially as described by Eis *et al* (18) except 1uM Probe was used for all probe sets and 0.25 uM of Invader® oligonucleotides were used for the IIIb-IIIc and U-IIIc probe sets as described in Wagner *et al* (Wagner *et al* manuscript submitted). To analyze all splice variants for double exon transfected minigenes, the Invader® RNA assays were run in the biplex format using the following probe set combinations: IIIb-D/U-D and IIIb-IIIc/U-IIIc as previously described (Wagner *et al* manuscript submitted). To analyze splice variants for single exon transfected minigenes, the Invader® RNA assays were run in the biplex format using the following probe set combinations: IIIb-D/U-D and IIIc-D/U-D. Different concentrations of each RNA splice

variant were used to calculate a standard graph comparing attomoles of RNA to fluorescence. From the fluorescence readings, absolute levels of each splice variant were calculated. The data for single inclusion events are presented as the following percentages: $(IIIb/(IIIb + IIIc)) \times 100$ or $(IIIc/(IIIb + IIIc)) \times 100$. When calculating percentage of double inclusion we use the following formula: $((IIIb \cdot IIIc)/(IIIb \cdot IIIc + IIIb + IIIc + \text{skipped})) \times 100$.

RNA Structure Probing. An 84 nucleotide RNA that included the *R. norvegicus* IAS2 and ISAR core sequences (bold) separated by a six nucleotide loop (underlined) (5'-GGGAGAAGAGAAU**UCAUGGAAAAAUGCCCACAA**AUGCUCUGUGGGCU**GAUUUUUCCAUGCU**AGAGUCGACCUGCAGGCAUGCAUA-3') was synthesized using T7 RNA polymerase as described previously (11). Structure probing by limiting digestion with RNase A and RNase T1 followed by primer extension with a 5'end-radiolabeled oligonucleotide (5'-tgc~~at~~gcctgcagg~~tc~~-3') was performed as described in Mistry et al (38).

RESULTS

Non-sequence specific RNA structure mediates proper splicing regulation in DT3 cells

Compensatory mutations in IAS2 and ISAR core elements, which partially rescue function, as well as phylogenetic data strongly suggest that a stem-like structure forms between IAS2 and ISAR core (15, 28, 38, 40). In order to provide physical evidence for the predicted structure, we synthesized an RNA molecule containing the rat IAS2 and ISAR core sequences and probed its structure *in vitro* (11). After partial digestion by RNase T1, which cleaves after single stranded guanosine residues, or RNase A, which cleaves preferentially after single stranded uridine residues, we mapped cleavage sites with primer extension. Residues in the predicted stem-forming IAS2 and ISAR core sequences were protected from digestion, whereas, residues in the predicted GU bulge and the loop were cleaved (Fig. 1A). Both structure probing and phylogeny suggest a stem structure divided into three parts: a proximal stem, a 2-nucleotide bulge, and a distal stem (Fig. 1A).

The primary sequence of the proximal stem has been conserved from mammals to *S. purpuratus*; of particular interest is the stretch of adenosines and uridines in IAS2 and ISAR, respectively (38). Also conserved is a predicted two nucleotide bulge that was shown above to form in the rat stem structure. Although the presence of the bulge has been maintained throughout evolution, the nucleotide content of the bulge has varied, as has the primary sequence of the distal portion of the stem. These observations led us to question whether both sequence of the proximal stem and overall structure were critical for the proper regulation of FGFR2. In order to test the importance of sequence

composition, we made several minigene constructs shown in Figure 1B. Two of these minigenes (pI12DE-Blue Blue(c) and -Blue(c) Blue) have the capacity to form a stem containing a two nucleotide bulge, while the other two minigenes (-Blue Blue and -Blue(c) Blue(c)) cannot (Fig 1B and 1C). These minigenes were transfected into DT3 and AT3 cells, and RNA from stably transfected cell populations was analyzed by RT-PCR or the Invader[®] RNA assay (18, Wagner *et al* manuscript submitted). The transfections into AT3 cells were performed to control for any effect on the silencing of exon IIIb, which is mediated by silencing elements flanking IAS2. Alterations of IAS2 and ISAR were not expected to affect IIIc inclusion in AT3 cells, and indeed we observed nearly exclusive use of exon IIIc with each minigene tested (data not shown). In DT3 cells transfected with pI12DE-Blue Blue(c) and -Blue(c) Blue, we observed 80% and 76% exon IIIb inclusion respectively (Fig 1D). These heterologous stems allowed for even greater exon IIIb inclusion than pI12DE-Rep (80% and 76% compared to 61%), which contains the authentic IAS2 and ISAR core sequences (Fig 1C and 1D). The constructs that could not form a stem lost the ability to include exon IIIb compared to pI12DE-Rep. To determine if the different stem structures were separately involved in activating exon IIIb and repressing exon IIIc, we made minigenes that contained only exon IIIb or exon IIIc as the internal exon (7). These single exon constructs revealed stem formation in epithelial cells activated exon IIIb inclusion and repressed exon IIIc inclusion (data not shown). These data and the recent report of Muh et al (40) suggested that the replacement of IAS2 and ISAR core with presumably unrelated complementary sequences could elicit cell-type specific regulation of exon IIIb inclusion.

We noticed; however, that all functional stems, including those reported in Muh et al (40), contained stretches of purines in one strand and complementary pyrimidines on the other (Fig 1C). Indeed, a stretch of five adenosines and two guanosines in IAS2 and a stretch of five uridines and two cytosines are highly conserved in vertebrates (38). To test whether a stretch of purines and a complementary track of pyrimidines were important, we generated pI12DE-PyPu, which contains alternating pyrimidines and purines in the stem structure (Fig 1B and 1C). When this construct was transfected into AT3 cells, almost exclusive use of exon IIIc was observed (data not shown). When this construct was transfected into DT3 cells, pI12DE-PyPu included exon IIIb 40% of the time, which is slightly lower than the 61% IIIb inclusion observed with pI12DE-Rep (Fig 1D). This result suggested the stretches of purines and pyrimidines, while not critical, may influence the proper regulation of FGFR2 alternative splicing (see below). Combined with the results discussed above and the recent findings of Muh et al (40), we conclude that many different stems can substitute for IAS2 and ISAR core; however, clearly not all stems regulate exon choice equally.

Deletion of the two-nucleotide bulge has no effect on FGFR2 splicing regulation

Bulges in RNA secondary structures tend to function by providing unique recognition sites for protein interactions, either by creating a specific RNA topography for protein binding in an otherwise helical structure, or by kinking the RNA backbone allowing access for protein recognition (24). In the case of the human immunodeficiency virus type 1 (HIV-1) *trans*-activation response element (TAR) RNA stem structure, a tri-

nucleotide bulge serves as a docking site for the binding of Tat. Mutating the bulge destroys the ability for the RNA to bind Tat (45, 46).

Given that both the *in vitro* structure probing and phylogenetic data indicated the presence of a two-nucleotide bulge, we wanted to determine if mutating the bulge would affect exon choice. To that end, we created pI12DE-PyPu Δ Bulge, which contains the same stem as pI12DE-PyPu with a deletion of the bulge (Fig 1B and 1C). When this minigene was transfected into AT3 cells, exon IIIc was included almost exclusively (data not shown). Interestingly, when pI12DE-PyPu Δ Bulge was transfected into DT3 cells, it gave 69% IIIb inclusion, which is higher than the 40% and 61% IIIb inclusion observed with pI12 PyPu and pI12 Rep, respectively (Fig 1D). This result demonstrates that the presence of a two-nucleotide bulge is not necessary for IIIb activation; indeed the presence of this bulge decreased exon IIIb inclusion in the context of the PyPu stem. Moreover, given that pI12DE-PyPu Δ Bulge lacks any stretches of pyrimidines and purines, these data argue against any role for the conserved sequence composition in the proximal stem of the IAS2-ISAR core structure.

In order to analyze the function of the GU bulge in the authentic stem formed between IAS2 and ISAR core (Fig 1A), we created pI12DE- Δ U, which contains a deletion of the U, - Δ G, which contains a deletion of the G, -+G, which adds an extra G to the bulge, and - Δ Bulge, which deletes the bulge entirely (Fig 1E). These minigenes were transfected into AT3 and DT3 cells, and RNA from stable cell populations was pooled and analyzed by RT-PCR and the Invader[®] RNA assay. All of the minigenes transfected into AT3 cells resulted in the nearly exclusive use of exon IIIc (data not shown). None of the minigenes tested in DT3 cells resulted in a significant decrease in exon IIIb inclusion

(Fig 1E). All the constructs tested included exon IIIb in greater than 80% of all single inclusion splicing events. These results were confirmed with the Invader® RNA assay (data not shown), demonstrating that the bulge has no apparent function in the proper regulation of exon choice.

A six nucleotide loop is sufficient to mediate proper regulation of FGFR2 splicing

The IAS2-ISAR core structure contains a 735-nucleotide loop. If loop sequences were to contribute to function, deletion of the loop would be predicted to impact splicing regulation. A previously reported loop deletion construct, which resulted in a 126-base pair loop, was shown to have no affect on FGFR2 exon choice (7). Moreover, it was recently shown that a deletion of the majority of the loop sequence between IAS2 and ISAR core resulted in the proper epithelial specific inclusion of exon IIIb (40); however, in this study the minimal spacer region between IAS2 and ISAR was not determined. To test the importance of these sequences, we created a minigene with a six-nucleotide loop (Fig. 2A). The six-nucleotide loop minigene (pI12DE-ΔLP) deleted the entire loop region between IAS2 and ISAR core with the exception of two nucleotides downstream of IAS2, three nucleotides of unrelated spacer sequence and one nucleotide upstream of ISAR core. Transcripts from this minigene included exon IIIc almost exclusively in AT3 cells and predominantly included exon IIIb in DT3 cells (Fig. 2B). Remarkably, pI12DE-ΔLP was more tightly regulated than the wild type minigene as exon IIIb was included in 92% of all single exon inclusion events in DT3 cells compared to 83% for pI12DE-WT, and exon IIIc was included 98.5 % of the time in AT3 cells compared to 93% for pI12DE-WT (Fig. 2B). Analysis of all possible splicing events further suggested tight

regulation of pI12DE- Δ LP, as double inclusion (transcripts that include both IIIb and IIIc) decreased from 28% for pI12DE-WT to 18% with pI12DE- Δ LP (not shown). This suggests that the decreased loop length allowed for greater repression of exon IIIc in epithelial cells, perhaps because smaller loops may facilitate stem formation. These results demonstrated that the loop was not essential for proper splicing regulation in either cell line.

Stem formation functions to approximate sequences upstream of IAS2 and downstream of ISAR core

The data presented above and data previously published by Muh et al (40) show that both the IAS2-ISAR core structure and the loop sequences between IAS2 and ISAR core can be replaced with heterologous stem-loop structures. How does this non-sequence specific structure mediate cell-type restricted activation of exon IIIb and repression of exon IIIc?

Two general scenarios provide an answer to this question. In the first scenario the RNA duplex must be recognized by cell-type specific *trans*-acting factors that control exon choice. These *trans*-acting factors would bind the stem without sequence specificity, which would be provided by neighboring *cis*-elements. In a second scenario the RNA duplex need not be recognized but rather functions by approximation of sequences.

Given that many and diverse stems can substitute for the IAS2-ISAR core structure, we favored approximation as the operative mechanism. In order to distinguish between the above scenarios we created a minigene that deleted IAS2, the loop sequence, and ISAR core (pI12DE- Δ STLP in Fig 3A). The deletion in - Δ STLP transcripts was designed to mimic the approximation of sequences caused by the IAS2-ISAR core stem. RT-PCR

and the Invader[®] RNA assay revealed that Δ STLP transcripts predominantly included exon IIIb in DT3 cells (70%) and almost exclusively exon IIIc in AT3 cells (Fig 3B and data not shown). Cell-type specific exon choice was achieved even though this construct lacked IAS2, ISAR core or any RNA stem. The fact that Δ STLP transcripts included predominantly IIIc in AT3 cells strongly suggests that exon IIIb was not globally activated by intron shortening or by unintended disruption of intronic silencer elements upstream of the deletion. These results ruled out the first scenario, in which dsRNA binding *trans*-acting factors are required for exon choice and demonstrated that approximating sequences upstream of IAS2 to sequences downstream of ISAR core was sufficient for splicing regulation. We concluded that approximation of elements upstream of IAS2 and downstream of ISAR allowed for epithelial-specific inclusion of exon IIIb and mesenchymal-specific inclusion of exon IIIc. Therefore a major function, possibly the only function, of the IAS2-ISAR stem is to approximate the sequences upstream of IAS2 and downstream of ISAR core.

Although approximation was sufficient for exon IIIb activation in DT3 cells, it may not have been sufficient for complete exon IIIc repression. We noted that double inclusion products increased from 20% of all spliced products for pI12DE-WT to 45% for pI12DE- Δ STLP (data not shown). These data suggest that although exon IIIb inclusion was not significantly affected by the deletion of the stem-loop structure, this structure may be independently required for complete exon IIIc repression in epithelial cells.

Sequences downstream of the ISAR core are important for regulating exon IIIb inclusion in DT3 cells

Downstream of ISAR core we had observed high conservation of sequence from echinoderms to mammals (38). Understanding that strong sequence conservation within introns can be a good predictor of important *cis* elements, we performed a mutational analysis of the sequence downstream of ISAR core. Initially we created six minigenes, which contained five-nucleotide substitutions sequentially positioned downstream of ISAR core (Fig 4A). These minigenes were transfected into DT3 cells, and the isolated RNA from stable cell populations was analyzed by RT-PCR. The C5, C25, and C30 mutations (in nucleotides 1-5, 21-25, and 26-30 downstream of ISAR core) had no effect on exon IIIb inclusion compared to wild type levels, and the C10 and C20 mutations (in nucleotides 6-10 and 16-20) had a slight decrease in exon IIIb inclusion compared to the wild type. When nucleotides 11-15 were mutated in the C15 construct, exon IIIb levels dropped from 85% to 51% (Fig 4B), suggesting that these nucleotides play a key role in exon IIIb inclusion and IIIc repression in DT3 cells. To determine if these nucleotides were separately involved in activating exon IIIb and repressing exon IIIc, we created single exon IIIb and single exon IIIc minigenes and transfected them into the DT3 cell line. This analysis demonstrated that the primary effect of mutating these nucleotides is to lower IIIb inclusion from 60% to 36%; moreover, the C15 mutation also allowed a slight increase from 21% to 32% exon IIIc inclusion in DT3 cells (data not shown). These results suggest that an important *cis* element is located 11-15 nucleotides downstream of ISAR core, and its effect is more critical for exon IIIb inclusion than for exon IIIc repression. This region contains the sequence GCAUGCAUG, which has two

overlapping GCAUG motifs and the C15 mutation is the only one to destroy both GCAUG copies. These GCAUG motifs could be intronic control elements downstream of ISAR core that are approximated by the IAS2-ISAR core RNA duplex.

Spacing between ISAR and the downstream exon is required for proper inclusion of exon IIIb in DT3 cells

Having found the GCAUG element downstream of ISAR core, we sought to determine if there were other important *cis*-elements further downstream of ISAR. We created the following single exon IIIb minigenes: Δ ISAR Δ 193, which deletes ISAR and 193 nucleotides downstream; +ISAR Δ 193, which restores ISAR to the *Nsi*I site; and ISAR +58, which restores ISAR and 58 base pairs of wild type FGFR2 sequence downstream of ISAR (Fig 5A). We transfected these minigenes into DT3 cells and pooled the RNA from stable cell populations. As expected, the deletion of ISAR and everything downstream of ISAR caused a decrease in levels of exon IIIb inclusion from 60% to 20% as analyzed by RT-PCR (Fig 5A). When just ISAR was restored, levels of IIIb inclusion increased slightly to 23%; however, when ISAR and 58 bases of FGFR2 sequence downstream of ISAR were restored, levels of IIIb inclusion approached that of the wild type (Fig 5A). Results were confirmed with the Invader[®] RNA assay (data not shown). We also performed scanning mutagenesis downstream of ISAR targeting areas of sequence conservation. Eight different 5-base pair mutations were made in double exon, single exon IIIb and single exon IIIc constructs. When the constructs were transfected in DT3 cells, none of the eight mutations had a significant affect on activation of exon IIIb inclusion or repression of exon IIIc inclusion (data not shown).

Since none of the five-nucleotide substitutions significantly affected levels of exon IIIb inclusion, we postulated that perhaps spacing rather than specific sequences governed the amount of exon IIIb inclusion. To address that idea, we created pI2IIIb-ISAR BS1 and ISAR BS2, which contained 193 nucleotides cloned from different portions of pBluescript (Stratagene) (Fig 5B). These mutants were transfected into DT3 cells along with a wild type and +ISAR Δ 193 construct. RT-PCR analysis demonstrated that substituting the random sequence downstream of ISAR nearly recovered wild type activity for exon IIIb inclusion (Fig 5B). These results suggest that distance between ISAR and the downstream exon, rather than specific sequences, is important for proper inclusion of exon IIIb in DT3 cells.

DISCUSSION

Proper exon IIIb or exon IIIc choice in FGFR2 transcripts depends on basepairing between IAS2 and ISAR core sequences (15), as revealed by compensatory mutations (15, 28) and phylogenetic analysis (38, 40). The latter revealed remarkable conservation of the IAS2-ISAR core secondary structure between echinoderms and mammals, whose common ancestor was last extant 600 million years ago (38). Perhaps equally impressive was the conservation of sequence noted for the proximal stem of the IAS2-ISAR core structure (Ibid) (Fig. 1A). Although at first glance this could be taken as evidence for the importance of the primary sequence, the specific nucleotides conserved, GAAAAAU(U) in IAS2 and AUUUUU(U) in ISAR core, hint otherwise. The conserved tracts, A₅ in IAS2 and U₅ in ISAR core, could be the result of evolutionary drift secondary to the lower mutability of A and T vs. G and C, as has been observed in human pseudogenes

(21). Indeed, the results obtained with the PyPu Δ Bulge transcript (above), which although fully functional does not have a tract of purines basepaired to a tract of pyrimidines, demonstrate that structure and not sequence was important. Yet, not all stem structures provided equal regulation. Even though we cannot categorically explain these differences between RNA structures, their relative stability, as calculated from the predicted ΔG (Fig 1C), correlated well with activation of exon IIIb inclusion (see discussion of Brown et al. below). Thus we conclude, in agreement with Muh et al (40), that base pairing between IAS2 and ISAR core, rather than the unique sequences of these elements, is critical for regulation of FGFR2 alternative splicing.

Secondary structures have been proposed to act as *cis*-elements and their action can be exerted in multiple ways. RNA duplexes can be recognized, usually in a sequence-independent fashion, by double stranded RNA binding proteins (ds RNA BPs) (19, 47). Specificity can be provided by direct or indirect interactions to neighboring *cis*-acting elements or single stranded regions within the structures (30). RNA duplexes can also either occlude or favorably display other *cis*-acting elements (2, 3, 41). Finally RNA duplexes can approximate otherwise distant *cis*-elements. In this manuscript we show that the major, if not the sole, function of the IAS2-ISAR core structure is to approximate elements upstream of IAS2 to elements downstream of the ISAR core. To properly mimic the propinquity mediated by the IAS2-ISAR core structure we deleted all the sequences from the 5' end of IAS2 to the 3' end of ISAR core, inclusive, in the plasmid of Δ STLP. Δ STLP transcripts included predominantly exon IIIb in DT3 cells and almost exclusively exon IIIc in AT3, which indicated correct regulation in the absence of IAS2, ISAR core and the structure they form. Therefore, we conclude that the IAS2-ISAR core

structure works by bringing together other elements. We should note that a previous approximation that did not precisely mimic IAS2-ISAR core stem formation did not promote exon IIIb inclusion in epithelial cells (15). Approximation of *cis*-elements by RNA secondary structures has precedent in pre-mRNA processing. The elaborate RexRE structure promotes polyadenylation of HTLV-1 transcripts by approximating two required elements, the canonical AAUAAA hexanucleotide and the downstream G/U element, which in the primary sequence lie hundreds of nucleotides away (1). Brown et al (4) showed that many RNA secondary structures can substitute for the RexRE to activate polyadenylation in this context and suggested that the strength of the basepairing interaction and the spatial distance between the approximated elements were critical for activity. RNA duplexes have also been shown to enhance splice site pairing in single intron transcripts (9, 31, 42) and exon inclusion in two intron transcripts in yeast (25). In these cases the proximity of sequences presumably enhances the interactions between splicing complexes assembled at the ends of introns. Here we report a case of duplex-mediated approximation of intronic control elements in FGFR2 transcripts, a first for cell-type specific regulatory sequences.

Even though several questions remain about how approximation leads to exon IIIb activation in epithelial cells, parsimony suggests that the IAS2-ISAR core stem exists in both epithelium and mesenchyme, but only in the former are the approximated sequences recognized by epithelial specific factors.. The identity of the approximated sequences has not been unambiguously ascertained; however, data shown above and prior work suggest likely candidates. In this manuscript, we show that exon IIIb activation requires nucleotides 11-15 downstream of ISAR core. These nucleotides are found within the

sequence (+10) GCAUGCAUG (+18), which contains two repeats of the previously characterized intronic activating sequence, GCAUG (5, 13, 23, 26, 29, 32, 39). This *cis*-element has been shown to interact with several *trans*-acting factors and is believed to counteract the action of splicing repressors, such as PTB (27, 33, 37). Thus it is likely that the GCAUG containing element is the relevant sequence downstream of ISAR core. Our previous work suggests that the pertinent sequence upstream of IAS2 is the intronic splicing silencer (ISS) immediately upstream of IAS2 (50). The juxtaposition of the GCAUG element to the ISS, which binds PTB, must be required to counteract the silencer and mediate inclusion of exon IIIb in epithelial cells.

Although our data indicate that cell-type specific factor(s) that control(s) exon IIIb inclusion need not interact with IAS2-ISAR core sequences, it should be noted, however, that approximation does not fully restore repression of exon IIIc in epithelial cells. Careful quantification of exon IIIc (single inclusion) and exons IIIb and IIIc (double inclusion) transcript levels by the Invader[®] RNA assay demonstrated reproducibly higher levels of exon IIIc inclusion in Δ STLP transcripts than in WT transcripts. While it is possible that the topology of the Δ STLP transcripts does not fully reproduce the approximation created by the IAS2-ISAR core structure, it is also conceivable that the IAS2-ISAR core structure plays a direct, albeit minor, role in repressing exon IIIc in epithelial cells. One could envision an exon IIIc repressor that interacts with the IAS2-ISAR core and also with adjacent single stranded RNA *cis*-elements. This could be similar to the interactions observed between the Sm protein heterohexamer and multiple sites within U snRNAS (35).

The tissue specific use of exon IIIb appears to be regulated by the superimposition of three layers of control (Fig. 6). The first layer is determined by the weak splice sites bordering exon IIIb (e.g., 5' splice site is GUAACA instead of the canonical GURAGU) and leads to poor exon definition. The second layer is provided by dual ISSs, upstream and downstream of exon IIIb, which mediate their action via PTB and other unidentified repressors. Whereas exon IIIb silencing is dominant in fibroblasts, all the required factors for silencing are also present in epithelial cells. In these cells, however, a cell-type specific third layer that requires the IAS2-ISAR core structure activates exon IIIb. We propose that exon IIIb activation is carried out by approximation of the GCAUG element to the neighborhood of the ISS. Only in epithelial cells is this element active, very likely because of the differential expression of factors that recognize the GCAUG element. The coordinated repression of exon IIIc requires an overlapping but not identical set of elements and factors.

It is not surprising that tissue-specific regulation of alternative splicing requires multiple layers each integrating the action of multiple factors. Much has already been discussed about the importance of combinatorial regulation as a way of providing diversity of functional states with a small number of regulators (48). The existence of tiers of regulation is also to be expected since alternative splicing systems have developed by sequential evolution and are not established *de novo* (38). In the case of FGFR2 transcripts the top tier of control is determined by the approximation of *cis*-elements via a stable RNA duplex.

ACKNOWLEDGEMENTS

We thank Drs. Robert Brazas and Robin Wharton for critical reading of the manuscript, and members of the Garcia-Blanco laboratory for many helpful discussions. We also thank Ms. Annette Kennett for her assistance in the preparation of the manuscript. The research was supported by PHS grants to M.A G-B. (GM63090). E. J. W. and A. P. B. acknowledge the support of a Department of Defense predoctoral fellowship and A. P. B. also acknowledges the support of a PHS training grant.

1. **Ahmed, Y. F., G. M. Gilmartin, S. M. Hanly, J. R. Nevins, and W. C. Greene.** 1991. The HTLV-I Rex response element mediates a novel form of mRNA polyadenylation. *Cell* **64**:727-37.
2. **Blanchette, M., and B. Chabot.** 1997. A highly stable duplex structure sequesters the 5' splice site region of hnRNP A1 alternative exon 7B. *Rna* **3**:405-19.
3. **Bratt, E., and M. Ohman.** 2003. Coordination of editing and splicing of glutamate receptor pre-mRNA. *Rna* **9**:309-18.
4. **Brown, P. H., L. S. Tiley, and B. R. Cullen.** 1991. Effect of RNA secondary structure on polyadenylation site selection. *Genes Dev* **5**:1277-84.
5. **Carlo, T., D. A. Sterner, and S. M. Berget.** 1996. An intron splicing enhancer containing a G-rich repeat facilitates inclusion of a vertebrate micro-exon. *Rna* **2**:342-53.
6. **Carstens, R. P., J. V. Eaton, H. R. Krigman, P. J. Walther, and M. A. Garcia-Blanco.** 1997. Alternative splicing of fibroblast growth factor receptor 2 (FGF-R2) in human prostate cancer. *Oncogene* **15**:3059-65.
7. **Carstens, R. P., W. L. McKeehan, and M. A. Garcia-Blanco.** 1998. An intronic sequence element mediates both activation and repression of rat fibroblast growth factor receptor 2 pre-mRNA splicing. *Mol Cell Biol* **18**:2205-17.
8. **Carstens, R. P., E. J. Wagner, and M. A. Garcia-Blanco.** 2000. An intronic splicing silencer causes skipping of the IIIb exon of fibroblast growth factor receptor 2 through involvement of polypyrimidine tract binding protein. *Mol Cell Biol* **20**:7388-400.
9. **Chebli, K., R. Gattoni, P. Schmitt, G. Hildwein, and J. Stevenin.** 1989. The 216-nucleotide intron of the E1A pre-mRNA contains a hairpin structure that permits utilization of unusually distant branch acceptors. *Mol Cell Biol* **9**:4852-61.

10. **Chomczynski, P., and N. Sacchi.** 1987. Single-step method of RNA isolation by acid guanidinium thiocyanate- phenol-chloroform extraction. *Anal Biochem* **162**:156-9.
11. **Colvin, R. A., and M. A. Garcia-Blanco.** 1992. Unusual structure of the human immunodeficiency virus type 1 trans- activation response element. *J Virol* **66**:930-5.
12. **De Moerlooze, L., B. Spencer-Dene, J. Revest, M. Hajihosseini, I. Rosewell, and C. Dickson.** 2000. An important role for the IIIb isoform of fibroblast growth factor receptor 2 (FGFR2) in mesenchymal-epithelial signalling during mouse organogenesis. *Development* **127**:483-92.
13. **Degullien, M., S. C. Huang, M. Moriniere, N. Dreumont, E. J. Benz, Jr., and F. Baklouti.** 2001. Multiple cis elements regulate an alternative splicing event at 4.1R pre-mRNA during erythroid differentiation. *Blood* **98**:3809-16.
14. **Del Gatto, F., and R. Breathnach.** 1995. Exon and intron sequences, respectively, repress and activate splicing of a fibroblast growth factor receptor 2 alternative exon. *Mol Cell Biol* **15**:4825-34.
15. **Del Gatto, F., A. Plet, M. C. Gesnel, C. Fort, and R. Breathnach.** 1997. Multiple interdependent sequence elements control splicing of a fibroblast growth factor receptor 2 alternative exon. *Mol Cell Biol* **17**:5106-16.
16. **Del Gatto-Konczak, F., C. F. Bourgeois, C. Le Guiner, L. Kister, M. C. Gesnel, J. Stevenin, and R. Breathnach.** 2000. The RNA-binding protein TIA-1 is a novel mammalian splicing regulator acting through intron sequences adjacent to a 5' splice site. *Mol Cell Biol* **20**:6287-99.

17. **Del Gatto-Konczak, F., M. Olive, M. C. Gesnel, and R. Breathnach.** 1999. hnRNP A1 recruited to an exon in vivo can function as an exon splicing silencer. *Mol Cell Biol* **19**:251-60.
18. **Eis, P. S., M. C. Olson, T. Takova, M. L. Curtis, S. M. Olson, T. I. Vener, H. S. Ip, K. L. Vedvik, C. T. Bartholomay, H. T. Allawi, W. P. Ma, J. G. Hall, M. D. Morin, T. H. Rushmore, V. I. Lyamichev, and R. W. Kwiattkowski.** 2001. An invasive cleavage assay for direct quantitation of specific RNAs. *Nat Biotechnol* **19**:673-6.
19. **Fierro-Monti, I., and M. B. Mathews.** 2000. Proteins binding to duplexed RNA: one motif, multiple functions. *Trends Biochem Sci* **25**:241-6.
20. **Gilbert, E., F. Del Gatto, P. Champion-Arnaud, M. C. Gesnel, and R. Breathnach.** 1993. Control of BEK and K-SAM splice sites in alternative splicing of the fibroblast growth factor receptor 2 pre-mRNA. *Mol Cell Biol* **13**:5461-8.
21. **Graur, D., and W.-H. Li.** 2000. *Fundamentals of molecular evolution*, 2nd ed. Sinauer, Sunderland, Mass.
22. **Hajihosseini, M. K., S. Wilson, L. De Moerlooze, and C. Dickson.** 2001. A splicing switch and gain-of-function mutation in FgfR2-IIIc hemizygotes causes Apert/Pfeiffer-syndrome-like phenotypes. *Proc Natl Acad Sci U S A* **98**:3855-60.
23. **Hedjran, F., J. M. Yeakley, G. S. Huh, R. O. Hynes, and M. G. Rosenfeld.** 1997. Control of alternative pre-mRNA splicing by distributed pentameric repeats. *Proc Natl Acad Sci U S A* **94**:12343-7.
24. **Hermann, T., and D. J. Patel.** 2000. RNA bulges as architectural and recognition motifs. *Structure Fold Des* **8**:R47-54.

25. **Howe, K. J., and M. Ares, Jr.** 1997. Intron self-complementarity enforces exon inclusion in a yeast pre-mRNA. *Proc Natl Acad Sci U S A* **94**:12467-72.
26. **Huh, G. S., and R. O. Hynes.** 1994. Regulation of alternative pre-mRNA splicing by a novel repeated hexanucleotide element. *Genes Dev* **8**:1561-74.
27. **Jin, Y., H. Suzuki, S. Maegawa, H. Endo, S. Sugano, K. Hashimoto, K. Yasuda, and K. Inoue.** 2003. A vertebrate RNA-binding protein Fox-1 regulates tissue-specific splicing via the pentanucleotide GCAUG. *Embo J* **22**:905-12.
28. **Jones, R. B., R. P. Carstens, Y. Luo, and W. L. McKeehan.** 2001. 5'- and 3'-terminal nucleotides in the FGFR2 ISAR splicing element core have overlapping roles in exon IIIb activation and exon IIIc repression. *Nucleic Acids Res* **29**:3557-65.
29. **Kawamoto, S.** 1996. Neuron-specific alternative splicing of nonmuscle myosin II heavy chain- B pre-mRNA requires a cis-acting intron sequence. *J Biol Chem* **271**:17613-6.
30. **Lehmann, K. A., and B. L. Bass.** 1999. The importance of internal loops within RNA substrates of ADAR1. *J Mol Biol* **291**:1-13.
31. **Libri, D., F. Stutz, T. McCarthy, and M. Rosbash.** 1995. RNA structural patterns and splicing: molecular basis for an RNA-based enhancer. *Rna* **1**:425-36.
32. **Lim, L. P., and P. A. Sharp.** 1998. Alternative splicing of the fibronectin EIIIB exon depends on specific TGCATG repeats. *Mol Cell Biol* **18**:3900-6.
33. **Markovtsov, V., J. M. Nikolic, J. A. Goldman, C. W. Turck, M. Y. Chou, and D. L. Black.** 2000. Cooperative assembly of an hnRNP complex induced by a tissue-specific homolog of polypyrimidine tract binding protein. *Mol Cell Biol* **20**:7463-79.

34. **Mathews, D. H., J. Sabina, M. Zuker, and D. H. Turner.** 1999. Expanded sequence dependence of thermodynamic parameters improves prediction of RNA secondary structure. *J Mol Biol* **288**:911-40.
35. **McConnell, T. S., R. P. Lokken, and J. A. Steitz.** 2003. Assembly of the U1 snRNP involves interactions with the backbone of the terminal stem of U1 snRNA. *Rna* **9**:193-201.
36. **Miki, T., D. P. Bottaro, T. P. Fleming, C. L. Smith, W. H. Burgess, A. M. Chan, and S. A. Aaronson.** 1992. Determination of ligand-binding specificity by alternative splicing: two distinct growth factor receptors encoded by a single gene. *Proc Natl Acad Sci U S A* **89**:246-50.
37. **Min, H., C. W. Turck, J. M. Nikolic, and D. L. Black.** 1997. A new regulatory protein, KSRP, mediates exon inclusion through an intronic splicing enhancer. *Genes Dev* **11**:1023-36.
38. **Mistry, N., W. Harrington, E. Lasda, E. J. Wagner, and M. A. Garcia-Blanco.** 2003. Of urchins and men: evolution of an alternative splicing unit in fibroblast growth factor receptor genes. *Rna* **9**:209-17.
39. **Modafferi, E. F., and D. L. Black.** 1997. A complex intronic splicing enhancer from the c-src pre-mRNA activates inclusion of a heterologous exon. *Mol Cell Biol* **17**:6537-45.
40. **Muh, S. J., R. H. Hovhannisyan, and R. P. Carstens.** 2002. A Non-sequence-specific double-stranded RNA structural element regulates splicing of two mutually exclusive exons of fibroblast growth factor receptor 2 (FGFR2). *J Biol Chem* **277**:50143-54.

41. **Muro, A. F., M. Caputi, R. Pariyarath, F. Pagani, E. Buratti, and F. E. Baralle.** 1999. Regulation of fibronectin EDA exon alternative splicing: possible role of RNA secondary structure for enhancer display. *Mol Cell Biol* **19**:2657-71.
42. **Newman, A.** 1987. Specific accessory sequences in *Saccharomyces cerevisiae* introns control assembly of pre-mRNAs into spliceosomes. *Embo J* **6**:3833-9.
43. **Oldridge, M., E. H. Zackai, D. M. McDonald-McGinn, S. Iseki, G. M. Morriss-Kay, S. R. Twigg, D. Johnson, S. A. Wall, W. Jiang, C. Theda, E. W. Jabs, and A. O. Wilkie.** 1999. De novo alu-element insertions in FGFR2 identify a distinct pathological basis for Apert syndrome. *Am J Hum Genet* **64**:446-61.
44. **Orr-Urtreger, A., M. T. Bedford, T. Burakova, E. Arman, Y. Zimmer, A. Yayon, D. Givol, and P. Lonai.** 1993. Developmental localization of the splicing alternatives of fibroblast growth factor receptor-2 (FGFR2). *Dev Biol* **158**:475-86.
45. **Puglisi, J. D., R. Tan, B. J. Calnan, A. D. Frankel, and J. R. Williamson.** 1992. Conformation of the TAR RNA-arginine complex by NMR spectroscopy. *Science* **257**:76-80.
46. **Roy, S., U. Delling, C. H. Chen, C. A. Rosen, and N. Sonenberg.** 1990. A bulge structure in HIV-1 TAR RNA is required for Tat binding and Tat-mediated trans-activation. *Genes Dev* **4**:1365-73.
47. **Ryter, J. M., and S. C. Schultz.** 1998. Molecular basis of double-stranded RNA-protein interactions: structure of a dsRNA-binding domain complexed with dsRNA. *Embo J* **17**:7505-13.
48. **Smith, C. W., and J. Valcarcel.** 2000. Alternative pre-mRNA splicing: the logic of combinatorial control. *Trends Biochem Sci* **25**:381-8.

49. **Wagner, E. J., and M. A. Garcia-Blanco.** 2001. Polypyrimidine tract binding protein antagonizes exon definition. *Mol Cell Biol* **21**:3281-8.
50. **Wagner, E. J., and M. A. Garcia-Blanco.** 2002. RNAi-mediated PTB depletion leads to enhanced exon definition. *Mol Cell* **10**:943-9.
51. **Yan, G., Y. Fukabori, G. McBride, S. Nikolaropolous, and W. L. McKeehan.** 1993. Exon switching and activation of stromal and embryonic fibroblast growth factor (FGF)-FGF receptor genes in prostate epithelial cells accompany stromal independence and malignancy. *Mol Cell Biol* **13**:4513-22.
52. **Yu, K., A. B. Herr, G. Waksman, and D. M. Ornitz.** 2000. Loss of fibroblast growth factor receptor 2 ligand-binding specificity in Apert syndrome. *Proc Natl Acad Sci U S A* **97**:14536-41.

Figure Legends

Figure 1. Functional characterization of stem composition on cell-type specific inclusion of exon IIIb. Stem formation dictates exon IIIb inclusion. (A) The structure of an *in vitro* synthesized 84-nucleotide RNA molecule containing the rat IAS2 and ISAR core sequences separated by a 6-nucleotide loop was probed with RNase A and RNase T1. Strong RNase A cleavage sites are indicated by large black arrowheads and strong RNase T1 cleavage sites are indicated by large gray arrowheads. A small gray arrowhead indicates the weak RNase T1 cleavage site. (B) Minigenes used to test the sequence specificity of stem formation for exon IIIb activation in epithelial cells. pI12DE-Rep, -Blue Blue(c), -Blue(c) Blue, -PyPu, and -PyPu Δ Bulge are capable of stem formation, while -Blue Blue and -Blue(c) Blue(c) are not capable of stem formation. IAS2 and ISAR core or the sequences that replace them are indicated as black boxes (C) Sequence composition of the stems formed by the corresponding minigenes in (B). Pu and Py demarcate the stretches of purines and pyrimidines in the stem structures. ΔG indicates the predicted Gibbs free energy for each stem in kcal/mole as calculated by mFold (34). (D) Minigenes that are capable of stem formation recover activation of exon IIIb inclusion to varying degrees (see discussion). Percent exon inclusion for minigenes in (B) that were stably transfected into DT3 cells was determined by Invader[®] RNA assay. (E) The two-nucleotide bulge in the stem structure is not necessary for IIIb inclusion. Left panel shows the minigenes used to test the effects of bulge mutations on exon IIIb inclusion. Right panel shows the quantification of RT-PCR analysis of stably transfected minigenes in DT3 cells.

Figure 2. Loop sequences are not necessary for cell-type specific exon inclusion. (A) Minigenes used to test the importance of loop sequence on cell-type specific exon inclusion. pI12DE-WT contains 735 nucleotides between IAS2 and ISAR, whereas pI12DE-ΔLP contains 6 nucleotides between IAS2 and ISAR. IAS2 and ISAR core are indicated as black boxes. (B) Quantification of RT-PCR analysis of stably transfected minigenes in DT3 and AT3 cells.

Figure 3. Approximation of sequences upstream of IAS2 to sequences downstream of ISAR core allows for the proper cell-type specific exon inclusion. (A) Minigenes used to test the importance of approximating sequences upstream of IAS2 with sequences downstream of ISAR core. pI12DE-WT is described in Figure 2A. The pI12DE-ΔSTLP minigene contains a deletion of the entire IAS2-ISAR core stem-loop structure from the 5' end of IAS2 to the 3' end of ISAR core, which mimics the predicted outcome of IAS2-ISAR stem formation. The pI12DE-Blue Blue minigene, which is not capable of stem formation, is described in Figure 1D. IAS2 and ISAR core are indicated as black boxes. (B) Quantification of RT-PCR analysis of stably transfected minigenes in DT3 and AT3 cells.

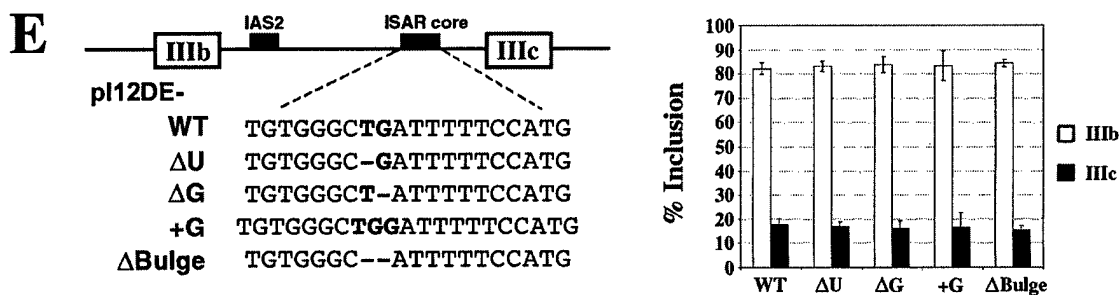
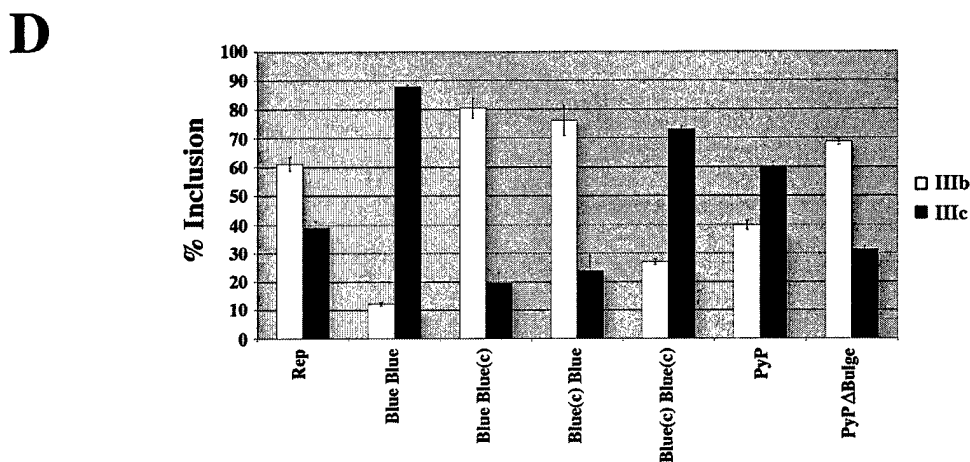
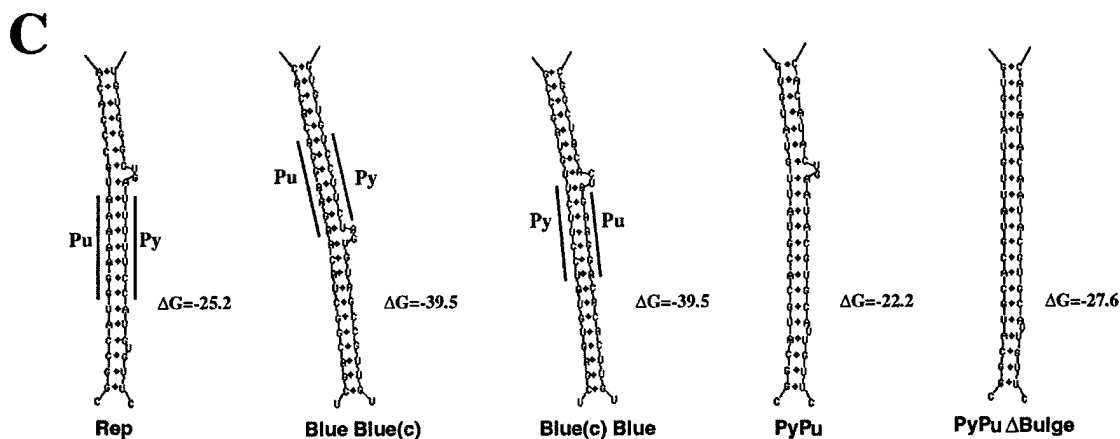
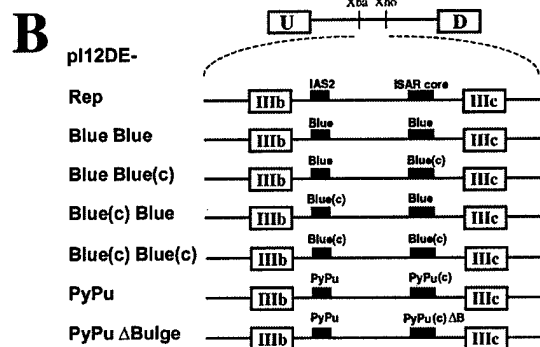
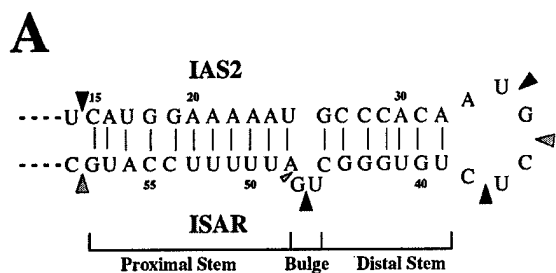
Figure 4. GCAUG element immediately downstream of ISAR core plays a role in exon IIIb inclusion. (A) Minigenes with 5 nucleotide mutations downstream of ISAR core. The 5-base pair substitution mutations are indicated with bold print. IAS2 and ISAR core are indicated as black boxes; ISAR core resides within the full ISAR element (indicated

as a gray box). Nucleotides in the gray box are within ISAR. (B) Quantification of RT-PCR analysis of stably transfected minigenes in DT3 cells.

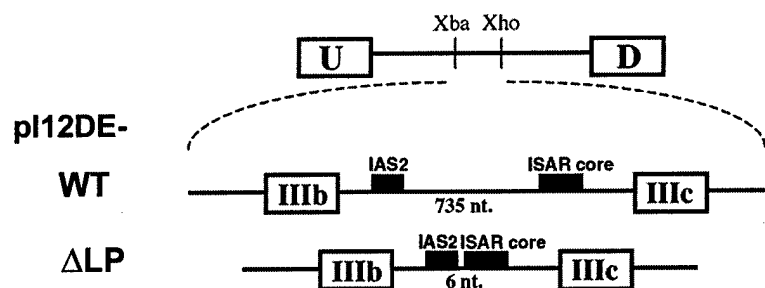
Figure 5. Spacing between ISAR and downstream exon is required for the proper inclusion of exon IIIb. (A) Left panel shows a diagram of single exon IIIb minigenes. pI12IIIb-WT contains exon IIIb flanked with intronic FGFR2 sequences as previously described (7). pI12IIIb- Δ ISAR Δ 193 contains a deletion of ISAR and 193 nucleotides of downstream FGFR2 sequence. pI12IIIb-+ISAR Δ 193 restores ISAR, and pI12IIIb-+ISAR +58 contains ISAR and 58 nucleotides of downstream FGFR2 sequence. The right panel shows quantification of RT-PCR analysis of stably transfected minigenes in DT3 cells. IAS2, ISAR core and ISAR are indicated as described in Figure 4. (B) Left panel shows a diagram of single exon IIIb minigenes used to test the importance of maintaining the proper minimum distance between ISAR and the 3'splice site. pI12IIIb-WT and pI12IIIb-+ISAR Δ 193 are described in A. pI12IIIb-+ISAR BS1 and pI12IIIb-+ISAR BS2 both contain ISAR and each contains a different 193 nucleotides of unrelated sequence derived from sequences of pBluescript (Stratagene). Right panel shows quantification of RT-PCR analysis of stably transfected minigenes in DT3 cells.

Figure 6. Layers of control in the alternative splicing of FGFR2 transcripts. The schematic shows three layers of control that determine the choice between inclusion of exon IIIb or exon IIIc. A primary transcript from the FGFR2 gene is shown containing the IAS2-ISAR core structure within intron 8. Layer 1 shows the negative effect of weak splice sites on the definition of exon IIIb. Layer 2 represents the influence of silencer

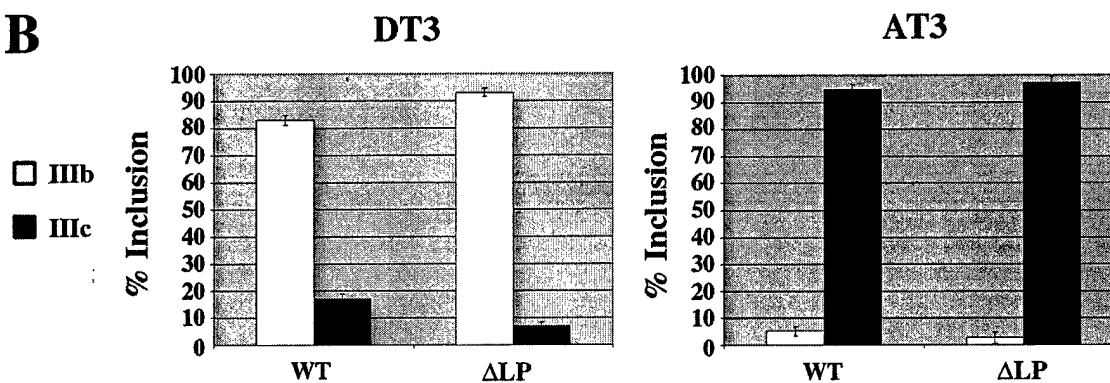
elements that regulate exon IIIb inclusion. These elements operate in both mesenchymal and epithelial cells. Layer 3 depicts epithelial-specific activity that promotes inclusion of IIIb and repression of IIIc. We propose that approximation of sequences downstream of the ISAR core to the vicinity of intronic silencers counters these elements and promotes inclusion of exon IIIb.



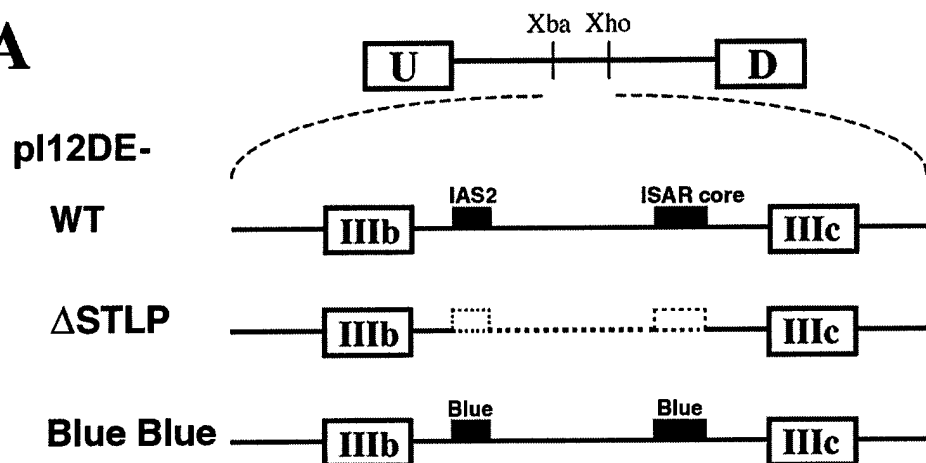
A



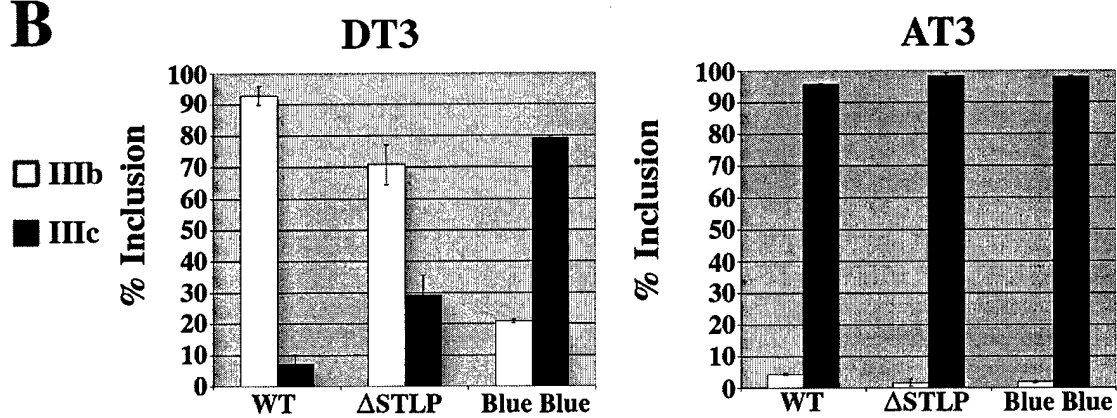
B



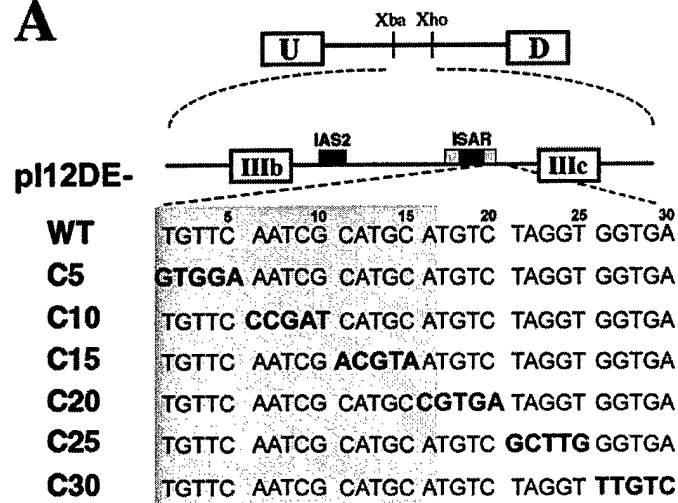
A



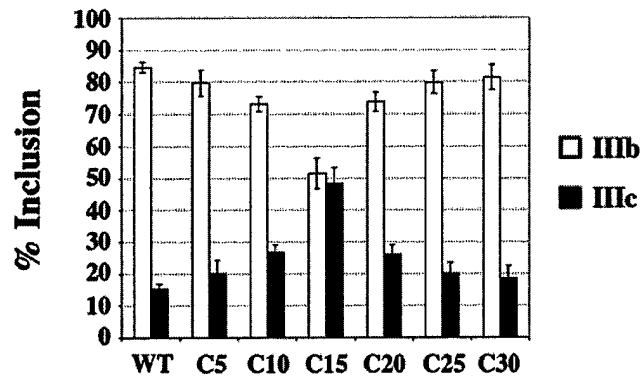
B



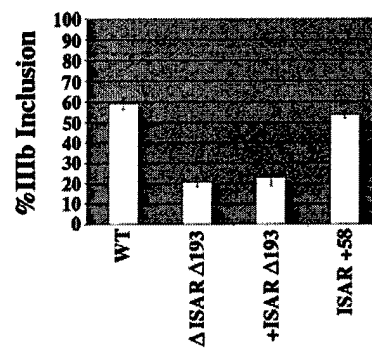
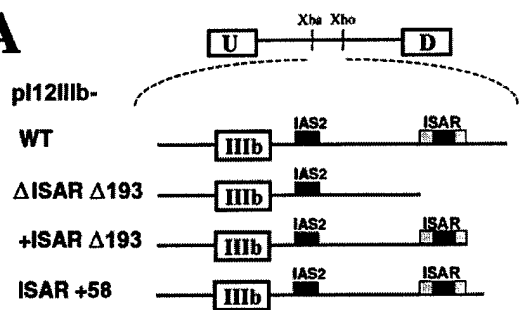
A



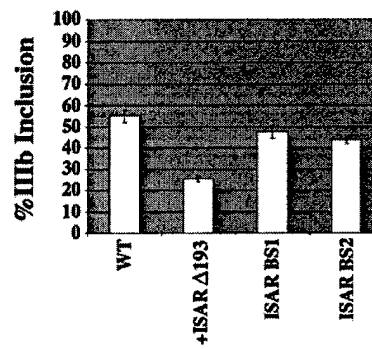
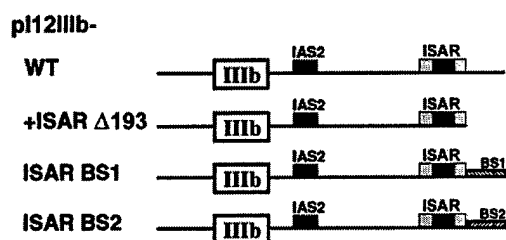
B

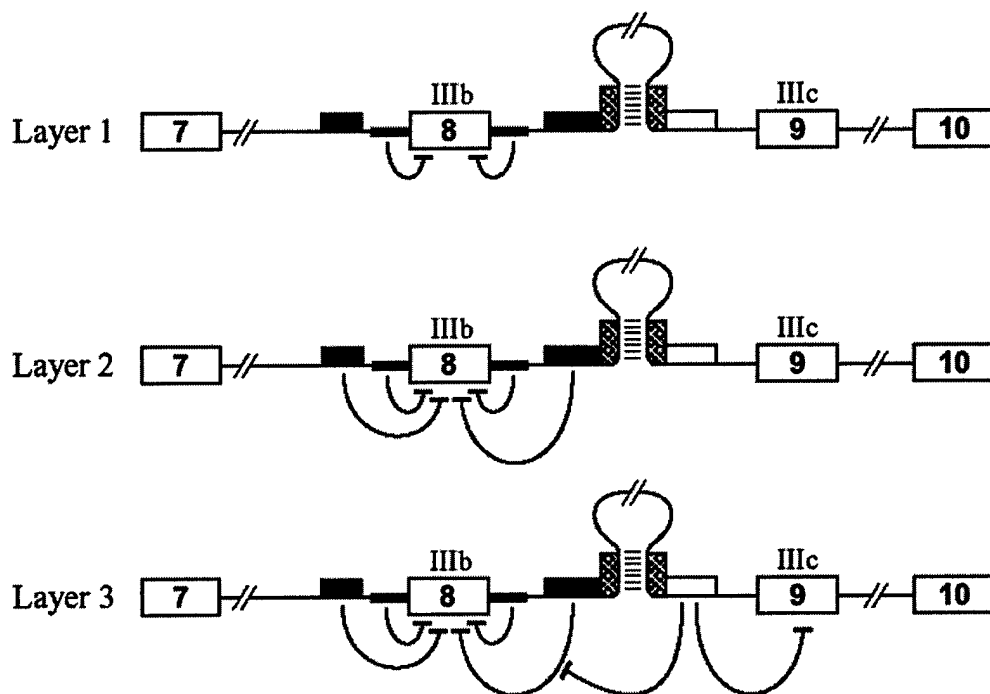


A



B





RNAi-Mediated PTB Depletion Reveals a Requirement in IRES-Dependent Translation and Picornavirus Propagation

Eric J. Wagner ^{1,2,†}, Paola Florez ^{1,†}, October Sessions ¹, Matthias Gromeier ^{1,3}, and
Mariano A. Garcia-Blanco ^{1,3,*}

¹Department of Molecular Genetics and Microbiology,

²Program in Molecular Cancer Biology, ³Department of Medicine,

Duke University Medical Center, Durham, North Carolina, 27710

*Correspondence should be sent to M. A. Garcia-Blanco at garci001@mc.duke.edu

[†]These two authors contributed equally to this work.

Mammalian factors required for cap-independent IRES-driven translation have been recalcitrant to genetic analysis. Here we use RNA interference to deplete mammalian cells of the polypyrimidine tract binding protein (PTB) and test its controversial requirement in IRES function. PTB depletion decreased expression of a reporter driven by a viral IRES, while it did not affect cap-dependent translation of the same reporter. RNAi-mediated PTB depletion also resulted in a profound reduction in encephalomyocarditis virus and poliovirus gene expression and propagation. These data demonstrate a critical role for PTB in IRES-mediated translation and suggest general utility for RNAi in the analysis of cellular factors required for cap-independent translation initiation and viral replication.

Picornaviruses, which include important pathogens such as poliovirus and foot and mouth disease virus (FMDV), encode a single polypeptide in one (+) strand RNA that is missing a 5' guanosine cap (Nomoto et al. 1976). The uncapped genomic RNA directs translation initiation via the IRES, a highly structured cis-acting element in the 5' untranslated region (5' UTR or 5' NTR) of the viral RNA (reviewed in Hellen and Sarnow 2001; Pestova et al. 2001; Vagner et al. 2001) (Jackson 2000). Based on structural differences picornavirus IRESs are classified as type I (*enterovirus* and *rhinovirus* genera) or type II (*cardiovirus* and *aphthovirus* genera). In addition to picornaviruses, other viral RNAs (e.g. hepatitis C virus (HCV)) and some cellular mRNAs contain IRESs (reviewed in Hellen and Sarnow 2001). As its name suggests, the IRES recruits the 40S ribosomal subunits and translation factors, which are also required for cap-dependent translation (Pestova et al. 1996), in a 5'-end- and cap-independent manner. IRESs also recruit other cellular proteins that have no known role in cap-dependent translation, but activate IRES function *in vitro* (reviewed in Hellen and Sarnow 2001). These activating proteins, or IRES trans-acting factors (ITAFs), are: ITAF₄₅ (which is also known as *Mpp1*) (Pilipenko et al. 2000), the La autoantigen (Meerovitch et al. 1993), poly(rC) binding protein2 (PCBP2) (Blyn et al. 1996), *unr* and *unr*-interacting protein (Hunt et al. 1999), and the polypyrimidine tract binding protein (PTB) (Borman et al. 1993; Hellen et al. 1993) (Witherell et al. 1993).

Although PTB has been implicated in the function of viral and cellular IRESs *in vitro*, a PTB requirement remains controversial (Pestova et al. 1996; Pilipenko et al. 1999; Kaminski and Jackson 1998; Hunt and Jackson 1999; Ali and Siddiqui 1995; Mitchell et

al. 2001). Depletion of PTB *in vitro* results in an inhibition of IRES translation, however, the addition of purified PTB has failed to restore activity (Hellen et al. 1993). Addition of PTB to *in vitro* translation systems enhances translation driven by an encephalomyocarditis virus (EMCV) IRES only two-fold, whereas PTB addition is required for translation driven by the FMDV IRES and the Theiler's murine encephalomyelitis virus (TMEV) IRESs (Pestova et al. 1996; Pilipenko et al. 1999; Kaminski and Jackson 1998; Hunt and Jackson 1999). The variability of the effects observed, the inability to obtain biochemical complementation, and inherent questions about *in vitro* systems have clouded the conclusion that PTB is an ITAF *in vivo*. Some attempts have been made to extend the analysis *in vivo*. Gosert et al (2000) showed that PTB overexpression leads to increased reporter expression when translation is driven by a picornavirus (poliovirus or hepatitis A virus) or a flavivirus (HCV) IRES (Gosert et al. 2000). Pilipenko et al. (2001) showed that the capacity of variant TMEV IRESs to bind neural PTB, a homologue of PTB, correlates with the ability to promote viral replication suggesting a role *in vivo* (Pilipenko et al. 2001). A further attempt to demonstrate *in vivo* relevance employed the expression of RNA decoys selected to bind and sequester PTB. Although these decoys inhibited IRES-dependent translation *in vivo*, it was not possible to assess the specificity of their effect (Anwar et al. 2000). None of these previous observations, however, demonstrated a requirement for PTB in IRES function and more importantly in picornavirus replication *in vivo*. In this report we make this previously controversial requirement evident. We took advantage of RNA interference (RNAi) methods, which can efficiently and specifically deplete PTB *in vivo*, to show that PTB is required for picornavirus IRES-dependent translation and viral propagation. Our study

has implications for the study of viral and cellular IRES-driven translation, and demonstrates the power of RNAi methods in unraveling the role of host factors required for pathogenicity.

Results and discussion

In order to test a role for PTB in IRES function *in vivo*, we used a small interfering RNA (siRNA) to specifically deplete PTB levels in HeLa R19 cells (Figure 1A) (Wagner and Garcia-Blanco 2002). The PTB depleted cells (P9) were transfected with plasmids that encode a green fluorescent protein (GFP) whose translation is either cap-dependent or EMCV IRES-dependent. Treatment with a control non-specific siRNA (C2) had no effect on GFP expression from either construct (Figure 1B). RNAi-mediated PTB depletion did not affect cap-dependent translation of GFP (Figure 1B, CMV-GFP), but severely compromised expression of GFP from mRNAs that required EMCV IRES function (Figure 1B, CMV-IRES-GFP). Because transcription of CMV-GFP and CMV-IRES-GFP was driven by the same cytomegalovirus immediate early promoter it is very unlikely that depletion of PTB affected transcription. These data directly support an *in vivo* requirement for PTB in IRES function.

To evaluate the importance of PTB for EMCV IRES function in the context of a viral genome we tested the effect of PTB depletion on EMCV gene expression and propagation. We used a *wild type* EMCV to infect HeLa-S3 cells that have been mock depleted with C2 siRNA or depleted of PTB with P9 siRNA (Figure 2A, left panel). Unless otherwise noted, this and all other infections described in this report were carried

out at a multiplicity of infection (m.o.i.) of 10. Cells treated with non-specific siRNA (C2) supported robust expression of viral proteins, whereas, PTB knockdown caused a profound and enduring inhibition of viral 3D protein accumulation (Figure 2A, right panel). Cellular proteins that crossreact with the anti-3D monoclonal antibody were not affected by PTB depletion (asterisk in Figure 2A, right panel). Most importantly, the depletion of PTB resulted in markedly decreased EMCV replication (Figures 2B & 2C). Representative plaque assays show that treatment with the P9 siRNA led to an almost ten fold inhibition of viral replication (Figure 2B). The quantification of the plaque assays, which is shown in Figure 2C, revealed that PTB depletion led to a delay in the appearance of viral progeny and to a persistent decrease in propagation of the virus. These data indicate that PTB is required for gene expression and replication of *wild type* EMCV. Together with the data obtained with the GFP reporter constructs this experiment suggested that PTB is critically required for EMCV IRES function.

The EMCV IRES used in the GFP minigene reporters contains an insertion of a single adenosine residue in the "A-bulge" of the IRES so the bulge contains seven adenosines rather than the six found in most isolates of EMCV (Kaminski and Jackson 1998). This additional adenosine makes this IRES PTB-dependent *in vitro*, whereas a six adenosine IRES was minimally PTB-dependent (Kaminski and Jackson 1998). The EMCV IRES in *wild type* EMCV, however, has a six adenosine bulge (data not shown) and was sensitive to PTB depletion *in vivo* (Figure 2). In order to investigate this discrepancy between prior *in vitro* results and our *in vivo* data we decided to test the two "A-bulge" variants in the same context. To this end we infected cells with PV1(ENPOS)

and PV1(ENPOS)-6A viruses, chimeric poliovirus type 1 (Sabin) (PV1(S)) where the cognate IRES has been replaced with a seven-adenosine or a six-adenosine EMCV IRES respectively (Alexander et al. 1994; Gromeier et al. 1996). Cells treated with non-specific siRNA (C2) supported robust expression of viral proteins, whereas, in PTB-depleted cells (P9) expression of viral proteins was profoundly diminished regardless of the chimeric virus used (data not shown). The reduction of viral protein levels was accompanied by a significant reduction in PV1(ENPOS) and PV1(ENPOS)-6A progeny (data not shown). These data showed that *in vivo*, in the same context, the six-adenosine "A-bulge" IRES was sensitive to PTB depletion (data not shown) and confirmed a PTB requirement for EMCV (type II) IRES function *in vivo*.

To examine the PTB requirement for type I IRES function we depleted PTB in HeLa R19 cells and infected these cells with PV1(S). PTB-depletion (P9) clearly delayed expression of PV1(S) gene products (P2, 2BC and 2C in Figure 3A). Although the expression of PV1(S) proteins in PTB depleted cells increased at late times p.i. (e.g., 6 hours p.i.) the levels never reached the same as those in the mock-depleted cells. The reduction of viral protein levels was accompanied by a significant decline in PV1(S) progeny, particularly at early times p.i. (Figure 3B). These data indicated that both poliovirus and EMCV IRESs, representatives of the two classes of picornavirus IRESs, require PTB. A common requirement for *trans*-activation of translation for the structurally unrelated type I and II picornaviral IRESs suggested PTB to be essential for the function of other IRESs as well. Indeed, the function of the HCV IRES was sensitive to PTB depletion *in vivo* (Florez et al., unpublished results).

Given that RNAi is likely an ancient anti-viral mechanism, its induction could have led to non-specific anti-viral activities in cells depleted of PTB (Hannon 2002). The non-specific C2 siRNA control could not rule out such an effect because this siRNA did not target any mRNA in HeLa cells and therefore did not activate RNAi effectors (e.g., RISC) (Ibid.). We wanted to test whether activation of RNAi *per se* would affect picornavirus replication. To that end, we constructed HeLa cells expressing pGL2 luciferase (HeLa^{Luc}) and confirmed that luciferase activity but not PTB could be specifically depleted with an siRNA (Luc) targeted to the luciferase mRNA (Elbashir et al. 2001) (Figures 4A & 4B). The Luc-depleted HeLa^{Luc} cells, which had normal levels of PTB were ideal controls to evaluate any non-specific anti-viral effects of RNAi. RNAi-mediated depletion of luciferase did not significantly affect the chimeric virus PV1(ENPOS2) gene expression (Figure 4C), whereas, as already shown, PTB-depletion resulted in greatly diminished levels of viral proteins at four and six hours p.i. (Figure 4C). Luc-depletion minimally decreased viral growth (<2 fold), contrasted to the greater than 8-fold reduction of viral replication when PTB was depleted (Figure 4D). These data suggest that activation of RNAi *per se* could not explain the results we had observed with PTB depletion. A second type of experiment was carried out to further rule out non-specific anti-viral effects of RNAi. We demonstrate that respiratory syncytial virus gene expression, which is not dependent on IRES function, was not affected by RNAi-mediated depletion of PTB (data not shown). We concluded from these experiments that non-specific activation of RNAi does not activate a non-specific antiviral state.

Although PTB has been found to shuttle between the nucleus and the cytoplasm (Kamath et al. 2001) its localization is predominantly nuclear (Huang et al. 1997). Very low levels of cytoplasmic PTB may be incompatible with robust IRES function, therefore we predicted that PTB would be recruited to the cytoplasm early during picornavirus infection. Others have reported relocation of nuclear factors following poliovirus infection (Shiroki et al. 1999) possibly due to poliovirus induced degradation of nuclear pore complex components (Gustin and Sarnow 2001). Previously, Back et al. (2002) showed that PTB is localized in the cytoplasm by 6 hours after poliovirus infection. By that time, however, PTB is cleaved by the viral protease 3C^{pro} and most of the cytoplasmic PTB must be proteolysed (Ibid.). In order to evaluate PTB localization and integrity early after infection, we performed indirect immunofluorescence and western blots. Whereas in uninfected cells PTB was almost exclusively nuclear, poliovirus infection led to the appearance of PTB in the cytoplasm, which could be seen as early as 3 hours p.i. (Figure 5A). The cytoplasmic relocation of PTB is not due to a global loss of nuclear integrity since the localization of splicing factor SC35 is unaffected at 3 hours p.i. (Figure 5A) (Gustin and Sarnow 2001). It should be also noted that at 3 hours p.i. there is no evidence of PTB cleavage (Figure 5B). These data led us to conclude that intact PTB accumulates in the cytoplasm early after poliovirus infection, which is consistent with a requirement for PTB in poliovirus IRES function.

Our work provides the first direct evidence that PTB is required for IRES dependent translation in living cells. While this work validates and extends biochemical experiments, it also raises some important questions about these *in vitro* assays. For

example these assays suggested that an EMCV IRES containing a six adenosine A-bulge is not dependent on PTB (Kaminski and Jackson 1998), but here we show this IRES was clearly sensitive to PTB depletion *in vivo*. Although the *in vitro* assays may be unreliable when assigning function they should be invaluable in unraveling how PTB mediates its ITAF function. PTB binds pyrimidine-rich sequences in IRESs (Pestova et al. 2001; Hellen and Sarnow 2001; Vagner et al. 2001), and must exert its function by modifying the RNA structure and/or by interacting with another ITAF or a translation factor. PTB has also been implicated in other RNA transactions (Valcarcel and Gebauer 1997). PTB is required for silencing alternative exons in FGF-R2 and fibronectin transcripts and is likely involved in silencing many other regulated exons (Charlet et al. 2002; Chou et al. 2000; Liu et al. 2002; Wagner and Garcia-Blanco 2001; Wagner and Garcia-Blanco 2002; Wollerton et al. 2001). Additionally PTB has been implicated in localization of the Vg-1 mRNA in *Xenopus laevis* oocytes (Cote et al. 1999). It is not clear if these other roles are mechanistically related to PTB ITAF function.

Cells devoid of PTB are poor hosts for both EMCV and poliovirus replication indicating that PTB is an essential host factor for efficient propagation of picornaviruses. We show that soon after picornaviral infection PTB is summoned out of the nucleus to facilitate IRES driven translation. As infection progresses PTB is cleaved, possibly to enable a switch from viral gene expression to viral replication and packaging (Back et al. 2002). The cleavage appears selective since the PTB1 isoform is more resistant and persists late in infection, which may be significant since the PTB1 isoform is more potent as an ITAF than PTB4 *in vitro* (Wollerton et al. 2001). The experiments presented here

also suggest that siRNA-mediated depletion can be a powerful tool to study the role of host factors required for viral replication, and consequently in the discovery and validation of anti-viral drug targets. PTB depletion represses viral replication suggesting that an early event in the viral life cycle, i.e. IRES dependent translation, is critically dependent on PTB. A similar delay in viral replication was observed when siRNAs targeted poliovirus RNA directly (Gitlin et al. 2002). It is reasonable to assume that anti-viral agents targeting the PTB-IRES interaction would affect viral replication similarly to PTB-depletion. This has implications not only for all picornavirus IRESs but also for the HCV IRES, which has been singled out as a target for antiviral therapy (Jubin 2001). The disruption of essential ITAF achieved by RNAi impressively demonstrates the potential for identifying molecular targets for antiviral chemotherapy *in vivo*. Furthermore, our study also impinges on the study of cellular processes that require IRES-dependent translation.

Materials and Methods

Viruses. PV1(S) cDNA was obtained from Akio Nomoto (Tokyo, Japan) and was used to derive virus. *Wild-type* EMCV was obtained from the ATCC (#VR-129B). Chimeric virus PV1(ENPOS) contains two changes in the coding region for the VP1 viral capsid protein, E16S and T17S, and has delayed growth kinetics relative to PV1(S) (Gromeier et al. 1996). PV1(ENPOS)-6A was derived from PV1(ENPOS). PV1(ENPOS2) has the Sabin VP1 viral capsid, but is otherwise identical to PV1(ENPOS).

siRNA transfection. PTB9 siRNA was created by annealing the sense RNA oligo 5'GC CUCUUUAUUCUUUUCGGdTdT3' to the antisense, 5'CCGAAAAGAAUAAAGAGG CdTdT3' (Dharmacon). The C2 siRNA duplex was described in Wagner and Garcia-Blanco (2002) and the Luc siRNA was as described in (Elbashir et al. 2001). siRNA transfections were performed essentially as previously described (Wagner and Garcia-Blanco 2002). Briefly, cells were transfected with siRNAs using Lipofectamine 2000 (Invitrogen) at 0 hrs and then again at 48 hrs. The following day (72 hrs), cells were recounted and plated to a density of 5×10^6 cells per well in a six well plate and then infected with virus the next day.

Viral gene expression and propagation. Following treatment with C2 or P9 siRNA, HeLa R19 or HeLa S3 cells were infected at an m.o.i. of 10 with either, PV1(ENPOS), PV1(ENPOS2), PV1(S), or *wild type* EMCV. Infected cells were rocked for 30 min at room temperature and washed three times with 2mL of serum free Dulbecco's minimal essential medium (DMEM). After adding 1.5 mL of DMEM containing 2% Fetal Bovine Serum (FBS), the cells were incubated at 37°C. At the indicated time points, the cells were freeze-thawed twice, resuspended, and vortexed. A 50ul aliquot was removed to determine the virus titer by plaque assay as described elsewhere (Gromeier et al. 1996) PV1(ENPOS), PV1(ENPOS2), and PV1 (S) were plaqued on HeLa R19 cells, whereas EMCV was plaqued on Vero cells. The results of the one step growth curves indicated as plaque forming units (PFU) per mL were the average of triplicate samples per time point, except for the P9 6-hour p.i. time point in figure 3, which was the average of duplicate samples. The remaining lysate was centrifuged at 13.2K rpm for 3 minutes. The pellet

fractions were resuspended in 200ul phosphate-buffered saline (PBS) containing 0.5% NP40 lysis buffer. After determination of the total protein concentration through Bradford assay (Bio-Rad) the sample was processed for SDS-PAGE and Western blot essentially as described previously (Wagner and Garcia-Blanco 2002) (Dobrikova et al. 2002). Poliovirus or EMCV gene expression was assayed by Western Blots using anti-P2/2BC/2C monoclonal antibody or anti-3D monoclonal antibody, respectively.

Immunofluorescence. Cells were fixed in 3.7% formaldehyde for 15 minutes and quenched for 15 minutes using ammonium chloride. PTB was probed using Ig purified rabbit polyclonal antiserum (Intronn Inc.) at a 1:1000 dilution. SC35 was probed using a mouse monoclonal at a 1:3000 dilution. Both were incubated on fixed cells for 1 hour, followed by 3 five minute washes in PBS+ (5 mg/ml BSA and .4% Tween 20) and then incubated with anti-rabbit rhodamine and anti-mouse fluorescein secondary antibodies according to manufacturers protocol (Jackson Immunolabs). Cells were imaged using standard techniques.

Acknowledgements

We thank E. Wimmer (SUNY Stony Brook) for the anti-poliovirus 2C monoclonal antibody and A. Palmenberg (U. of Wisconsin, Madison) for the anti-EMCV 3D monoclonal antibody. We thank Drs. Glen Coburn, Matt Wollerton and Robert Brazas for critical reading of the manuscript and members of the Garcia-Blanco and Gromeier laboratories for helpful discussions. We also thank Ms. Annette Kennett for her assistance in the preparation of the manuscript. The research was supported by PHS grants to M.A G-B. (GM63090) and to M.G. (CA87537), and by the ABC² Foundation

(to M.G.). M. G. is a recipient of a Burroughs Wellcome Career Award in the Biomedical Sciences. E. J. W. acknowledges the support of a Department of Defense predoctoral fellowship.

References

- Alexander, L., H.H. Lu, and E. Wimmer. 1994. *Polioviruses containing picornavirus type 1 and/or type 2 internal ribosomal entry site elements: genetic hybrids and the expression of a foreign gene. Proc Natl Acad Sci U S A* **91**: 1406-10.
- Ali and Siddiqui. 1995. *Interaction of polypyrimidine tract-binding proteins with the 5' noncoding region of the hepatitis C virus RNA genome and its functional requirement in internal initiation of translation. J. Virology* **69**: 6367-6375.
- Anwar, A., N. Ali, R. Tanveer, and A. Siddiqui. 2000. *Demonstration of functional requirement of polypyrimidine tract-binding protein by SELEX RNA during hepatitis C virus internal ribosome entry site-mediated translation initiation. J Biol Chem* **275**: 34231-5.
- Back, S.H., Y.K. Kim, W.J. Kim, S. Cho, H.R. Oh, J.E. Kim, and S.K. Jang. 2002. *Translation of polioviral mRNA is inhibited by cleavage of polypyrimidine tract-binding proteins executed by polioviral 3C(pro). J Virol* **76**: 2529-42.
- Blyn, L.B., K.M. Swiderek, O. Richards, D.C. Stahl, B.L. Semler, and E. Ehrenfeld. 1996. *Poly(rC) binding protein 2 binds to stem-loop IV of the poliovirus RNA 5' noncoding region: identification by automated liquid*

- chromatography- tandem mass spectrometry. Proc Natl Acad Sci U S A* **93**: 11115-20.
- Borman, A., M.T. Howell, J.G. Patton, and R.J. Jackson. 1993. *The involvement of a spliceosome component in internal initiation of human rhinovirus RNA translation. J Gen Virol* **74**: 1775-88.
- Charlet, B.N., P. Logan, G. Singh, and T.A. Cooper. 2002. *Dynamic antagonism between ETR-3 and PTB regulates cell type-specific alternative splicing. Mol Cell* **9**: 649-58.
- Chou, M.Y., J.G. Underwood, J. Nikolic, M.H. Luu, and D.L. Black. 2000. *Multisite RNA binding and release of polypyrimidine tract binding protein during the regulation of c-src neural-specific splicing. Mol Cell* **5**: 949-57.
- Cote, C.A., D. Gautreau, J.M. Denegre, T.L. Kress, N.A. Terry, and K.L. Mowry. 1999. *A Xenopus protein related to hnRNP I has a role in cytoplasmic RNA localization. Mol Cell* **4**: 431-7.
- Dobrikova, E., P. Florez, and M. Gromeier. 2002. *Virology, In Press.*
- Elbashir, S.M., J. Harborth, W. Lendeckel, A. Yalcin, K. Weber, and T. Tuschl. 2001. *Duplexes of 21-nucleotide RNAs mediate RNA interference in cultured mammalian cells. Nature* **411**: 494-8.
- Gitlin, L., S. Karelsky, and R. Andino. 2002. *Short interfering RNA confers intracellular antiviral immunity in human cells. Nature* **418**: 430-4.
- Gosert, R., K.H. Chang, R. Rijnbrand, M. Yi, D.V. Sangar, and S.M. Lemon. 2000. *Transient expression of cellular polypyrimidine-tract binding protein stimulates cap-independent translation directed by both picornaviral and flaviviral internal ribosome entry sites In vivo. Mol Cell Biol* **20**: 1583-95.

- Gromeier, M., L. Alexander, and E. Wimmer. 1996. *Internal ribosomal entry site substitution eliminates neurovirulence in intergeneric poliovirus recombinants. Proc Natl Acad Sci U S A* **93**: 2370-5.
- Gustin, K.E. and P. Sarnow. 2001. *Effects of poliovirus infection on nucleocytoplasmic trafficking and nuclear pore complex composition. Embo J* **20**: 240-9.
- Hannon, G.J. 2002. *RNA interference. Nature* **418**: 244-51.
- Hellen, C.U. and P. Sarnow. 2001. *Internal ribosome entry sites in eukaryotic mRNA molecules. Genes Dev* **15**: 1593-612.
- Hellen, C.U., G.W. Witherell, M. Schmid, S.H. Shin, T.V. Pestova, A. Gil, and E. Wimmer. 1993. *A cytoplasmic 57-kDa protein that is required for translation of picornavirus RNA by internal ribosomal entry is identical to the nuclear pyrimidine tract-binding protein. Proc Natl Acad Sci U S A* **90**: 7642-6.
- Huang, S., T.J. Deerinck, M.H. Ellisman, and D.L. Spector. 1997. *The dynamic organization of the perinucleolar compartment in the cell nucleus. J Cell Biol* **137**: 965-74.
- Hunt, S.L., J.J. Hsuan, N. Totty, and R.J. Jackson. 1999. *unr, a cellular cytoplasmic RNA-binding protein with five cold-shock domains, is required for internal initiation of translation of human rhinovirus RNA. Genes Dev* **13**: 437-48.
- Hunt, S.L. and R.J. Jackson. 1999. *Polypyrimidine-tract binding protein (PTB) is necessary, but not sufficient, for efficient internal initiation of translation of human rhinovirus-2 RNA. Rna* **5**: 344-59.

- Jackson, R.J. 2000. A Comparative View of Initiation Site Mechanisms. In *Translational Control of Gene Expression* (ed. N. Sonenberg, H. J.W.B., and M. M.B.), pp. 127-183. Cold Spring Harbor Laboratory Press, Cold Spring Harbor, NY.
- Jubin, R. 2001. *Hepatitis C IRES: translating translation into a therapeutic target. Curr. Opin. Mol. Ther.* 3: 278-287.
- Kamath, R.V., D.J. Leary, and S. Huang. 2001. *Nucleocytoplasmic shuttling of polypyrimidine tract-binding protein is uncoupled from RNA export. Mol Biol Cell* 12: 3808-20.
- Kaminski, A. and R.J. Jackson. 1998. *The polypyrimidine tract binding protein (PTB) requirement for internal initiation of translation of cardiovirus RNAs is conditional rather than absolute. Rna* 4: 626-38.
- Liu, H., W. Zhang, R.B. Reed, W. Liu, and P.J. Grabowski. 2002. *Mutations in RRM4 uncouple the splicing repression and RNA-binding activities of polypyrimidine tract binding protein. Rna* 8: 137-49.
- Meerovitch, K., Y.V. Svitkin, H.S. Lee, F. Lejbkowitz, D.J. Kenan, E.K. Chan, V.I. Agol, J.D. Keene, and N. Sonenberg. 1993. *La autoantigen enhances and corrects aberrant translation of poliovirus RNA in reticulocyte lysate. J Virol* 67: 3798-807.
- Mitchell, S.A., E.C. Brown, M.J. Coldwell, R.J. Jackson, and W. A.E. 2001. *Protein factor requirements of the Apaf-1 internal ribosome entry segment: roles of polypyrimidine tract binding protein and upstream of N-ras. Mol Cell Biol* 21: 3364-3374.

- Nomoto, A., Y.F. Lee, and E. Wimmer. 1976. *The 5' end of poliovirus mRNA is not capped with m7G(5')ppp(5')Np. Proc Natl Acad Sci U S A 73: 375-80.*
- Pestova, T.V., C.U. Hellen, and I.N. Shatsky. 1996. *Canonical eukaryotic initiation factors determine initiation of translation by internal ribosomal entry. Mol Cell Biol 16: 6859-69.*
- Pestova, T.V., V.G. Kolupaeva, I.B. Lomakin, E.V. Pilipenko, I.N. Shatsky, V.I. Agol, and C.U. Hellen. 2001. *Molecular mechanisms of translation initiation in eukaryotes. Proc Natl Acad Sci U S A 98: 7029-36.*
- Pilipenko, E.V., T.V. Pestova, V.G. Kolupaeva, E.V. Khitrina, A.N. Poperechnaya, V.I. Agol, and C.U. Hellen. 2000. *A cell cycle-dependent protein serves as a template-specific translation initiation factor. Genes Dev 14: 2028-45.*
- Pilipenko, E.V., E.G. Viktorova, S.T. Guest, V.I. Agol, and R.P. Roos. 2001. *Cell-specific proteins regulate viral RNA translation and virus-induced disease. Embo J 20: 6899-908.*
- Pilipenko, E.V., E.G. Viktorova, E.V. Khitrina, S.V. Maslova, N. Jarousse, M. Brahic, and V.I. Agol. 1999. *Distinct attenuation phenotypes caused by mutations in the translational starting window of Theiler's murine encephalomyelitis virus. J Virol 73: 3190-6.*
- Shiroki, K., T. Isoyama, S. Kuge, T. Ishii, S. Ohmi, S. Hata, K. Suzuki, Y. Takasaki, and A. Nomoto. 1999. *Intracellular redistribution of truncated La protein produced by poliovirus 3Cpro-mediated cleavage. J Virol 73: 2193-200.*
- Vagner, S., B. Galy, and S. Pyronnet. 2001. *Irresistible IRES. Attracting the translation machinery to internal ribosome entry sites. EMBO Rep 2: 893-8.*

- Valcarcel, J. and F. Gebauer. 1997. *Post-transcriptional regulation: the dawn of PTB. Curr Biol 7*: R705-8.
- Wagner, E.J. and M.A. Garcia-Blanco. 2001. *Polypyrimidine tract binding protein antagonizes exon definition. Mol Cell Biol 21*: 3281-8.
- . 2002. *RNAi-Mediated Depletion of PTB Leads to Enhanced Exon Definition. Mol Cell 10*: 943-949.
- Witherell, G.W., A. Gil, and E. Wimmer. 1993. *Interaction of polypyrimidine tract binding protein with the encephalomyocarditis virus mRNA internal ribosomal entry site. Biochemistry 32*: 8268-75.
- Wollerton, M.C., C. Gooding, F. Robinson, E.C. Brown, R.J. Jackson, and C.W. Smith. 2001. *Differential alternative splicing activity of isoforms of polypyrimidine tract binding protein (PTB). Rna 7*: 819-32.

Figure Legends

Figure 1. IRES dependent reporter gene expression is inhibited by RNAi-mediated PTB knockdown. **A.** Western Blot analysis demonstrates knockdown of endogenous PTB in cells transfected with P9 siRNA compared to the control C2 siRNA. Levels of the unrelated CA150 were unaffected by either siRNA. CMV-GFP driven by the immediate early cytomegalovirus (CMV) promoter and translated through a canonical cap-dependent mechanism, whereas CMV-IRES-GFP is controlled by the same promoter, but GFP translation depends on the EMCV IRES upstream of the EGFP ORF.

B. Upper panels show GFP fluorescence of cells treated with either C2 or P9 siRNAs and transfected with the reporter constructs. The lower panels show results of fluorescent

activated cell sorting of these same cells. Data are plotted as the number of EGFP positive cells vs. the siRNA used to treat the cells.

Figure 2. PTB knockdown inhibits translation and replication of *wild type* EMCV.

A. Western Blot analysis demonstrates knockdown of endogenous PTB in HeLa-S3 cells transfected with P9 siRNA compared to the control C2 siRNA (left panel). A crossreacting protein, which is seen in HeLa-S3 cells, is not affected by P9 treatment. Western Blot analysis of lysates collected from HeLa-S3 cells treated with either control (C2) or PTB (P9) siRNA, and infected with EMCV. Blots were probed for the EMCV 3D protein, the asterisk marks a crossreacting protein band used as control. . **B.** EMCV progeny after infection of HeLa-S3 as determined by plaque assay from lysates shown in **A.** **C.** One-step growth curve in HeLa-S3 cells treated with either control (C2) or PTB (P9) siRNA, and infected with EMCV.

Figure 3. PTB knockdown reduces translation and replication of poliovirus. A.

Western Blot analysis of lysates collected from HeLa-R19 cells treated with either control (C2) or PTB (P9) siRNA, and infected with PV1(S). Blots were probed for poliovirus protein P2 and its proteolytic fragments 2BC and 2C. **B.** One-step growth curve in HeLa-R19 cells treated with either control (C2) or PTB (P9) siRNA, and infected with PV1(S).

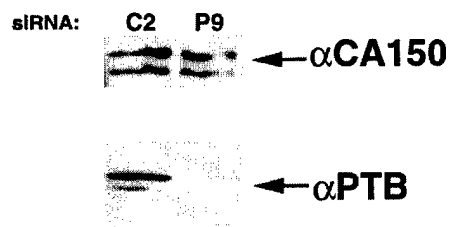
Figure 4. Activation of RNAi *per se* does not affect viral gene expression and

replication. A. Western Blot analysis of PTB levels in HeLa-R19-Luc cells transfected

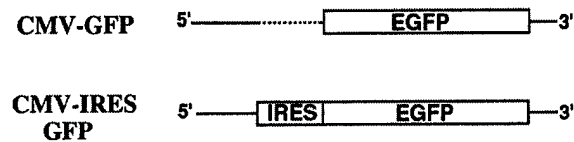
with C2, P9, or Luc siRNA, blots were also probed for TBP as a control. **B.** Luciferase activity in the cell lysates analyzed in (A). **C.** Western Blot analysis of two time points post infection with PV1(ENPOS2) probed for the polioviral P2 protein and its proteolytic products 2BC and 2C. **D.** One-step growth curve in HeLa-R19 cells treated with either control (C2), Luc or PTB (P9) siRNA, and infected with PV1(ENPOS2).

Figure 5. PTB is relocated to the cytoplasm early after poliovirus infection and prior to cleavage by the poliovirus 3C^{pro} protease. **A.** HeLa-R19 cells infected with PV1(S) were fixed every hour p.i. The subcellular localization of PTB or SC35 was determined by indirect immunofluorescence and the nuclei were stained with DAPI. **B.** The integrity of PTB was assayed by Western Blot analysis of lysates collected at the indicated times.

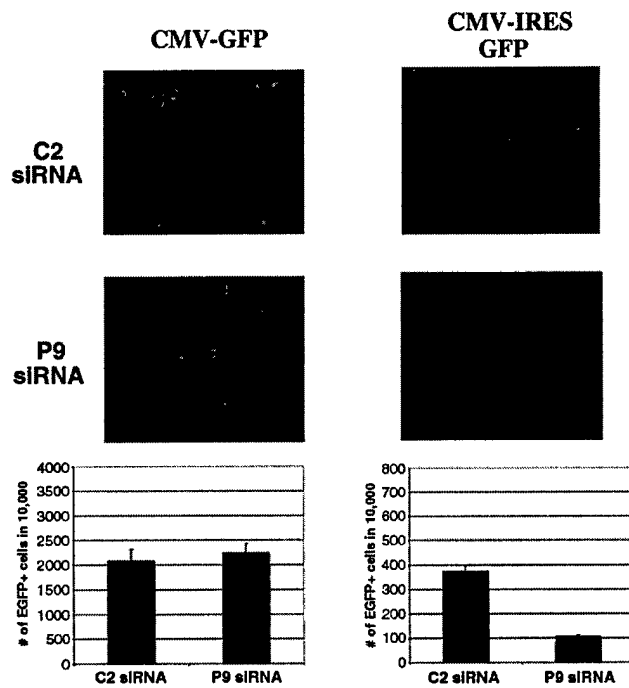
A



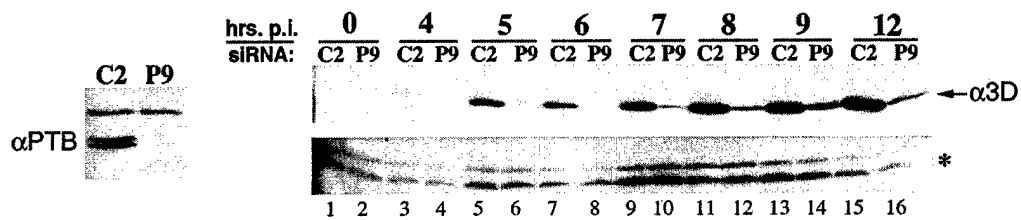
B



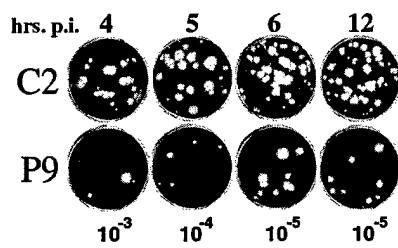
C



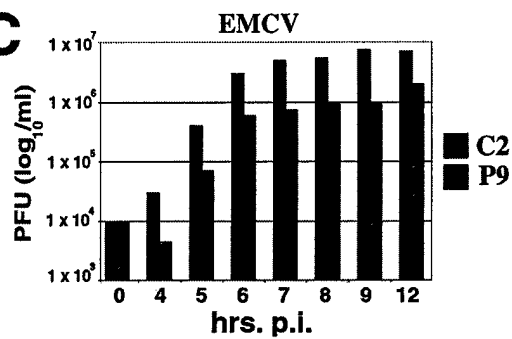
A



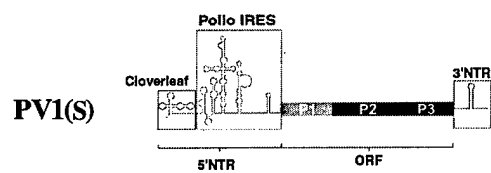
B



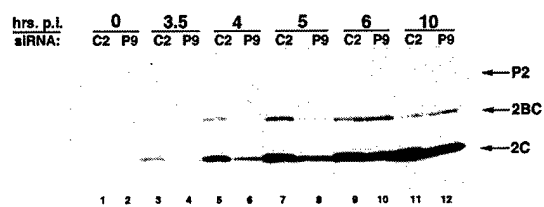
C



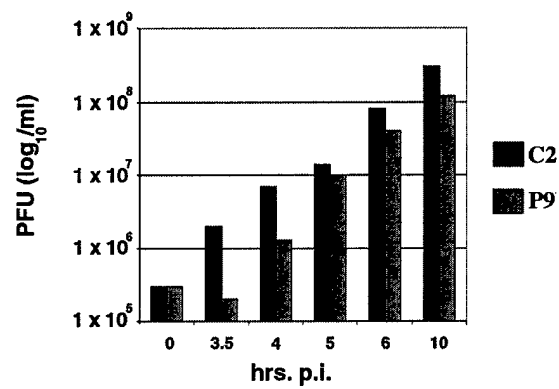
A

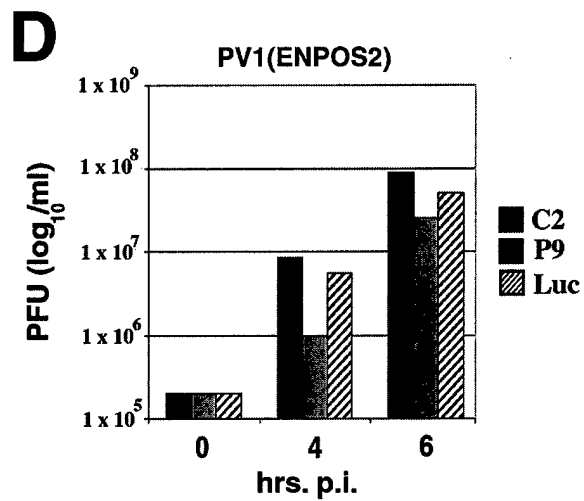
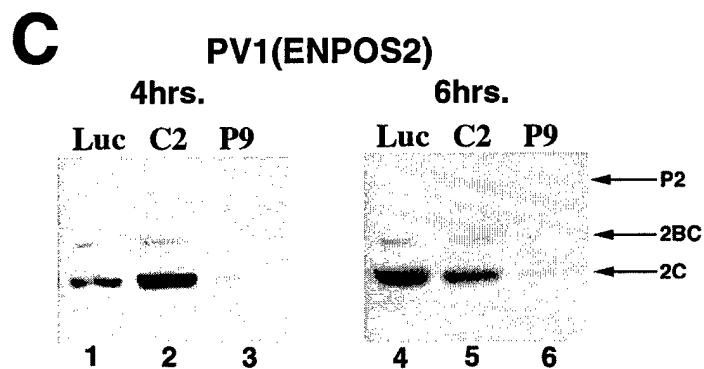
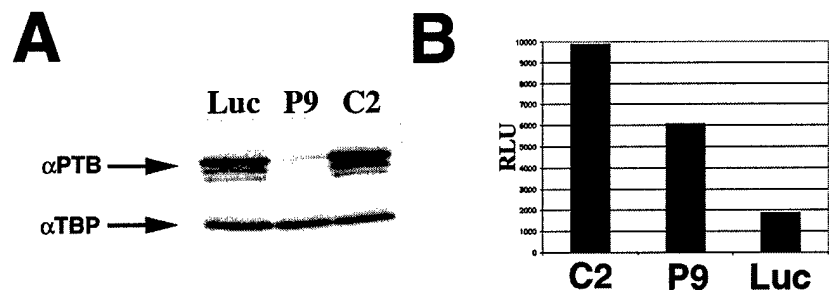


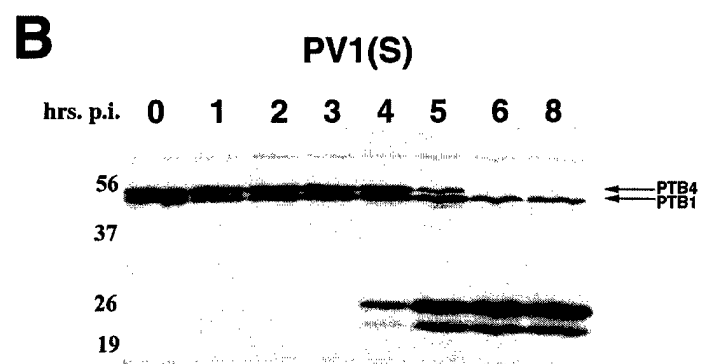
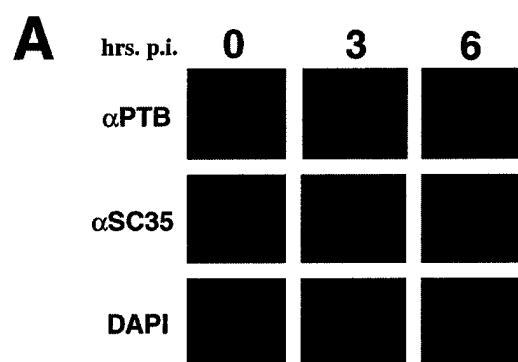
B



C







Quantification of Alternatively Spliced FGFR2 RNAs

Using the RNA Invasive Cleavage Assay

Eric J. Wagner^{1,2,†‡}, Michelle L. Curtis^{3,†}, Peggy S. Eis^{3,*†},

and Mariano A. Garcia-Blanco^{1,4,*}

¹ Departments of Molecular Genetics and Microbiology,
and ⁴ Medicine, ² Program in Molecular Cancer Biology, Duke University Medical Center
Durham, North Carolina 27710

³Third Wave Technologies, Inc., 502 South Rosa Road, Madison, Wisconsin 53719-1256.

†E. J. Wagner and M. L. Curtis contributed equally to this manuscript.

*Corresponding authors. Address correspondence to garcia001@mc.duke.edu or to Third Wave Technologies, Inc., 502 South Rosa Road, Madison, Wisconsin 53719-1256

‡Current addresses: For E. J. Wagner: Department of Molecular Biology and Biochemistry, CB# 7100, University of North Carolina, Chapel Hill, North Carolina 27599, and for P. S. Eis: GeneOhm Sciences, 6146 Nancy Ridge Drive, San Diego, CA 92121

Running Head Title: Quantification of Alternatively Spliced *FGFR2* RNAs

Key Words: alternative splicing, *FGFR2*, gene expression, Invader[®] assay, invasive cleavage, RNA quantification.

ABSTRACT

The regulated splicing of fibroblast growth factor receptor-2 (FGFR2) transcripts leads to the tissue specific expression of distinct receptor isoforms. These isoforms contain two different versions of the ligand binding Ig-like domain III, which are encoded by exon IIIb or exon IIIc. The mutually exclusive use of exon IIIb and exon IIIc can be recapitulated in tissue culture using the DT3 and AT3 rat prostate carcinoma cells. We used this well-characterized system to evaluate the precision and accuracy of the RNA invasive cleavage assay to specifically measure *FGFR2* alternative splicing outcomes. Experiments presented here demonstrated that the RNA invasive cleavage assay could specifically detect isoforms with discrimination levels that ranged from 1 in 5×10^3 to 1 in 10^5 . Moreover the assay could detect close to 0.01 attomole of *FGFR2* RNAs. The RNA invasive cleavage assay detected significant levels of transcripts containing both exons IIIb and IIIc, and surprisingly high levels of IIIb-IIIc double inclusion events. This finding, which has important implications for the role of exon silencing and of mRNA surveillance mechanisms, had been missed by RT-PCR. Additionally, we used the RNA invasive cleavage assay to demonstrate a novel function for the regulatory element IAS2 in repressing exon IIIc inclusion. We also show here that purification of RNA is not necessary for the invasive cleavage assay since crude cell lysates could be used to accurately measure alternative transcripts. The ability to measure RNA from crude extracts makes the assay less labor-intensive without sacrificing accuracy and performance. The data presented here indicate that the RNA invasive cleavage assay is an important addition to the repertoire of techniques available for the study alternative splicing.

INTRODUCTION

The sequencing and preliminary annotation of the human genome provides evidence of a preponderance of large and complex protein coding genes. The majority of these genes encode primary transcripts that undergo alternative splicing (Modrek and Lee, 2002), a process that generates different mRNAs from one gene (Black, 2000). Properly regulated alternative splicing is critical for normal development, and a breakdown in the regulation of alternative splicing leads to cellular abnormalities and to human disease (Cartegni et al. 2002; Cartegni and Krainer, 2002; Savkur, et al. 2001). These functional implications of alternative splicing underscore the importance of assays that can quantitatively and specifically measure alternative transcripts. Alternative splicing of fibroblast growth factor receptor 2 (FGFR2) transcripts leads to the formation of multiple mRNAs. The differential inclusion of exon 8 (IIIb) or exon 9 (IIIc) leads to the expression of FGFR2 isoforms with different ligand specificity. Exon IIIb is predominantly included in epithelial cells, whereas exon IIIc is exclusively used in mesenchymal cells (Fig. 1). As a consequence of expressing FGFR2(IIIb), epithelial cells respond to FGF10 and FGF7, while in mesenchymal cells the FGFR2(IIIc) responds to FGF2. Inappropriate expression of FGFR2(IIIb) in fibroblasts induces transformation in culture (Miki et al., 1991) and loss of FGFR2(IIIb) expression leads to absent or malformed epithelial compartments in many organs in mice (De Moerloose et al., 2000). A switch from the IIIb to the IIIc isoform accompanies the progression of androgen-sensitive, well-differentiated prostate carcinomas to androgen-insensitive, poorly differentiated tumors in both rats and humans (Yan et al., 1993; Carstens et al., 1997). The governance of cell-type specific FGFR2 isoform expression is therefore important in normal development and tumor progression.

Functional FGFR2 mRNAs constitutively include exon 7 and exon 10 and different regulatory pathways select exon IIIb or IIIc to produce 7-IIIb-10 and 7-IIIc-10 transcripts in a tissue-specific manner (Fig. 1). Two other variant RNAs have been described: one is the result of splicing between exons 7 and 10 (7-10) and is called the skipped product, and the other includes both IIIb and IIIc (7-IIIb-IIIc-10) is known as the double inclusion product. Both of these mRNAs, which encode truncated, non-functional receptors, are destabilized by nonsense mediated decay (Jones, et al. 2001). Thus, the choice of including either IIIb or IIIc, and the decision to skip or double include, must be controlled. The regulation of FGFR2 alternative splicing represents a complex interplay between positive and negative acting factors. There is documentation for at least ten *cis*-acting elements, which are the targets for splicing activators and repressors (reviewed in Wagner and Garcia-Blanco, 2001). We have studied the cell-type specific expression of 7-IIIb-10 in DT3 cells, which are derived from a well-differentiated rat prostate carcinoma, and the expression of 7-IIIc-10 in AT3 cells, a related but poorly differentiated rat prostate tumor line (Yan et al., 1993; Carstens et al., 1997). This exon choice is regulated by the interplay of *cis*-acting elements, two of which appear to be cell-type specific, and the *trans*-acting factors that recognize them. In DT3 cells, two elements, the intronic activation sequence 2 (IAS2) and the intronic splicing activator and repressor (ISAR; also called IAS3), activate exon IIIb (Carstens, et al. 1998; Del Gatto, et al. 1997), whereas in AT3 cells these elements have no discernable function (Fig. 1). The ISAR element, as its name suggests, also represses exon IIIc in DT3 cells (Carstens et al., 1998). To date, the tissue specific *trans*-acting factors that regulate exon choice have not been identified.

To further investigate the complex alternative splicing of FGFR2, we required higher resolution analysis than had been previously provided by RT-PCR. To this end we investigated the

quantitative capability of the RNA invasive cleavage assay (Eis et al. 2001; de Arruda et al., 2002), herein termed the Invader¹ RNA assay. The Invader RNA assay utilizes an engineered 5' nuclease (Cleavase¹ enzyme) to cleave a DNA oligonucleotide probe bound to a target RNA in a sequence- and structure-specific manner (Lyamichev et al. 1999; Ma, et al. 2000; Eis et al. 2001). In this report we demonstrate that the Invader RNA assay can quantitatively discriminate between four alternatively spliced FGFR2 transcripts using purified total cellular RNA or crude cell lysates. Furthermore, the Invader RNA assay revealed two novel observations previously obscured by the RT-PCR analysis. First, surprisingly high levels of double inclusion product were found, and second, the levels of skipped product were much lower than previously measured. These findings have important implications, which will be discussed below. Our studies also led us to the unexpected observation that the IAS2 element, which had previously been described as an activator of splicing, was observed to be a repressor of exon IIIc.

RESULTS AND DISCUSSION

To facilitate the study of FGFR2 splicing regulation we have constructed minigene constructs that recapitulate the cell-type specific regulation of endogenous FGFR2 transcripts (Carstens et al., 1998, 2000; Wagner and Garcia-Blanco, 2002). In these double exon minigenes the 7 and 10 *FGFR2* exons have been replaced with heterologous upstream (U) and downstream (D) exons derived from the Adenovirus2 major late promoter transcription unit (Carstens et al., 1998). The transcription products of these minigenes, which are synthesized *in vitro* using a T7 RNA polymerase promoter or *in vivo* from the human cytomegalovirus immediate early promoter, can

¹Invader[®] and Cleavase[®] are registered trademarks of Third Wave Technologies, Inc.

be alternatively spliced to produce four RNA variants: U-D, U-IIIb-D, U-IIIc-D, and U-IIIb-IIIc-D (Fig. 2).

Invader probe sets were designed to recognize unique junctions in each of the four RNA variants (Fig. 2). Binding of the probe, stacking and Invader oligonucleotides to the RNA sequence at or near the splice junctions creates an invasive cleavage structure that enables cleavage of the probe's 5' flap by the Cleavase enzyme (vertical arrowheads in Fig. 2) (Eis et al., 2001; Ma et al., 2000). Probes contain a Target Specific Region (TSR) and a non-complementary 5' flap (red or green). Since the assay is run isothermally near the melting temperature of the probe's TSR, the process of probe turnover (probe binding, cleavage, and dissociation of cleaved fragments) results in the specific, linear accumulation of cleaved 5' flaps in a target- and time-dependent manner. Each cleaved 5' flap then forms a second invasive cleavage structure along with a Secondary Reaction Template (SRT) and a Fluorescence Resonance Energy Transfer (FRET) oligonucleotide (Fig. 2, right side). Fluorescence signal is generated in a cleaved 5' flap-dependent manner when the Cleavase enzyme cleaves the FRET oligonucleotide between its fluorophore and quencher (vertical arrowhead). An arrestor oligonucleotide (not shown), complementary to the entire probe TSR and a portion of the 5' flap region, hybridizes with the uncleaved probe. This prevents the uncleaved probes, but not the 5' flaps, from binding to the SRT during the secondary reaction, which enhances signal generation (de Arruda et al., 2002; Eis et al., 2001).

We synthesized the four variant RNAs *in vitro* and used these to test the ability of the Invader RNA assay to quantify each and to discriminate between them. Five Invader probe sets readily discriminated between the four RNA variants (Fig. 3). For example, the IIIb-D probe set, which was designed to detect a junction found only in the U-IIIb-D RNA, preferentially

recognized this RNA over the other three variants with a 1 in 500,000 discrimination level (Fig. 3A, 3C). Likewise, the U-IIIc probe set specifically detected the U-IIIc-D RNA (Fig. 3B, 3C). The least robust discrimination level by the U-IIIc probe set was 1 in 5,000 for the U-D RNA (Fig. 3C), which is still well outside the quantitative range for the U-IIIc probe set and thus not regarded as problematic. These data indicated that the Invader RNA assay could specifically quantify the levels of all four alternatively spliced RNA variants (summarized in Fig. 3C) with a sensitivity ranging from 0.01 to 0.04 amole.

We have previously shown that the double exon minigene constructs described above recapitulate the cell-type specific choice of IIIb vs. IIIc when transfected into DT3 and AT3 cells (Carstens et al., 1998). These double exon minigenes provided us with an excellent system to test the utility of the Invader RNA assay in quantifying alternative splice site RNA variants. Thus, we transfected DT3 and AT3 cells with the pI12DE:Wt minigene construct (Fig. 4A) and quantified the levels of the four variant RNAs (U-D, U-IIIb-D, U-IIIc-D, and U-IIIb-IIIc-D) using the probe sets described in Figure 2. When transfected with this minigene, DT3 cells preferentially include exon IIIb and AT3 cells almost exclusively use exon IIIc (Fig. 4B). The data derived from the Invader RNA assay supported our prior conclusions regarding the cell-type specific expression of U-IIIb-D in DT3 cells and U-IIIc-D in AT3 cells (Carstens et al., 1998). Although the same general trend was observed with the Invader RNA assay (gray bars) and with RT-PCR (white bars), significant over-representation of the U-D product by RT-PCR led to lower relative values for the U-IIIb-D and U-IIIc-D levels. This anomaly is likely due to the propensity of PCR to favor the smaller U-D product. Perhaps most importantly the Invader RNA assay revealed a surprisingly high level of double inclusion (U-IIIb-IIIc-D) RNA, reaching 30% of all RNA variants, in both DT3 and AT3 cells. It is important to note that because these

transcripts do not encode an open reading frame, the U-D and U-IIIb-IIIc-D transcripts are not destabilized by nonsense mediated decay. These data suggest that the regulation of exon choice in *FGFR2* transcripts is not as stringent as previously assumed (see discussion below).

The cell-type specific regulation of *FGFR2* alternative splicing was previously shown to be controlled by several cis-elements. Among these, ISAR activates exon IIIb and silences exon IIIc in DT3 cells (Fig. 1) (Carstens et al., 1998). Data of others had suggested that IAS2 works in concert with ISAR to activate IIIb in cells of epithelial origin (Fig. 1) (Del Gatto et al., 1997). The requirements for IAS2 and ISAR were tested using the Invader RNA assay and RT-PCR. Once again, the observed trends for the Invader RNA assay generally corresponded with previous and current RT-PCR results (Fig. 4). In AT3 cells, deletion of either IAS2 (Δ IAS2), ISAR (Δ ISAR), or both (Δ, Δ) had no perceptible effect on the percent inclusion of IIIb or IIIc (Fig. 4B, 4C; first and second panels), which was expected. However, in DT3 cells, Δ IAS2, Δ ISAR, or Δ, Δ led to a significant decrease in the expression of U-IIIb-D and increased expression of U-IIIc-D (Fig. 4B, 4C; first and second panels). Interestingly, deletion of IAS2 led not only to increased levels of U-IIIc-D, but also of U-IIIb-IIIc-D. This is the first evidence implicating IAS2 in the repression of exon IIIc.

In order to distinguish between the role of IAS2 in IIIb activation and IIIc repression, we transfected DT3 cells with single exon minigene constructs. We had previously employed similar single exon minigenes (constructs that contain either IIIb or IIIc) to show that ISAR was independently required for the activation of IIIb and the repression of IIIc (Carstens et al., 1998) (Fig. 5A). Deletion of IAS2 in the context of the minigene constructs had no effect in AT3 cells (data not shown), but in DT3 cells this deletion decreased IIIb inclusion and independently increased IIIc inclusion. These trends were observed using both the Invader RNA assay (gray

bars) and RT-PCR (white bars) and established that IAS2 can mediate repression of exon IIIc in epithelial cells.

Given the ability of the Invader RNA assay to specifically quantify alternatively spliced RNA variants and prior reports that the assay could be carried out using crude cell lysates (Eis et al., 2001), we wanted to test whether alternative FGFR2 variants could be measured without the need to purify cellular RNA. Crude cell lysate and purified RNA samples were prepared from DT3 cells transfected with the single exon minigene constructs, which have either IIIb or IIIc as a single internal exon (Fig. 5A), and the splicing products were quantified with the Invader RNA assay. This experiment demonstrated nearly identical results from purified RNA and crude cell lysates (Fig. 6). The use of cell lysates saves several hours of sample preparation and provides accurate monitoring of gene expression and alternative splicing in a simple, high-throughput format.

The functional implications of the high frequency of alternative splicing among human transcripts are far-reaching. Thus, there is a need for RNA assays that are not only quantitative, but that are also specific since alternatively spliced variants can differ by very few nucleotides. Such high-resolution analysis of gene expression profiles for differentially spliced mRNA variants will provide insight into this complex phenomenon. In this manuscript we investigated the potential of the Invader RNA assay to report on alternative splicing. The Invader RNA assay confirmed our suspicion that RT-PCR consistently over-represented the skipped product and skewed the results accordingly. This propensity of PCR to favor smaller products is a problem in all PCR reactions, including QRT-PCR, where different products are in competition. The accurate quantification of FGFR2 alternative splicing by the Invader RNA assay permitted the detection of significant levels of IIIb-IIIc double exon inclusion. This finding suggests that the

repression of exon IIIc in epithelium (Carstens et al., 1998) and of exon IIIb in mesenchyme (Wagner and Garcia-Blanco, 2002) may not be as tightly controlled as previously thought. If true for endogenous FGFR2, this indicates that RNA surveillance mechanisms must dispose of significant levels of FGFR2 transcripts that include both IIIb and IIIc (Jones et al., 2001). These studies clearly establish the significant value of the Invader RNA assay in the study of alternative splicing.

Although selection of specific Invader assay probe sets can be more complex than the selection of RT-PCR primers, the assay offers some significant advantages. The Invader RNA assay not only exhibits remarkable isoform discrimination, but it is also highly quantitative and sensitive, routinely detecting 0.005-0.05 attomole of transcript (Fig. 3 and data not shown). Accurate quantification is achieved through its linear signal amplification mechanism, which can reproducibly detect 1.2-fold changes in mRNA (Eis et al., 2001). In the present study, the Invader RNA assay was performed in a biplex detection format, thus enabling the quantification of an included exon relative to an internal control (e.g., U-D) in the same sample. This type of measurement affords additional accuracy in the analysis of the splice variant profiles. An added advantage over most other methods is the capacity to carry out the assay in crude cell lysates, which saves time and reduces errors associated with increased manipulations. The data presented in this report demonstrate that the Invader RNA assay is a valuable tool for the investigation of alternative splicing.

MATERIALS AND METHODS

Minigene constructs and *in vitro* transcript generation. Short transcripts (containing only the oligonucleotide-binding regions) were used for all standard curves except those generated for the discrimination experiments, which used full-length transcript standards. The short and full-length transcripts performed equivalently in the Invader RNA assay (data not shown). For generation of the short transcript standards, two synthetic oligonucleotides containing the T7 promoter and the binding region for the oligonucleotides for each assay were annealed. To generate the full-length transcripts, which span the exon-exon junctions shown in Figure 2, double exon minigene constructs (Fig. 4A) or single exon minigene constructs (Fig. 5A) were obtained by cloning PCR products of genomic segments of the rat *FGFR2* gene into the pI-12 vector as described in Carstens et al (1998). The sequences of all oligonucleotides used for cloning will be available upon request. The minigene constructs, which contain a T7 or T3 promoter, were linearized with either HindIII or ApaI, and served as templates for *in vitro* transcription. Transcription reactions were performed using the T7 Ribomax™ Large Scale RNA Production System (Promega Corporation, Madison, WI) or the T3 MEGAshortscript *in vitro* transcription kit (Ambion, Austin, TX). The sequences of the full length RNAs will be made available upon request. The transcripts were purified using Trizol Reagent (Invitrogen Corporation, Carlsbad, CA) or gel-purified on denaturing polyacrylamide gels and quantified by A₂₆₀ measurement. All transcripts were diluted with 20 ng/μl transfer RNA (tRNA) (Sigma, St. Louis, MO) or 1X Cell Lysis Buffer (Third Wave Technologies, Inc., Madison, WI).

Transfections, cell lysates and isolation of cellular RNA. The growth and transfection of DT3 and AT3 cells and the isolation of total cellular RNA were performed as previously described in Wagner and Garcia-Blanco (2002). Cell lysate samples were prepared as previously

described in Eis et al (2001). Assays were performed using either total RNA (50-200 ng) or cell lysate samples prepared from approximately 900 cells.

Invader RNA assay and semi-quantitative RT-PCR. The Invader RNA assay was carried out as described in Eis et al (2001) except 1 μ M probe was used for all probe sets and 0.25 μ M of Invader oligonucleotide was used for the IIIb-IIIc and U-IIIc probe sets. Invader RNA Assay Generic Reagents (Third Wave Technologies, Inc., Madison, WI) were used for all assays. The four alternate RNAs were quantified with the biplex format of the Invader RNA assay (Eis et al., 2001), using the following probe set combinations: U-D/IIIb-D and IIIb-IIIc/U-IIIc (for double inclusion IIIb-IIIc minigene constructs), U-D/IIIb-D (for single inclusion IIIb minigene construct), or U-D/IIIc-D (for single inclusion IIIc minigene construct). Semi-quantitative RT-PCR was carried out as previously described (Carstens et al., 1998; Wagner and Garcia-Blanco, 2002). All oligonucleotides used in the RT-PCR and Invader RNA assays are listed in Table 1.

Data analysis. The expression levels of each construct were calculated for each sample using the net signal values and the equations generated from the standard curves as previously described in Eis et al. (2001). These expression levels were then used to determine % inclusion for any given construct by using the following equation: (expression level of the construct of interest)/(combined expression levels of all constructs) x 100.

ACKNOWLEDGEMENTS

We thank Andrew Baraniak and David Mauger for critical reading of this manuscript and members of the Garcia-Blanco laboratory, especially Erika Lasda, for important suggestions. We thank James Dahlberg, Marilyn Olson, Tsetska Takova, Victor Lyamichev, and Laura

Heisler for insightful discussions and revisions of the manuscript. We thank Annette Kennett for her help in the preparation of this manuscript. The work in the Garcia-Blanco laboratory was funded by a grant from the NIH (GM63090). M. A. G-B. was a scholar of the Raymond and Beverly Sackler Foundation. E. J. W. acknowledges the support of a Department of Defense predoctoral fellowship.

TABLE 1. Oligonucleotides used in the Invader RNA and RT-PCR assays

Invader		
Probe Set	Oligonucleotide	Sequence* (5' to 3')
U-D	Probe	CCGTCGCTGCGTCTGGTAGGGT-NH ₂
	Invader Oligo	TCCTGCAGCTCAACCGCGACA
	Stacking Oligo	ACCUCGCAGACAGCG
	Arrestor Oligo	ACCCUACCAGACGCAG
	FRET Oligo	FAM-CAC(DQ)TGCTTCGTGG
	Secondary Reaction Template	CCAGGAAGCAAGTGACGCAGCGAC GGU
	Synthetic Target Oligo (coding)	GGTAATACGACTCACTATAGGGACGCATCGCTGTCTGCGAGGTACCTACCAGGTCGCGTTGAGCTGCAGGACAAAC
	Synthetic Target Oligo (non-coding)	GTTTGTCTGCAGCTCAACCGCGACCTGGTAGGGTACCTGCAGACAGCGATGCGTCCCTATAGTGAGTCGTATTACC
IIIb-D	Probe	CCGTCACGCCTCCTTGCTGTTTG-NH ₂
	Invader Oligo	TCCTGCAGCTCAACCGCGACA
	Stacking Oligo ²	GGCAGGACAGUGAGCC
	Arrestor Oligo ²	CAAACAGCAAGGAGGCG
	FRET Oligo ³	Red-CTC(DQ)TTCTCAGTGCG
	Secondary Reaction Template ²	CGCAGTGAGAATGAGGAGGCGTGAC GGU
	Synthetic Target Oligo (coding)	GGTAATACGACTCACTATAGGGATGCGCTGCTGCTGCTGCCAAACAGCAAGGTCGCGTTGAGCTGCAGGACAAAC
	Synthetic Target Oligo (non-coding)	GTTTGTCTGCAGCTCAACCGCGACCTTGCTGTTTGGCAGGACAGTGAGCCAGGCATCCCTATAGTGAGTCGTATTACC
U-IIIc	Probe	CCGTCGCTGCGTCTGGTAGGGT-NH ₂
	Invader Oligo	CGTGGTGTAAACACCGGCGGCA
	Stacking Oligo ²	ACCUCGCAGACAGCG
	Arrestor Oligo ²	ACCCUACCAGACGCAG
	FRET Oligo ³	FAM-CAC(DQ)TGCTTCGTGG
	Secondary Reaction Template ²	CCAGGAAGCAAGTGACGCAGCGAC GGU
	Synthetic Target Oligo (coding)	GGTAATACGACTCACTATAGGGACGCATCGCTGCTGCGAGGTACCTACCAGGCGCGGTTGTTAACACCGGACAA
	Synthetic Target Oligo (non-coding)	TTGTCCGTGGTGTAAACACCGCGCGCTTGCTGTTTGGCAGGACAGTGAGCCAGGCATCCCTATAGTGAGTCGTATTACC
IIIb-IIIc	Probe	CCGTCACGCCTCCTTGCTGTTTG-NH ₂
	Invader Oligo	CGTGGTGTAAACACCGGCGGCA
	Stacking Oligo ²	GGCAGGACAGUGAGCC
	Arrestor Oligo ²	CAAACAGCAAGGAGGCG
	FRET Oligo ³	Red-CTC(DQ)TTCTCAGTGCG
	Secondary Reaction Template ²	CGCAGTGAGAATGAGGAGGCGTGAC GGU
	Synthetic Target Oligo (coding)	AGGTAATACGACTCACTATAGGGATGCGCTGCTGCTGCTGCCAAACAGCAAGGCGCGGTTGTTAACACCGGACAA
	Synthetic Target Oligo (non-coding)	ATTGTCCGTGGTGTAAACACCGCGCGCTTGCTGTTTGGCAGGACAGTGAGCCAGGCATCCCTATAGTGAGTCGTATTACC
IIIc-D	Probe	CCGTCACGCCTCCTGGCAGAAC-NH ₂
	Invader Oligo	TCCTGCAGCTCAACCGCGACA
	Stacking Oligo ²	UGUCAACCAUGCAGAGU
	Arrestor Oligo ²	GUUCUGCCAGGAGGCG
	FRET Oligo ³	Red-CTC(DQ)TTCTCAGTGCG
	Secondary Reaction Template ²	CGCAGTGAGAATGAGGAGGCGTGAC GGU
	Synthetic Target Oligo (coding)	GGTAATACGACTCACTATAGGGACCTTCACTCTGCATGGTTGACAGTTCTGCCAGGTCGCGTTGAGCTGCAGGACAAAC
	Synthetic Target Oligo (non-coding)	GTTTGTCTGCAGCTCAACCGCGACCTGGCAGAACTGTCAACCATGCAGAGTGAAAGTCCCTATAGTGAGTCGTATTACC
RT-PCR	T7 Primer	GTAATACGACTCACTATAGG
	SP6 Primer	TACGATTTAGGTGACACTATAG

*Underlined bases indicate 2'-O-methylated nucleotides. Redmond Red (Red) and Eclipse Dark Quencher (DQ) were obtained from Epoch Biosciences (Bothell, WA).

REFERENCES

- Black, D. L. 2000. Protein diversity from alternative splicing: a challenge for bioinformatics and post-genome biology. *Cell*. **103**: 367-70.
- Carstens, R. P., McKeehan, W. L. and Garcia-Blanco, M. A. 1998. An intronic sequence element mediates both activation and repression of rat fibroblast growth factor receptor 2 pre-mRNA splicing. *Mol Cell Biol*. **18**: 2205-17.
- Cartegni, L., Chew, S. L. and Krainer, A. R. 2002. Listening to silence and understanding nonsense: exonic mutations that affect splicing. *Nat Rev Genet*. **3**: 285-98.
- Cartegni, L. and Krainer, A. R. 2002. Disruption of an SF2/ASF-dependent exonic splicing enhancer in SMN2 causes spinal muscular atrophy in the absence of SMN1. *Nat Genet*. **30**: 377-84.
- de Arruda, M., Lyamichev, V. I., Eis, P. S., Iszczyszyn, W., Kwiatkowski, R. W., Law, S. M., Olson, M. C. and Rasmussen, E. B. 2002. Invader technology for DNA and RNA analysis: principles and applications. *Expert Rev Mol Diagn*. **2**: 487-96.
- Del Gatto, F., Plet, A., Gesnel, M. C., Fort, C. and Breathnach, R. 1997. Multiple interdependent sequence elements control splicing of a fibroblast growth factor receptor 2 alternative exon. *Mol Cell Biol*. **17**: 5106-16.
- Eis, P. S., Olson, M. C., Takova, T., Curtis, M. L., Olson, S. M., Vener, T. I., Ip, H. S., Vedvik, K. L., Bartholomay, C. T., Allawi, H. T., Ma, W. P., Hall, J. G., Morin, M. D., Rushmore, T. H., Lyamichev, V. I. and Kwiatkowski, R. W. 2001. An invasive cleavage assay for direct quantitation of specific RNAs. *Nat Biotechnol*. **19**: 673-6.

- Jones, R. B., Wang, F., Luo, Y., Yu, C., Jin, C., Suzuki, T., Kan, M. and McKeehan, W. L. 2001. The nonsense-mediated decay pathway and mutually exclusive expression of alternatively spliced *FGFR2IIIb* and *-IIIc* mRNAs. *J Biol Chem.* **276**: 4158-67.
- Lyamichev, V., Mast, A. L., Hall, J. G., Prudent, J. R., Kaiser, M. W., Takova, T., Kwiatkowski, R. W., Sander, T. J., de Arruda, M., Arco, D. A., Neri, B. P. and Brow, M. A. 1999. Polymorphism identification and quantitative detection of genomic DNA by invasive cleavage of oligonucleotide probes. *Nat Biotechnol.* **17**: 292-6.
- Ma, W. P., Kaiser, M. W., Lyamicheva, N., Schaefer, J. J., Allawi, H. T., Takova, T., Neri, B. P. and Lyamichev, V. I. 2000. RNA template-dependent 5' nuclease activity of *Thermus aquaticus* and *Thermus thermophilus* DNA polymerases. *J Biol Chem.* **275**: 24693-700.
- Modrek, B. and Lee, C. 2002. A genomic view of alternative splicing. *Nat Genet.* **30**: 13-9.
- Savkur, R. S., Philips, A. V. and Cooper, T. A. 2001. Aberrant regulation of insulin receptor alternative splicing is associated with insulin resistance in myotonic dystrophy. *Nat Genet.* **29**: 40-7.
- Wagner, E. J. and Garcia-Blanco, M. A. 2002. RNAi-mediated PTB depletion leads to enhanced exon definition. *Mol Cell.* **10**: 943-9.
- Yan, G., Fukabori, Y., McBride, G., Nikolaropolous, S. and McKeehan, W. L. 1993. Exon switching and activation of stromal and embryonic fibroblast growth factor (FGF)-FGF receptor genes in prostate epithelial cells accompany stromal independence and malignancy. *Mol Cell Biol.* **13**: 4513-22.

FIGURE LEGENDS

FIGURE 1. Multiple layers of combinatorial interactions result in tissue-specific alternative splicing of FGFR2 transcripts. A schematic of exons 7-10 and introns 7-9 of *FGFR2* is shown indicating that silencing of exon IIIb dominates in mesenchymal cells. In epithelial cells, however, a layer of regulation combines activation of exon 8 (IIIb) with repression of exon 9 (IIIc). These activities are mediated by two cis-elements: IAS2 and ISAR.

FIGURE 2. Schematics of the Invader RNA assay probe sets and of the four FGFR2 RNA variants derived from the alternative splicing of exons IIIb and IIIc. Splice variants generated from the minigene constructs used in this report contain U and D exons, which are derived from Adenovirus2 L1 and L2 exons. Variants can also contain IIIb and/or IIIc exons, which are derived from the rat *FGFR2* gene (see Materials and Methods).

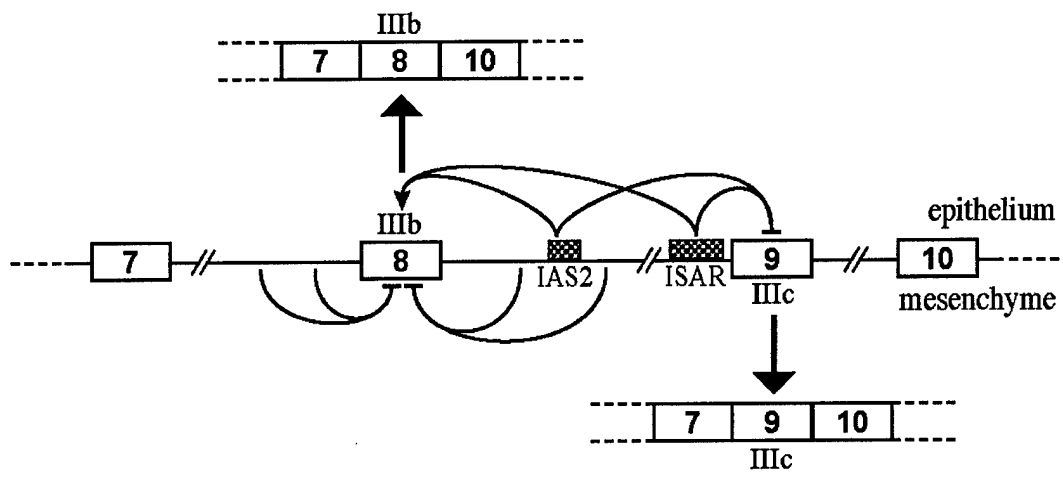
FIGURE 3. The Invader RNA assay discriminates between alternatively spliced FGFR2 transcripts. (A, B) The Invader RNA assay, using the IIIb-D (A) or the U-IIIc probe set (B) was carried out with increasing levels (0.01 to 10,000 amole) of the four variant RNAs (Fig. 2). Linear regression (R^2) values for the fitted regions of the data are 0.992 and 0.998 for IIIb-D and U-IIIc, respectively. (C) Table of the discrimination capability of the five probe sets on the four RNA variants. The discrimination capability for each probe set was calculated by dividing the highest target level in which no significant signal was detected for another RNA variant by the limit of detection for the probe set being tested. Values listed represent the inverse of the discrimination capability (e.g., the IIIb-D probe set has a limit of detection of 0.02 amole and it

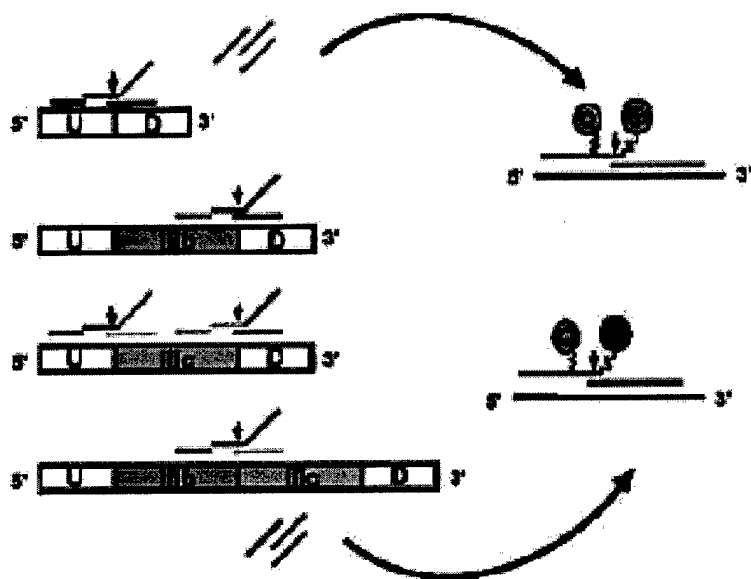
detects background signal from the U-D transcript at 5,000 amole: $10,000/0.02 = 250,000$ discrimination level).

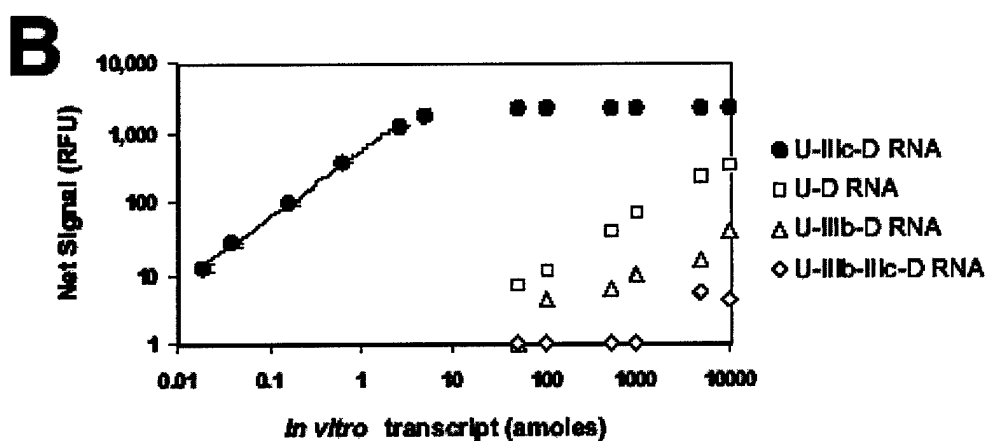
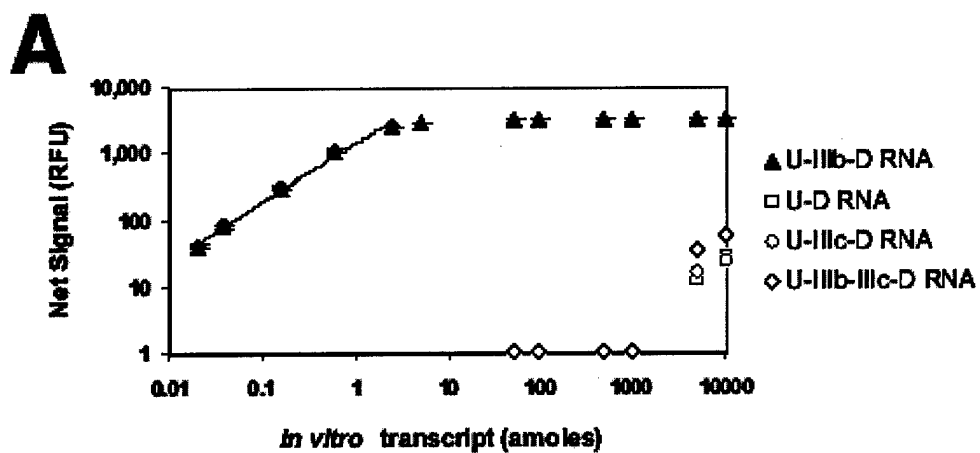
FIGURE 4. The Invader RNA assay accurately reports levels of alternatively spliced *FGFR2* RNAs. **(A)** Schematic of double exon minigene constructs used to study the cell-type specific inclusion of exons IIIb and/or IIIc. The presence or absence of IAS2 and ISAR is indicated. These minigenes can direct the expression of four RNAs produced by alternative splicing: skipping of IIIb and IIIc yields U-D RNA, inclusion of either IIIb or IIIc yields U-IIIb-D or U-IIIc-D, respectively, and double inclusion yields U-IIIb-IIIc-D. **(B)** DT3 cells and **(C)** AT3 cells were transfected with the minigene constructs in (A). Total RNA was extracted and analyzed with either the Invader RNA assay (gray bars) or semi-quantitative RT-PCR (white bars) for the presence of the four RNA variants.

FIGURE 5. IAS2 represses the IIIc exon in epithelial cells. **(A)** Schematic of single exon minigene constructs used to study the inclusion of exon IIIb and the repression of exon IIIc in DT3 cells. The presence or absence of IAS2 and ISAR is indicated. The IIIb minigenes can direct the expression of two RNAs produced by alternative splicing: skipping of IIIb leads to the U-D RNA, and the inclusion of IIIb leads to the U-IIIb-D RNA. The IIIc minigenes can direct the expression of two RNAs produced by alternative splicing: skipping of IIIc leads to the U-D RNA, and the inclusion of IIIc leads to the U-IIIc-D. **(B)** DT3 cells were transfected with the minigene constructs in (A) and total RNA was extracted and analyzed with either the Invader RNA assay (gray bars) or semi-quantitative RT-PCR (white bars) for the presence of the RNA variants.

FIGURE 6. The Invader RNA assay accurately reports levels of *FGFR2* alternatively spliced RNAs in crude cell extracts. DT3 cells were transfected with the single exon minigene constructs described in Figure 5, and either crude cell lysate (striped bars) or purified total RNA (gray bars) was analyzed for the presence of U-D, U-IIIb-D (left panel), or U-IIIc-D RNAs (right panel).



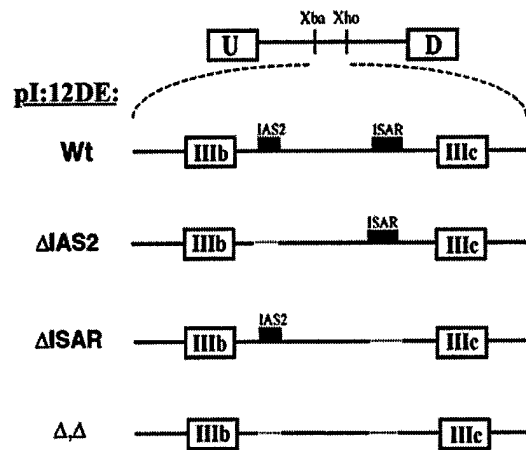




C

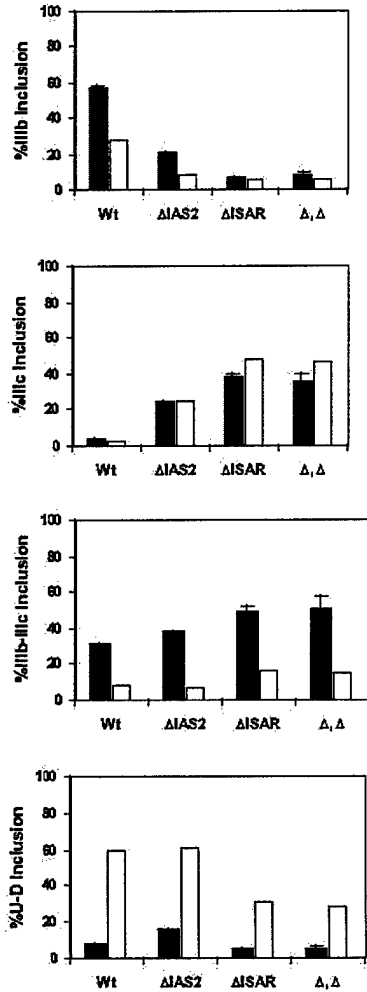
		RNA Control			
		U-D	U-IIIb-D	U-IIIc-D	U-IIIb-IIIc-D
Probe Set	U-D	1	500,000	5,000	10,000
	IIIb-D	500,000	1	500,000	500,000
	U-IIIc	5,000	50,000	1	>500,000
	IIIc-D	12,500	125,000	1	1
	IIIb-IIIc	>500,000	25,000	>500,000	1

A



B

DT3 cells



C

AT3 cells

